

PETROGENESIS OF THE KLONDIKE FORMATION,

YUKON TERRITORY

by

Paul Metcalfe

A Thesis

presented to the University of Manitoba

in partial fulfilment of the

requirements for the degree of

Master of Science

in

Department of Earth Sciences

University of Manitoba

Winnipeg, Manitoba, 1981

(c) P. Metcalfe, 1981

PETROGENESIS OF THE KLONDIKE FORMATION,

YUKON TERRITORY

BY

PAUL METCALFE

A thesis submitted to the Faculty of Graduate Studies of
the University of Manitoba in partial fulfillment of the requirements
of the degree of

MASTER OF SCIENCE

© 1981

Permission has been granted to the LIBRARY OF THE UNIVER-
SITY OF MANITOBA to lend or sell copies of this thesis, to
the NATIONAL LIBRARY OF CANADA to microfilm this
thesis and to lend or sell copies of the film, and UNIVERSITY
MICROFILMS to publish an abstract of this thesis.

The author reserves other publication rights, and neither the
thesis nor extensive extracts from it may be printed or other-
wise reproduced without the author's written permission.

I hereby declare that I am the sole author of this thesis. I authorize the University of Manitoba to lend this thesis to other institutions or individuals for the purpose of scholarly research.

P. Metcalfe

I further authorize the University of Manitoba to reproduce this thesis by photocopying or by other means, in whole or in part, at the request of other institutions or individuals for the purpose of scholarly research.

P. Metcalfe

The University of Manitoba requires the signatures of all persons using or photocopying this thesis. Please sign below, and give address and date.

ABSTRACT

The bedrock of the Klondike placer gold deposits in the Yukon Territory is here redefined as the Klondike Formation, using conventional litho-stratigraphic nomenclature. The formation comprises a 3000 m-thick cataclastically deformed sequence of bimodal blastomylonitic quartz feldspar muscovite schists, with intercalated quartz K-feldspar protomylonites near the observed base of the formation. Metamorphic grade is middle greenschist facies. The protomylonites are petrographically distinct from the blastomylonitic schists and are interpreted as minor rhyolitic volcanic members in a predominantly arkosic sedimentary succession, the latter derived from erosion of the rhyolites, or associated granitic rocks.

Rb-Sr isotopic studies on the metarhyolites indicate an age of 202 ± 11 Ma with an initial $^{87}\text{Sr}/^{86}\text{Sr}$ of 0.7140, interpreted as an age of metamorphism of the Klondike Formation. A decay constant for ^{87}Rb of $1.42 \cdot 10^{-11} \text{yr}^{-1}$ was used in the measurement. This age is consistent with K-Ar studies conducted on the formation. Rotation of the isochron to an assumed initial $^{87}\text{Sr}/^{86}\text{Sr}$ of 0.704 yields an age of 290 Ma for formation of the rhyolites, consistent with a U-Pb zircon age of 276 ± 5 Ma on genetically related granitic rocks. The minimum estimated age of the Klondike Formation is 250 Ma.

The Klondike Formation has a conformable basal contact with the structurally underlying metasedimentary rocks of the Nasina Series, although discordant cleavages in less competent lithologies of the Nasina Series possibly reflect a low angle thrust contact. The two formations were folded congruently during F2.

Chlorite-actinolite schists, in the area around King Solomon Dome, are associated with a serpentinite body. These have been excluded from the Klondike Formation and assigned to the Moosehide Assemblage of serpentinites, metagabbros and metabasalts on the grounds of lithologic similarity.

Tectonic models for the evolution of the Klondike Formation suggest that

it was an assemblage of immature sediments and rhyolitic volcanics which underwent cataclasis and metamorphism in the suture zone of an island arc-continent collision, during the late Triassic or early Jurassic. The results of petrographic, geochemical and isotopic studies on the formation are consistent with this theory.

ACKNOWLEDGEMENTS

Field work for this research project was funded by Cominco Ltd., of Vancouver. The Rb-Sr isotopic studies were supported by an N.S.E.R.C. grant to Dr. G.S. Clark. The author was funded by a graduate assistantship at the University of Manitoba.

The author wishes to thank Dr. H.D.B. Wilson for his supervision of this thesis and Dr. G.S. Clark for critical review of the thesis and assistance with the Rb-Sr isotopic studies. Special thanks are due to Dr. I.A. Paterson of Cominco Ltd., for his help in the field and for critical review of the completed thesis. Other members of the Department of Geology who rendered assistance are Dr. L.D. Ayres and Dr. A.C. Turnock, with petrography, Dr. F. Hawthorne, with computer programming, and Dr. W.C. Brisbin with structural studies.

Special thanks are due to Paul Beaudoin for his help with isotope dilution and mass spectrometry. Thanks are also due to Ron Pryhitko for advice on drafting and for photography; to Ron Chapman and Ken Ramlal for chemical analyses and to Irene Berta for thin sections. The Cominco laboratory in Vancouver also assisted in the making of 20 thin sections. I would like to thank my colleagues in graduate studies for their encouragement and constructive criticism of this research.

TABLE OF CONTENTS

	<u>Page</u>
ABSTRACT	iii
ACKNOWLEDGEMENTS	v
LIST OF FIGURES	ix
LIST OF TABLES	xi
CHAPTER I. INTRODUCTION	1
1.1 PURPOSE OF PRESENT STUDY	1
1.2 LOCATION OF AREA AND ACCESS	1
1.3 VEGETATION AND OUTCROP	1
1.4 PREVIOUS STUDIES	4
CHAPTER II. GENERAL GEOLOGY	7
2.1 NASINA SERIES	7
2.2 KLONDIKE SERIES	7
2.3 MOOSEHIDE ASSEMBLAGE	11
2.4 STRUCTURE	11
Deformation	11
Faults	12
CHAPTER III. STRATIGRAPHY AND PETROGRAPHY	13
3.1 STRATIGRAPHIC DEFINITION	13
3.2 TYPE SECTION	13
3.3 FIELD OBSERVATIONS	13
3.4 DETAILED PETROGRAPHY	15
Blastomylonites	16
Matrix	16
Quartz Fragments	17
Plagioclase	17
Compound Fragments	17
Protomylonites	18
Matrix	18
Quartz Fragments	18
K-Feldspar	19
Compound Fragments	19
Ferruginous Quartzites	19
Calc-Silicate Assemblages	20
Metamorphism	20
3.5 SUMMARY OF PETROGRAPHY	23
CHAPTER IV. CHEMISTRY OF THE KLONDIKE FORMATION	24
4.1 ANALYTICAL RESULTS	24
4.2 TREATMENT OF ANALYTICAL RESULTS	24
4.3 SUMMARY OF CHEMISTRY	38

	<u>Page</u>
CHAPTER V. ISOTOPIC STUDIES	41
5.1 PREVIOUS STUDIES	41
5.2 ISOTOPIC AGE OF THE KLONDIKE FORMATION METARHYOLITES	44
Isotopic Analysis	44
Analytical Results	45
5.3 DISCUSSION	45
5.4 SUMMARY	47
CHAPTER VI. CHLORITE-ACTINOLITE SCHIST ASSEMBLAGES	48
6.1 MOOSEHIDE ASSEMBLAGE	48
6.2 CHLORITE-ACTINOLITE SCHIST OF KING SOLOMON DOME	49
CHAPTER VII. CONCLUSION	53
7.1 TECTONIC SETTING	54
7.2 RECOMMENDATIONS FOR STUDY	58
REFERENCES CITED.. .. .	59
PHOTOGRAPHIC PLATES	64
APPENDICES	
A. PETROGRAPHIC DESCRIPTIONS OF KLONDIKE FORMATION	71
A.1 Member 1	71
A.2 Member 2	74
Submember 2a	74
A.3 Member 3	76
Submember 3a	76
A.4 Member 4	76
Submember 4a	79
Submember 4b	79
A.5 Member 5	79
A.6 Member 6	80
A.7 Upper Section	81
B. PROCEDURES FOR WHOLE ROCK ANALYSIS AND ISOTOPE DILUTION	84
B.1 WHOLE ROCK ANALYSIS	84
B.2 SAMPLE PREPARATION FOR RB-SR ISOTOPIC ANALYSIS	84
C. RENORM	87
C.1 FUNCTION	87
C.2 PROCESSING LOGIC	87
C.3 OPTIONS	88
C.4 OUTPUT	89

	<u>Page</u>
D. NORMATIVE CALCULATIONS ON KLONDIKE FORMATION	90
E. CHLORITE SCHISTS AND SERPENTINITES	95
E.1 PETROGRAPHIC DESCRIPTIONS	95
Moosehide Assemblage	95
Sample 4/6/1	95
Sample 27/5/3A	95
Sample 27/5/3B	95
Sample 27/5/5	96
Sample 29/7/3	96
Sample 29/7/4	97
King Solomon Dome Assemblage	97
Samples H-21, H-60, H-62, H-129	97
Sample H-65	98
Sample H-119	98
Sample 20/8/3	99
Sample H-16	99
Sample 26/7/5	100
E.2 CHEMICAL ANALYSES AND NORMATIVE CALCULATIONS	100

LIST OF FIGURES

<u>Figure</u>		<u>Page</u>
1	Regional geologic setting	2
2	Location of study area	3
3	Physiography and sample locations	8
4	Geology of the Dawson area	9
5	Structural elements in the Klondike Series	9
6	Diagrammatic structural section of type section	14
7	Stratigraphic column from type section	14
8	P-T chart of metamorphic conditions	22
9	Frequency variation diagrams for SiO_2 , Al_2O_3 , Fe_2O_3 and FeO	34
10	Frequency variation diagrams for MgO, CaO, Na_2O and K_2O	35
11	K_2O -MgO diagram for the Klondike Formation	36
12	Chemical classification of the Klondike Formation metasedimentary rocks	36
13	MacDonald diagram for volcanogenic samples	39
14	AFM diagram for volcanogenic samples	39
15	Normative plagioclase composition against normative colour index	40
16	Or-Ab-An diagram	40
17	Previous isotopic ages	43
18	Rb-Sr isochron for Klondike Formation metarhyolites	46
19	MacDonald diagram for chlorite schists and amphibolites	50
20	Normative plagioclase composition against Al_2O_3 for chlorite schists and amphibolites	50
21	Normative plagioclase composition against normative colour index for chlorite schists and amphibolites	51
22	Or-Ab-An diagram for chlorite schists and amphibolites	51

<u>Figure</u>		<u>Page</u>
23	Idealized cross section across the Quiet Lake and Finlayson Lake map-areas	55
24	Regional tectonic setting of the Yukon Cataclastic Complex	56
25	Model for formation of the Yukon Cataclastic Complex	57

LIST OF TABLES

<u>Table</u>		<u>Page</u>
1	Equilibrium metamorphic assemblages in the Klondike Formation type section	22
2	Whole rock analyses of the Klondike Formation	25
3	Previous isotopic ages of metamorphic rocks	42
4	Isotopic Analysis - Results	46
A-1	Member 1 - modes	72
A-2	Member 2 - modes	75
A-3	Member 3 - modes	77
A-4	Member 4 - modes	78
A-5	Member 5 - modes	80
A-6	Member 6 - modes	81
A-7	Upper section - modes	82
A-8	Stratigraphic height of samples from type section	83
B-1	Methods, precision and replicability of chemical analyses	85
D-1	Normative analyses of Klondike Formation	91
D-2	Parameter echo for norm calculation program	94
E-1	Normative calculations on greenschists	101
E-2	Parameter echo for norm calculation program	103

Chapter I

INTRODUCTION1.1 PURPOSE OF PRESENT STUDY

The purpose of this study is to investigate the premetamorphic nature of the Klondike Schist. This is predominantly composed of quartz-muscovite-feldspar cataclasite with prominent quartz and feldspar "eyes" and chlorite. The Klondike Schist underlies part of the Yukon Crystalline Terrain in the west-central Yukon Territory (Fig. 1), an area of medium to high-grade metamorphic rocks. This study comprises the petrography, chemistry and Rb-Sr geochronology of the Klondike Schist.

1.2 LOCATION OF AREA AND ACCESS

The Yukon Crystalline Terrain, or Yukon-Tanana Upland, is an upland region, deeply dissected by the Yukon river drainage. It extends southeastwards from Alaska through the west-central and south-central Yukon, merging with the Omenica Crystalline Belt in northern British Columbia (Fig. 1).

The Klondike Schist, in the type area, outcrops to the south and east of Dawson City, in an area bounded by latitudes $63^{\circ}45'N$ and $64^{\circ}05'N$ and by longitudes $138^{\circ}30'W$ and $139^{\circ}45'W$. The location of the area is shown in Figures 1 and 2. The valley of the Tintina Trench, on the northeastern edge of the study area, forms a physiographic and geologic boundary between the Yukon Crystalline Terrain and the Ogilvie Mountains (Plate 1, Fig. 1).

Field work was carried out during the summers of 1978 and 1979, as part of a reconnaissance exploration project for Cominco Ltd. Access to most parts of the area was by truck; the roads in this area are maintained for placer mining and for the tourist industry centred on Dawson City. Outcrops along the Yukon River were visited by boat from Dawson.

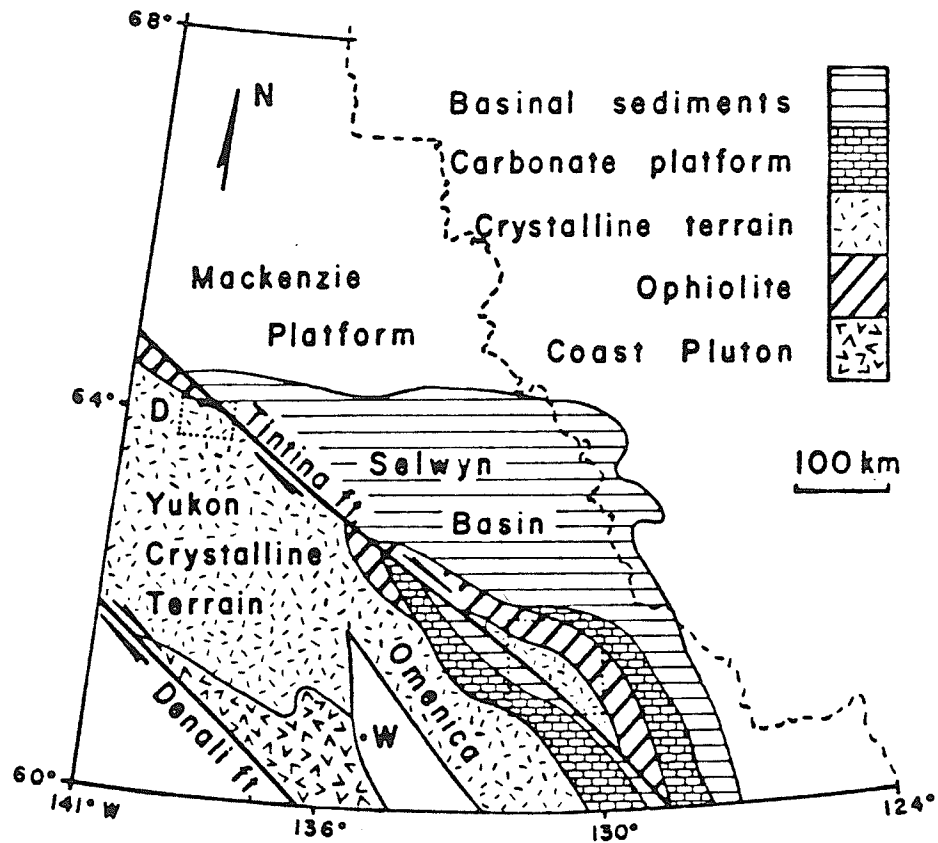


Figure 1. Regional geologic setting. The study area to the south of Dawson City (D) is shown. W = Whitehorse.

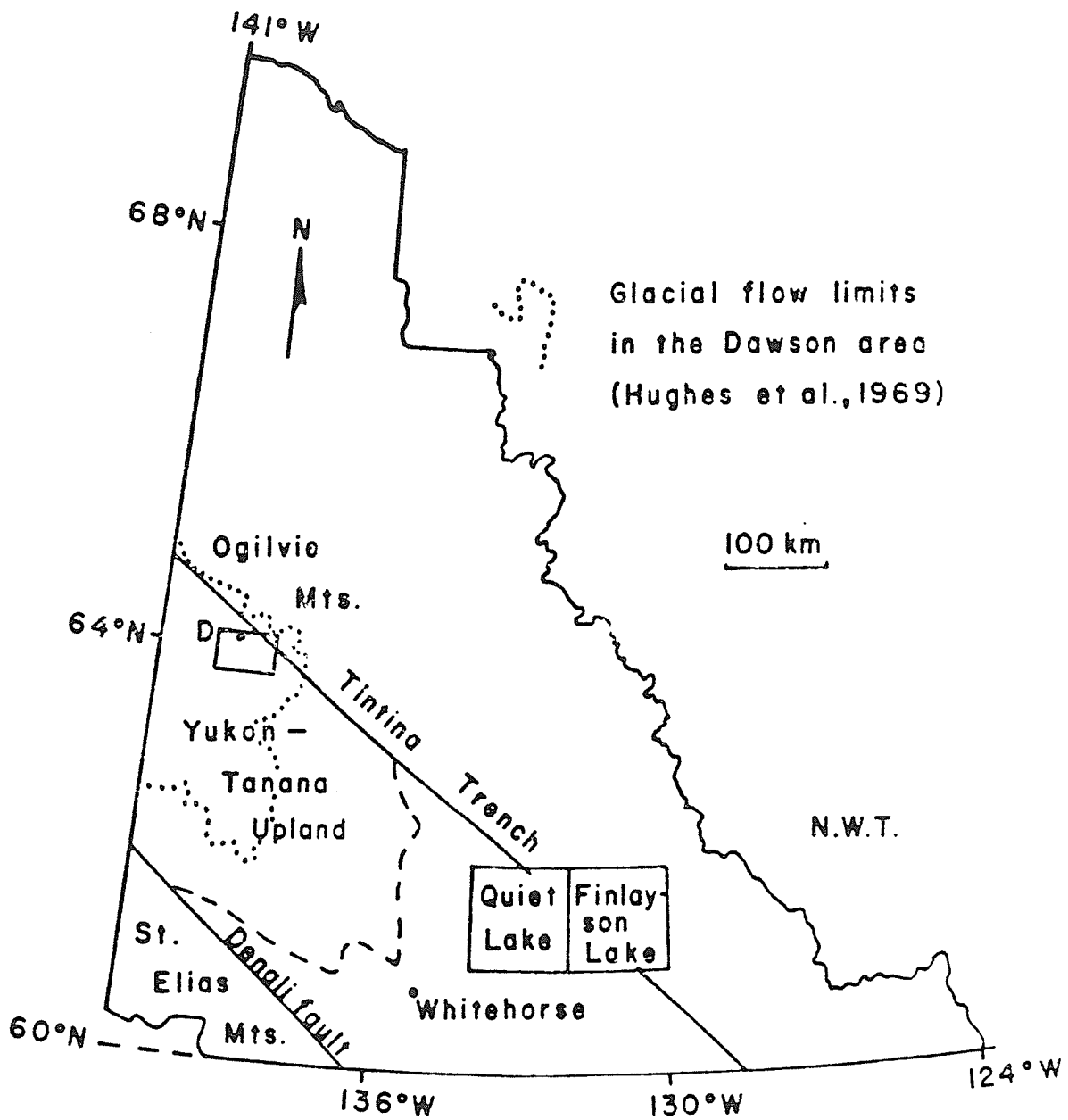


Figure 2. Location of study area to the south of Dawson City (D).
The physiographic boundary of the Yukon-Tanana Upland is shown (dashed line).

1.3 VEGETATION AND OUTCROP

The geography and geomorphology of the area were described by Green (1972). The area was not glaciated, due to low annual precipitation during the last 3 million years (Fig. 2). A large proportion of precipitation is retained as subsurface ice, although true permafrost is present only on north-facing slopes.

Deep weathering of bedrock took place between the early Eocene and Pliocene. Schistose horizons were preferentially weathered. Extensive Pliocene and Quaternary fluvial gravels were deposited in the area; some are auriferous.

Tree line is at an elevation of 900-1000 metres; all but the higher hill-tops are forested. Stunted black spruce and thick moss grow on the north-facing slopes underlain by permafrost; poplar and birch woodland is dominant on south-facing, permafrost-free, slopes.

Outcrops are scarce, comprising only 1% to 2% of the area (Plate 1, Fig. 1) and occur mainly as tors on ridge crests or in the valleys of swiftly-eroding streams and rivers (Plate 1, Fig. 2).

1.4 PREVIOUS STUDIES

McConnell (1890, pp.134-143) was the first to report on the geology of the region, using observations made during an ascent of the Yukon River. Detailed work was carried out in both Alaska and the Yukon Territory, following the discovery of gold in the Klondike area (Spurr, 1898; Spurr and Goodrich, 1898; McConnell, 1905). Many of these early reports, incorporating accounts of the placer and lode gold mining operations, are to be found in a later compilation by Bostock (1957).

McConnell (1905) first proposed the term "Klondike Series" for the quartz-muscovite-feldspar schists forming the bedrock of the placer goldfields. He considered these rocks to be sheared granitic intrusions, distinct from

the structurally underlying metasedimentary schists, to which he gave the name of Nasina Series. The latter are considered as lateral equivalents of Spurr's (1898) Fortymile and Birch Creek Series. McConnell's (1905) Moosehide Diabase was later found in the Sixtymile area (Cockfield, 1921).

Cairnes (1914), Cockfield (1921), Mertie (1937) and Bostock (1942) extended the mapped areas of the Yukon Crystalline Terrain. More recent mapping by Tempelman-Kluit (1974) completed the coverage of the immediate area. Assignment of the metamorphic rocks to the Precambrian by Cairnes (1914) was proved at least partly erroneous by Mertie (1937) on the basis of Devonian fossil assemblages in rocks of the Nasina Series. The structurally overlying Klondike Schist is assumed to be of later origin.

Recent studies in the Klondike (Green, 1972) have questioned McConnell's interpretation of the origin of the Klondike Schist. Green gives petrographic evidence of modal heterogeneity in the unit and suggests that it is of sedimentary origin. Gleeson (1970) conducted a heavy mineral study of the Klondike goldfields. Milner (1977) investigated the geology and geomorphology of the Klondike area in order to define the geomorphological processes leading to the formation of the placer deposits.

K-Ar, U-Pb and Rb-Sr radiometric studies have been conducted over much of the Yukon Crystalline Terrain (Lowdon, 1961, 1962; Lowdon et al., 1963; Leech et al., 1964; Wanless et al., 1965, 1966, 1967, 1968, 1970, 1972, 1978, 1979; Tempelman-Kluit and Wanless, 1975, 1980; leCouter and Tempelman-Kluit, 1976; Morrison et al., 1979). The studies include one K-Ar age from within the study area and several nearby. A detailed review is given in Chapter 5.

Tempelman-Kluit, in a series of papers (1976, 1977b, 1979) has produced a tectonic model which involves the Yukon Crystalline Terrain. His latest studies suggest that the Klondike Schist represents one of a series of allochthons emplaced during an island arc-continent collision. Resetting of the Tintina Trench (Roddick, 1967) places the type area for this model (the

Finlayson Lake area) adjacent to the present study area (Fig. 2). Such conclusions are thus of considerable significance in the interpretation of geological history in the Dawson area.

Chapter II

GENERAL GEOLOGY

The study area was mapped on a scale of 1:50,000 to determine stratigraphy and structure (Figs. 3 and 4). Particular attention was given to the Yukon River area, where exposures were more abundant, and to the King Solomon Dome area where the chlorite-rich members of the Klondike Schist could be examined.

2.1 NASINA SERIES

Structurally the lowermost unit in the Dawson area is the metasedimentary assemblage called the Nasina Series (McConnell, 1905). This is a sequence of graphitic schists, black quartzites and siliceous marbles, with minor chlorite schist and quartz-muscovite schist. The formation has been metamorphosed to grades ranging from upper greenschist to middle amphibolite facies. Higher grade assemblages occur outside the study area. Petrographic study of a siliceous marble revealed development of diopside after tremolite, with a second generation of tremolite replacing the diopside.

The Nasina Series is interpreted as a sedimentary sequence of siliceous limestones, sandstones and black shales, deposited in a quiet continental shelf environment. Limestone predominates in the lower part of the formation. The chlorite schist horizons are interpreted as basaltic volcanics, although detailed petrological studies have not been made. The Nasina succession can be correlated with the Lower Palaeozoic sedimentary succession of the Pelly-Cassiar Platform and Selwyn Basin (Tempelman-Kluit, 1977).

2.2 KLONDIKE SERIES

The Klondike Series comprises leucocratic quartz-feldspar-muscovite schists, commonly bearing fragments or "eyes" of quartz or, less commonly,

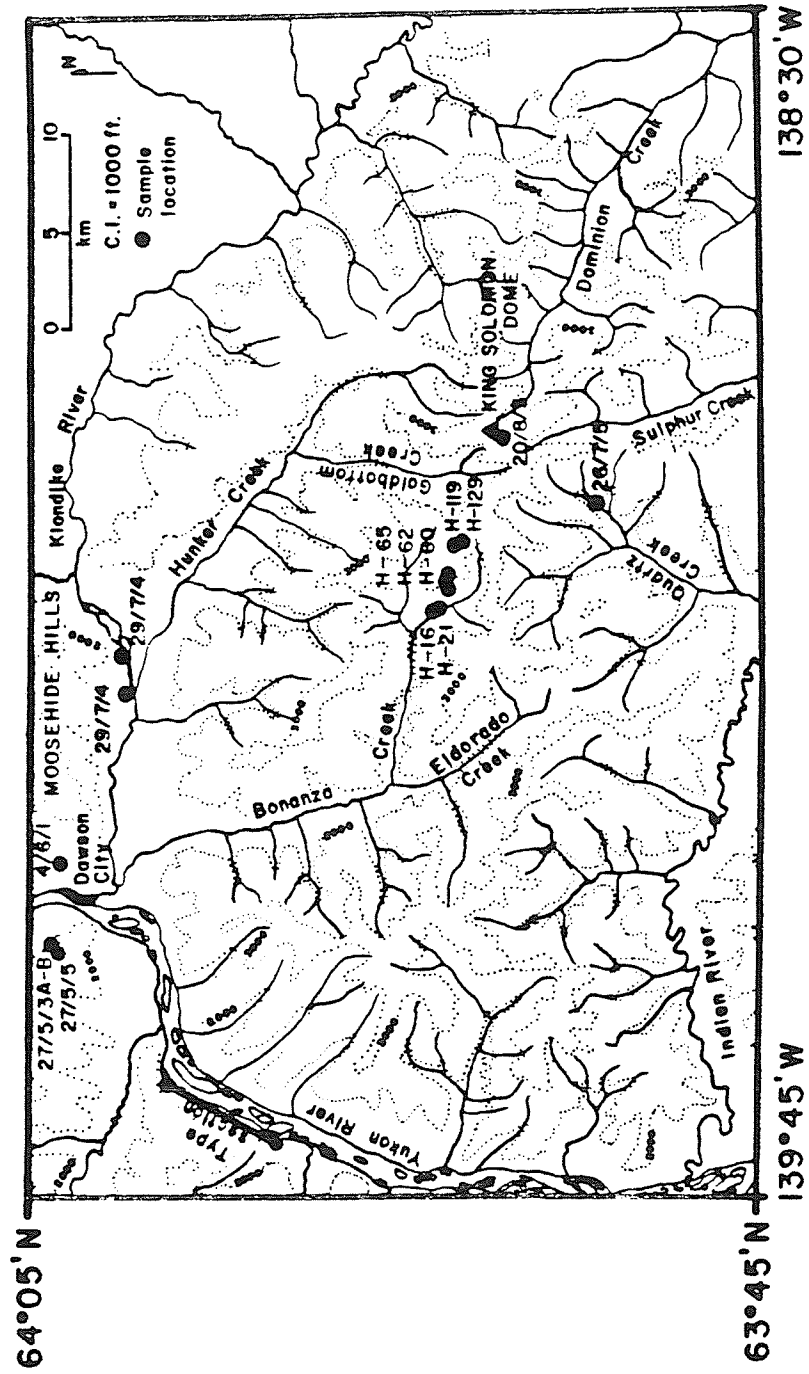


Figure 3. Physiography and sample locations for petrography and chemistry.

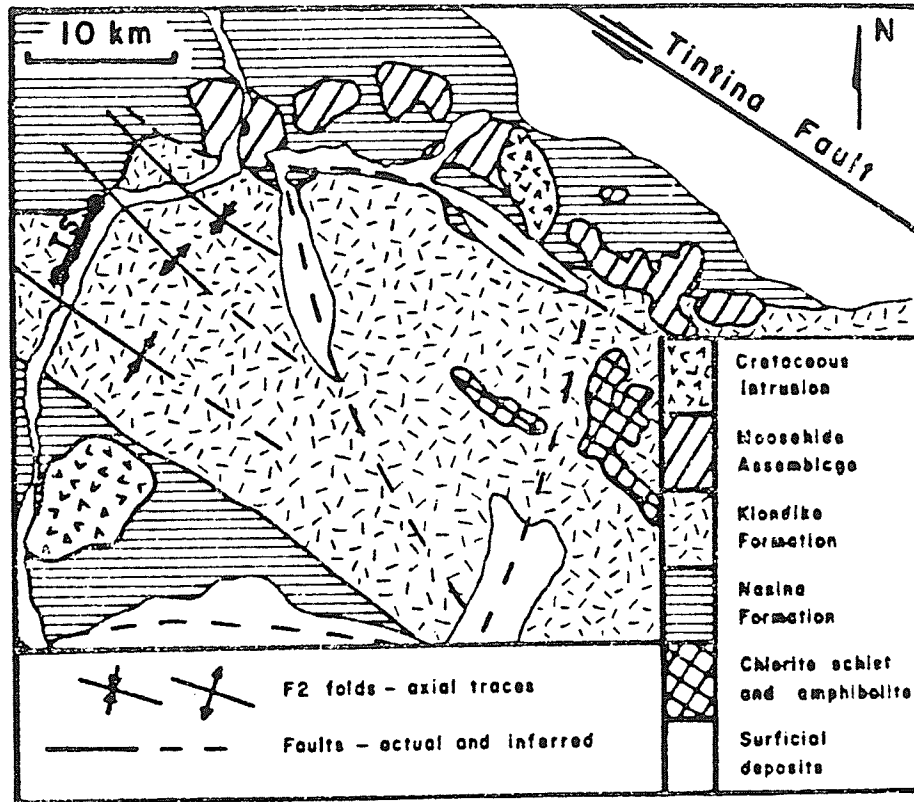


Figure 4. Geology of the Dawson area. TS = Type section.

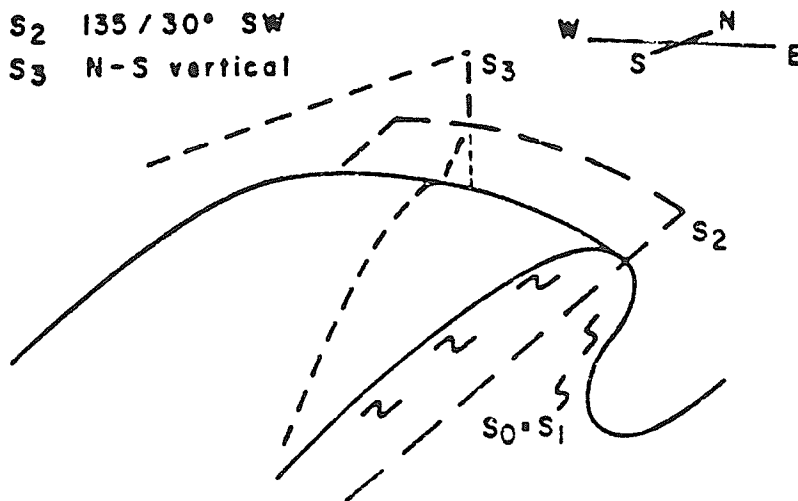


Figure 5. Structural elements in the Klondike Series.

feldspar, as much as 7 mm in diameter. Clast-free lithologies are common; calcareous and graphitic members are rare or absent. The schistosity reflects variations in mica content, hence the application of the term "schist-gneiss unit" to this lithologic type.

The Klondike Series lies with a conformable basal contact upon graphitic schist of the Nasina Series at all contacts examined. The contact itself is possibly a low-angle thrust, as suggested by discordant cleavages in the Nasina graphitic schists. The dip of the contact is of variable steepness, usually to the southwest. The quartz-feldspar-muscovite schists, near King Solomon Dome (Fig. 3) are overlain by amphibolites and chlorite schists spatially associated with a serpentinite body in the right fork of Hunker Creek. All contacts of the quartz-feldspar-muscovite schists with these "greenschists" are masked by surficial deposits; these schists have hitherto been assigned to the Klondike Schist. Lack of outcrop precluded studies of field relationships, but samples were taken from float over the contact in upper Bonanza Creek.

Evidence of an age of deposition is absent for the Klondike Series. Tempelman-Kluit (1976) postulated an Upper Devonian-Lower Mississippian age, based on the age of lithologically similar units elsewhere in the Cordillera. K-Ar isotopic ages, discussed in Chapter 5, indicate a late Triassic metamorphism of the unit, placing a minimum age on the Klondike Series.

Boulders of sheared intrusive rock occur near the head of the right fork of Hunker Creek. Outcrop was absent, but an intrusive margin against chlorite schist and quartz-muscovite schist of the Klondike Series could be inferred from the distribution of abundant float. The intrusion postdates deposition of the Klondike Series; the shearing indicates that it predates at least one of the deformational events. It is possible that the intrusion is part of the Pelly Gneiss of the Triassic Klotassin Suite (Tempelman-Kluit and Wanless, 1980).

2.3 MOOSEHIDE ASSEMBLAGE

McConnell (1905) first defined the assemblage of rocks extending eastward from Moosehide along the north bank of the Klondike River, thence southeastward along the ridge northeast of Hunker Creek (Figs. 3 and 4). His adoption of the name "Moosehide Diabase" for this assemblage has fallen into disuse; nevertheless, the name will be retained for the amphibolites, serpentinites, chlorite schists and talc schists associated with this belt. The name "Moosehide Assemblage" is here applied to these rocks.

Rocks of the Moosehide Assemblage appear to overlie both Nasina and Klondike Series on the ridge northeast of Hunker Creek. Metamorphic grade in both formations increases towards the contact; garnet appears in chloritic members of the Nasina Series and biotite in the more chlorite-rich members of the Klondike Series. The contact itself is masked by lack of outcrop.

The rocks of the Moosehide Assemblage are cataclastically deformed and tectonically mixed. The relationships between lithologies in the area of outcrop were beyond the scope of this study. The Moosehide Assemblage possibly forms part of the Anvil Allochthon of Tempelman-Kluit (1979) and others.

2.4 STRUCTURE

Deformation

Structural elements of the Klondike Series are presented in Figure 5. The F1 event comprised cataclastic deformation of the Klondike Series with development of augen and flaser structures, particularly in more micaceous lithologies. Lepidoblastic micas, dominantly muscovite, define a penetrative S1 cleavage, apparent on a mesoscopic and a microscopic scale. The S1 cleavage is approximately parallel to rarely observed compositional layering in the Klondike Series (Plate 2, Figs. 1-2).

Graphitic phyllites of the Nasina Series occasionally exhibit S0 compositional layering inconsistent with the S1 cleavage (Plate 2, Figs. 3-4). Infrequent shear zones distort both cleavage and compositional layering (Plate 2, Fig. 5). It is possible (Tempelman-Kluit, 1979) that the Klondike Series has been tectonically emplaced on the Nasina Series.

The S0/S1 planes have been deformed penetratively by an F2 event. The F2 folds are isoclinal and overturned, with a northeasterly vergence; their axes strike northwesterly. These folds are apparent on microscopic, mesoscopic and macroscopic scales. An S2 cleavage is defined microscopically by rotation of mica and amphibole crystalloblasts. The S2 cleavage has a northwest-southeast strike and dips southwesterly at 20-50° (Fig. 5). L2 lineations, defined by enrollment of S1, usually plunge at low angles to the southeast.

The latest deformational event was a gentle flexure about a north-south axis. A weak S3 cleavage is defined by graphite in graphitic phyllites of the Nasina Series. Minor fracturing is also associated with this event.

Faults

The fault systems in the area were studied by Milner (1977). Milner identified northwest-trending and northeast-trending fault systems (Figs. 3 and 4). The Hunker Creek, Eldorado and Indian River faults are examples of the former type and the Quartz Creek-Goldbottom Creek "lineament" is an example of the latter type. Both fault types have their traces obscured by surficial deposits. Under these conditions, it is improbable that an accurate estimate of relative movement can be made.

Chapter III

STRATIGRAPHY AND PETROGRAPHY3.1 STRATIGRAPHIC DEFINITION

It is here proposed that the quartzofeldspathic schists hitherto known as the Klondike Series be assigned the status of a formation according to conventional nomenclature (American Commission on Stratigraphic Nomenclature, 1961). Chlorite-bearing schists associated with the unit are tentatively included in the formation at this point. These will be discussed in a later chapter.

3.2 TYPE SECTION

Areal stratigraphic correlation was beyond the scope of this study, due to the scarcity of outcrop (Plate 1, Fig. 1). The author defined a type section to the south of Dawson City, where the Yukon River has cut a gorge through an F2 antiform and synform (Plate 1, Fig. 2). Exposures representative of approximately 3000 m of Klondike Formation above its basal contact were observed (Figs. 6-7). The top of the formation is not exposed. A less complete section of the Klondike Formation is exposed in the inverse flank of the synform, further to the south. A considerable thickness of the underlying Nasina Series is also exposed in this inverse flank.

High-angle faults, striking northwest, transect the type section (Plate 2 Fig. 6). Relative movement, determined in a few localities, showed these to be reverse faults with a throw of 5-10 m. Faults with greater topographic expression and of uncertain throw occur further up the section.

3.3 FIELD OBSERVATIONS

The basal member of the Klondike Formation rests with a conformable basal

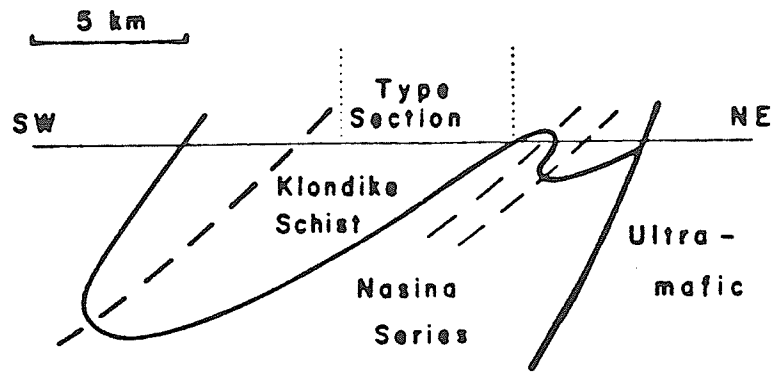


Figure 6. Diagrammatic structural section of type section.

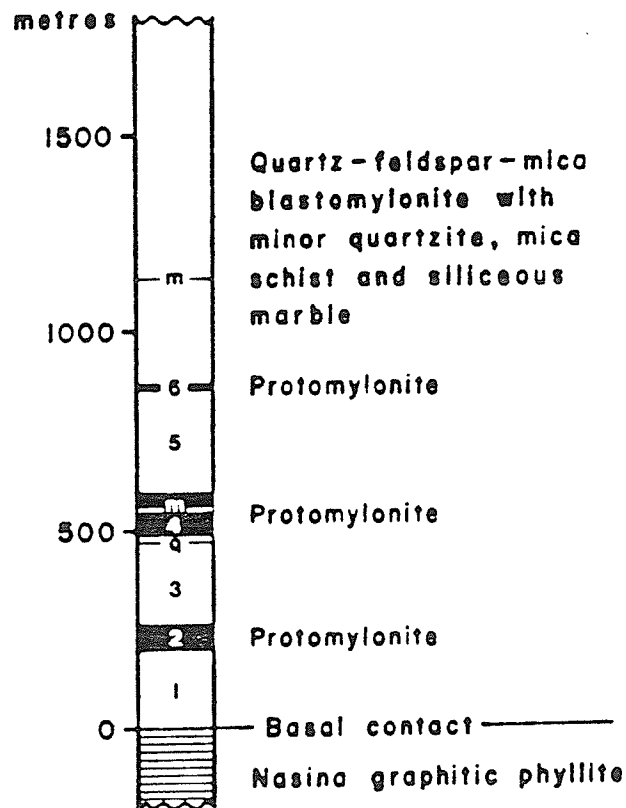


Figure 7. Stratigraphic column from type section. Members are numbered upwards from the base of the formation.
m = siliceous marble, q = ferruginous quartzite.

contact on the Nasina Series (Fig. 7). The contact zone comprises inter-foliated quartz-muscovite schist and graphitic schist over a distance of 20 m. Both lithologies are sheared and weather recessively, hence the contact is partially obscured.

The base of the Klondike Formation comprises white, pale green and blue-green quartz-feldspar-muscovite schists. Quartz and feldspar, as much as 7 mm and 4 mm in diameter respectively, occur in the rocks of the Klondike Formation. Quartz is blue, rounded and more abundant than feldspar. Feldspar grains are white and tabular.

Compositional layering, where observed, is parallel to the S1 cleavage (Plate 2, Figs. 1-2). Small chevron folds of S2 generation, flaser and augen structures are present in rocks of higher mica content. The lenticular augen are as much as 3 cm in length, surrounded by a mica-rich matrix. Three members (2, 4 and 6 of Fig. 7) with lower mica content occur near the base of the section; schistosity is absent and brittle fracturing replaces chevron folding. Irregular 10 m areas of pyrite mineralization were detected by their orange weathering. These areas conform neither to the S1 cleavage, nor to observed compositional layering. They are probably related to Tertiary dolerite dykes which transect the type section.

Samples were taken mostly from members 1 to 6 in the type section because exposure was more continuous and the absence of faults permitted better estimates of stratigraphic height. Less detailed sampling was conducted in the upper part of the exposed section. Table A-8, in Appendix A, contains a detailed list of samples, with their measured stratigraphic height above the base of the formation.

3.4 DETAILED PETROGRAPHY

Petrographic studies were conducted on all samples from the type section. Members within the formation were defined on the basis of petrographic

evidence and field observations. Petrographic descriptions of individual members are presented in Appendix A.

Models were determined by visual estimation and fine-grained feldspars were identified by staining polished sections with cold hydrofluoric acid and a saturated solution of sodium cobaltinitrite.

The Klondike Formation comprises two main lithologic types. The less competent, mica-rich, members are non-volcanogenic blastomylonites (Plate 3, Fig. 1). The three competent mica-poor members, each 10-90 m in thickness, are protomylonites (Plate 3, Fig. 2), with features suggestive of a volcanic origin. The distribution of these lithologies in the type section is shown in Figure 7. Protomylonitic members are absent in the upper part of the section.

Blastomylonites

The typical lithology of the Klondike Formation is a quartz-feldspar-muscovite schist with a blastomylonitic texture and bimodal grain size. The quartz-feldspar-muscovite matrix has a grain size of 0.4 mm; fragment diameters range from 2 to 7 mm. Chlorite is interlaminated with muscovite, giving the rock a greenish hue. Carbonate, epidote, pyrite, iron-titanium oxides and hydroxides are accessory minerals. Modes for each sample of the blastomylonite are presented in Appendix A. Modal composition varies widely as reported by Green (1972).

Matrix

The matrix of a blastomylonite comprises a granoblastic or sutured quartz-sodic plagioclase intergrowth with a penetrative S1 cleavage defined by lepidoblastic micas (Plate 3, Fig. 3). The grain size of the quartz-feldspar intergrowth ranges from 0.2 mm to 0.5 mm; that of the mica, usually muscovite, ranges from 0.3 mm to 1.0 mm. Variation in the grain size of the matrix outlines zones of cataclasis.

The F2 event has folded and fractured muscovite, amphibole and, rarely, feldspar (Plate 3, Fig. 4). Fractures replace folds in rocks of low mica content.

Quartz Fragments

Quartz fragments, as much as 7 mm in diameter (Plate 3, Fig. 5), occur in many samples. They are rounded and tectonically flattened in the plane of the penetrative S1 cleavage. Unrecrystallized fragments exhibit strained extinction. Recrystallized fragments are distinguished from the matrix, with difficulty in some samples, by coarser internal grain size. Recrystallized grain boundaries are straight or sutured (Plate 3, Fig. 5).

The marginal texture of quartz fragments is usually obscured by metamorphic recrystallization but rare, poorly preserved magmatic embayments are observed. It is doubtful whether all quartz fragments are volcanogenic; those exhibiting recrystallization were possibly sandstone, less resistant to metamorphism. Modal fragment content is less than 20%.

Plagioclase

Subhedral plagioclase occurs in some samples. The anorthite content, determined optically, ranges from 3% to 30%. Marginal textures are obscured by a recrystallized rim of clear, more sodic plagioclase. The plagioclase cores are clouded by sericitic alteration.

Compound Fragments

Rare rounded fragments, comprising an equigranular interlocking fabric of plagioclase and quartz, occur in the blastomylonites. The fragment size varies from 0.5 mm to 3 mm. Plagioclase composition, determined optically, ranges from An25 to An35.

Protomylonites

The lower part of the type section includes three protomylonitic members, each 10-90 m in thickness. These comprise a small, but significant, part of the stratigraphic column. Mica contents in all samples are low and many samples have an unrecrystallized fine-grained matrix. Detailed petrography for each member and modes of all samples are presented in Appendix A.

The protomylonitic members are quartz-feldspar protomylonites with accessory muscovite, carbonate, pyrite and iron-titanium oxide. The feldspar is predominantly K-feldspar.

Matrix

The matrices of the protomylonites are variably recrystallized, forming a granoblastic matrix of grain size 0.2 mm to 0.4 mm. Where unrecrystallized, the matrix is fine-grained (0.03 mm - 0.05 mm) and almost isotropic (Plate 4, Figs. 1-2). Relict spherulitic textures occur in some samples (Plate 4, Fig. 3) and rare fragments of devitrified glass are preserved in the pressure shadows of large crystals (Plate 4, Fig. 4).

Muscovite lepidoblasts, 0.3 mm to 0.5 mm, are oriented parallel to the S1 cleavage. Brittle fracturing replaces the F2 folding of S1; the fractures are filled with carbonate and quartz. Carbonate also occurs in stringers parallel to the S1 cleavage, forming as much as 15% of the rock. Iron-titanium oxide and pyrite are disseminated accessory phases.

Quartz Fragments

Rounded quartz fragments, as much as 4 mm in diameter, occur in most samples. These exhibit primary marginal textures, including well-developed magmatic embayments (Plate 4, Figs. 5-6), and are flattened parallel to the S1 cleavage. The embayments frequently contain unrecrystallized matrix with rare spherulites. Less commonly matrix rims the quartz grains.

K-Feldspar

K-feldspar occurs in many of the protomylonites whereas it is rare or absent in the blastomylonites. Euhedral to subhedral crystals are frequently elongate (Plate 5, Fig. 1) but do not exhibit a preferential orientation. They exhibit well-developed magmatic embayments infilled with unrecrystallized matrix (Plate 5, Figs. 2-3). Rarely, the crystals are rimmed with unrecrystallized matrix (Plate 5, Figs. 1 and 4). Feldspar margins are recrystallized to albite (Plate 5, Figs. 3 and 4) and albite is occasionally exsolved (Plate 5, Fig. 5).

Compound Fragments

Fragments of quartz and feldspar (0.5 mm to 3 mm), with an equigranular interlocking texture, are less common in the protomylonites than in the blastomylonites. Where present, they are rimmed with unrecrystallized matrix (Plate 5, Fig. 6). Plagioclase is the common feldspar in these fragments, although microcline was observed. The composition of the plagioclase ranges from An₂₅ to An₃₅.

Ferruginous Quartzites

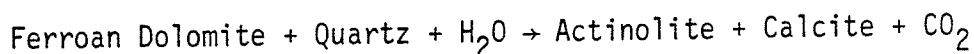
Three 10 cm thick beds of black quartzite occur near the top of member 3. Plate 6, Fig. 1 shows the texture of these rocks. Stringers of iron-titanium oxide grains (0.05 - 0.1 mm) transect a granoblastic matrix of quartz (0.4 mm). Crystoblasts of quartz enclose smaller grains of iron oxide. Aggregates of chlorite and carbonate, as much as 1 mm in diameter, occur infrequently (Plate 6, Fig. 2). These beds are interpreted as metamorphosed ferruginous chert.

The ferruginous quartzites are a significant lithology in the Klondike Foramation, suggesting that chemical sedimentation occurred during deposition of the unit. Their thickness suggests that depositional rates were sufficiently rapid as to preclude formation of significant chemical deposits

in the immediate area.

Calc-Silicate Assemblages

Rocks rich in quartz and carbonate in beds as much as 3 m in thickness occur in the section (Fig. 7). The carbonate present is usually ferroan dolomite, determined by staining with a 9% solution of Alizarin Red and potassium ferricyanide. Siderite is rare. In some samples the reaction:



has taken place. Elsewhere the reaction has reversed, forming pseudomorphs of ferroan dolomite and quartz after amphibole (Plate 6, Fig. 3).

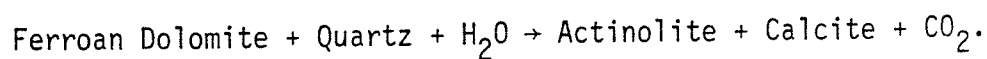
The calcareous rocks are interpreted as thin beds of siliceous marble. Their mode of deposition is unknown.

Metamorphism

Two deformational events are documented on a mesoscopic and microscopic scale. Metamorphic equilibrium assemblages for the associated metamorphic events are listed in Table 1. The metamorphic history of the Nasina Series, although similar, is inadequately documented.

The first recorded event in the Klondike Formation comprised cataclasis, leading to the development of augen and flaser structures 1 - 10 cm in length. Strain was concentrated in micaceous lithologies, hence the mica-poor protomylonites escaped severe cataclasis.

M1 metamorphism comprised recrystallization of granoblastic quartz and lepidoblastic muscovite, chlorite and biotite, forming an S1 cleavage. The grade of metamorphism is documented by the assemblage actinolite + calcite + quartz in calcareous assemblages. Actinolite may have been formed by the reaction:



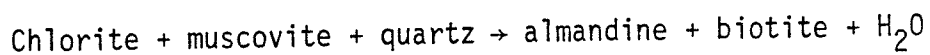
Saturated conditions are assumed with respect to water and carbon dioxide.

Talc does not form part of the metamorphic assemblage. This implies a high activity of carbon dioxide during metamorphism (Winkler, 1979, p.119).

Constraints for the F1 event are provided by the stable coexistence of the assemblage biotite-chlorite- muscovite. Staurolite and garnet are absent, indicating that neither pressure nor temperature rose above conditions expected for greenschist facies metamorphism.

A later F2 event folded the S1 cleavage and fractured mica, feldspar and amphibole in the matrix. M2 petrograde metamorphism, possibly related to F2, is indicated by the assemblage ferroan dolomite-quartz after actinolite and by the appearance of chlorite after biotite. Plagioclase is peripherally albitized (Plate 5, Fig. 4). Actinolite and biotite are preserved in the higher levels of the section. Fracturing of competent members, with later carbonate filling occurred.

Mineral assemblages were used to estimate P-T conditions during metamorphism. Actinolite and biotite are present and the coexistence of chlorite and muscovite was observed (Plate 6, Fig. 4), indicating low pressure metamorphism in the upper greenschist facies (Fig. 8). This possibility is further supported, in micaceous blastomylonites, by the absence of garnet, which would form from the reaction:



at pressures greater than 4-5 kb (Winkler, 1979, pp.220-221). The equilibrium curve for this phase change, being sensitive to garnet composition, is not presented here.

The observed deformational events, F1 and F2, can be correlated with the M1 and M2 metamorphic events. Uninterrupted recrystallisation and formation of S1 cleavage suggests that M1 metamorphism outlasted F1 deformation. Fs bending of M2 pseudomorphs after actinolite suggests that M2 and F2 were synchronous.

Table 1

Equilibrium Metamorphic Assemblages in the Klondike Formation Type Section

Lithology	M1	M2
Protomylonite	K - fsp + mu ± cc	K - fsp + mu ± cc
Blastomylonite	Mu + chl ± ep ± cc	Mu + chl ± ep ± cc
Micaceous blastomylonite	Mu + chl + bi ± ep	Mu + chl ± ep
Calcareous blastomylonite	Mu + act + cc ± ep	Mu + dol ± ep
Ferruginous quartzite	Chl + ep + cc	Chl + ep ± cc

All assemblages + (albite + quartz + Fe-Ti oxide)

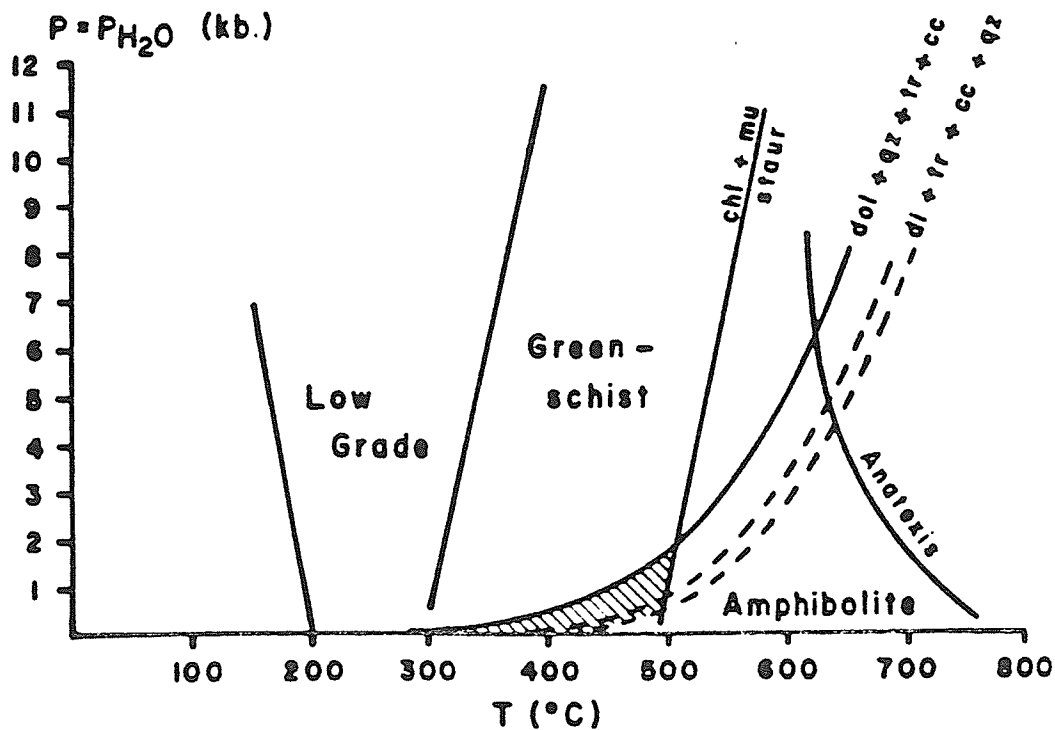


Figure 8. P-T chart of metamorphic conditions. The shaded area defines the probable region of conditions experienced by the Klondike Formation.

3.5 SUMMARY OF PETROGRAPHY

The Klondike Formation, herein defined, is a sequence of leucocratic blastomylonite schists with minor protomylonitic members. The latter retain primary textures indicative of volcanic origin, owing to concentration of deformational strain in the enclosing micaceous blastomylonitic members.

Textural studies indicate that the formation was initially subjected to cataclasis: recrystallization of phyllosilicates formed an S1 cleavage parallel to observed compositional layering. Refolding during a second deformation kinked and fractured the S1 cleavage.

Mineral assemblages indicate that the Klondike Formation was metamorphosed in a thermal gradient of approximately $70^{\circ}\text{C km}^{-1}$ to upper greenschist facies during M1. Subsequent thermal retrograde metamorphism has occurred.

Thin beds of ferruginous quartzite in the lower part of the section are possibly chemical sedimentary deposits. Rapid deposition of clastic sediments in this area precluded formation of extensive chemical deposits.

Chapter IV

CHEMISTRY OF THE KLONDIKE FORMATION4.1 ANALYTICAL RESULTS

Fifty-six samples were selected for analysis from the type section. All had been subjected to petrographic studies (Chapter III). Nine samples, from the "greenschists" of King Solomon Domes and from the Moosehide Assemblage, were also analysed; these are discussed in Chapter VI. All samples were analysed for major elements and for MnO, S, P₂O₅, Ba, Rb, Sr and Cs. The analytical procedure is described in Appendix B. Analyses for the Klondike Formation are presented in Table 2.

4.2 TREATMENT OF ANALYTICAL RESULTS

Major oxides are presented in frequency variation diagrams (Figs. 9 and 10). The purpose of these diagrams is to detect any bimodality in chemical composition.

Silica and alumina distributions are unimodal and skewed, silica negatively, alumina positively. The erratic distribution of iron-oxide concentrations reflects leaching by surface processes.

The major alkali and alkaline-earth oxides are plotted on Figure 10. CaO is positively skewed; carbonate veins and stringers noted in the samples suggest that the calcium is, at least in part, derived and is therefore an unsafe criterion upon which to base a classification. Na₂O is negatively skewed.

MgO and K₂O both exhibit clearly bimodal distributions. A plot of K₂O against MgO (Fig. 11) shows that the protomylonites are separated from the remainder of the samples. This chemical separation reflects the relative abundance of K-feldspar in the protomylonites and the presence of chlorite interfoliated with muscovite in the blastomylonites. It is apparent that

Table 2
Whole Rock Analyses of Klondike Formation

Member	1	1	1	1	1	1
Sample	14/8/1	14/8/2	14/8/5	14/8/9	14/8/14	16/8/7
SiO ₂	75.90	73.85	69.75	84.85	78.90	75.10
Al ₂ O ₃	12.67	14.20	16.28	7.48	10.94	10.22
Fe ₂ O ₃	1.20	0.85	1.27	0.74	1.27	0.92
FeO	0.40	0.48	0.48	0.56	0.20	0.36
CaO	0.05	0.03	0.02	0.45	1.21	2.94
MgO	1.14	0.81	1.84	0.69	0.65	2.34
Na ₂ O	3.48	5.30	2.52	2.62	1.68	0.82
K ₂ O	3.20	2.60	5.21	1.04	2.16	2.14
TiO ₂	0.16	0.18	0.22	0.10	0.23	0.17
P ₂ O ₅	0.01	0.01	0.02	0.02	0.01	0.04
MnO	0.02	0.01	0.02	0.02	0.02	0.03
S	0.041	0.018	0.009	0.005	0.020	0.081
CO ₂	0.09	0.06	0.11	0.98	1.14	2.64
H ₂ O ⁺	-	-	-	-	-	-
H ₂ O	1.49	1.29	2.15	0.89	1.52	2.00
Total	99.85	99.69	99.90	100.45	99.95	99.80
Ba (%)	0.195	0.162	0.320	0.073	0.181	0.171
Rb (ppm)	119	102	184	55	100	81
Sr (ppm)	31	44	44	71	70	54

- = Not Analyzed

Table 2 (continued)

Member	1	1	1	2	2	2
Sample	16/8/10	18/8/11	16/8/12B	14/8/15	16/8/1	16/8/2
SiO ₂	74.40	71.40	76.60	77.70	71.55	80.30
Al ₂ O ₃	12.65	15.06	12.57	12.58	10.36	10.95
Fe ₂ O ₃	0.93	1.37	0.87	0.26	-	0.10
FeO	0.46	0.46	0.20	0.32	0.36	0.08
CaO	1.41	0.39	1.04	0.06	5.58	0.13
MgO	2.13	3.06	1.39	0.07	0.07	0.08
Na ₂ O	1.45	2.33	1.08	2.27	1.88	2.10
K ₂ O	2.84	2.91	2.72	5.78	4.78	5.22
TiO ₂	0.16	0.18	0.17	0.10	0.12	0.10
P ₂ O ₅	0.01	0.03	0.05	0.02	0.02	0.00
MnO	0.02	0.02	0.02	0.01	0.10	0.01
S	0.000	0.000	0.000	0.005	0.003	0.014
CO ₂	1.30	0.38	1.05	0.20	4.65	0.12
H ₂ O+	-	-	-	0.61	0.38	0.55
H ₂ O	2.15	2.35	2.00	0.65	0.43	0.61
Total	99.91	99.94	99.76	100.03	99.90	99.81
Ba (%)	0.155	0.188	0.121	0.225	0.182	0.183
Rb (ppm)	88	108	175	161	147	136
Sr (ppm)	76	13	41	56	112	43

Table 2 (continued)

Member	2	2a	2a	2	2	2
Sample	16/8/12A	16/8/14	16/8/15C	16/8/15A	16/8/16	16/8/17A
SiO ₂	74.65	74.40	58.75	70.90	75.20	77.25
Al ₂ O ₃	13.36	13.98	20.10	15.67	13.06	11.66
Fe ₂ O ₃	0.57	0.61	2.14	0.06	0.38	0.38
FeO	0.40	0.52	1.28	0.40	0.20	0.10
CaO	0.30	0.86	0.81	0.15	0.84	1.03
MgO	0.14	0.46	2.68	0.31	0.09	0.04
Na ₂ O	1.40	2.39	0.25	2.67	2.32	2.01
K ₂ O	8.73	3.99	9.12	7.52	6.53	5.92
TiO ₂	0.15	0.12	0.26	0.17	0.12	0.13
P ₂ O ₅	0.00	0.02	0.10	0.06	0.02	0.01
MnO	0.02	0.02	0.04	0.01	0.03	0.03
S	0.007	0.017	0.018	0.024	0.119	0.078
CO ₂	0.24	0.82	0.85	0.22	0.73	0.87
H ₂ O ⁺	0.58	-	-	0.92	0.48	0.36
H ₂ O	0.65	1.45	3.41	0.98	0.53	0.40
Total	100.65	99.66	99.81	99.14	100.17	99.91
Ba (%)	0.234	0.373	0.242	0.291	0.207	0.208
Rb (ppm)	190	109	462	182	163	103
Sr (ppm)	44	59	27	35	56	59

Table 2 (continued)

Member	3	3	3a	3	4	4
Sample	25/8/3	25/8/4	25/8/5B	25/8/5C	25/8/6	25.8/7
SiO ₂	70.05	82.50	78.40	85.10	72.65	78.60
Al ₂ O ₃	15.64	8.44	10.96	6.26	14.16	11.12
Fe ₂ O ₃	1.47	0.82	2.06	1.07	1.56	1.53
FeO	0.30	0.48	0.36	0.10	0.60	0.48
CaO	0.44	1.39	0.40	1.45	0.74	0.93
MgO	2.36	0.69	1.09	0.51	2.04	0.41
Na ₂ O	0.18	1.54	1.05	2.05	2.25	0.08
K ₂ O	6.45	1.52	3.10	0.92	2.98	3.93
TiO ₂	0.19	0.21	0.27	0.18	0.36	0.33
P ₂ O ₅	0.04	0.02	0.04	0.03	0.05	0.05
MnO	0.02	0.02	0.02	0.03	0.03	0.03
S	0.003	0.074	0.000	0.000	0.000	0.010
CO ₂	0.44	1.16	0.38	1.31	0.45	0.74
H ₂ O ⁺	-	-	-	-	-	-
H ₂ O	2.51	1.07	1.66	0.88	1.89	1.63
Total	100.09	99.93	99.79	99.89	99.76	99.87
Ba (%)	0.339	0.065	0.229	0.028	0.167	0.099
Rb (ppm)	228	74	108	125	108	127
Sr (ppm)	54	89	31	32	68	48

Table 2 (cont'd)

Member	4	4	4	4	4a	4
Sample	26/8/1	26/8/2	26/8/3	26/8/4	26/8/5	26/8/6
SiO ₂	79.00	77.60	77.90	75.10	78.00	77.60
Al ₂ O ₃	11.04	11.24	11.02	11.74	11.36	11.58
Fe ₂ O ₃	0.39	0.49	0.55	1.41	0.72	0.65
FeO	0.90	0.58	0.64	0.72	0.98	0.50
CaO	0.28	0.16	1.35	0.58	0.58	0.80
MgO	0.25	0.08	0.34	0.38	2.08	0.29
Na ₂ O	0.75	0.17	1.43	1.43	1.63	1.98
K ₂ O	6.24	8.28	5.51	6.02	2.42	5.13
TiO ₂	0.06	0.09	0.06	0.13	0.10	0.05
P ₂ O ₅	0.02	0.14	0.02	0.01	0.02	0.00
MnO	0.02	0.03	0.04	0.01	0.02	0.01
S	0.037	0.026	0.007	0.078	0.036	0.100
CO ₂	0.34	0.16	1.10	1.32	0.38	0.77
H ₂ O ⁺	0.82	0.76	0.79	0.87	-	0.65
H ₂ O	0.89	0.90	0.85	0.95	1.86	0.71
Total	100.22	99.95	100.82	99.88	100.19	100.17
Ba (%)	0.183	0.225	0.185	0.255	0.076	0.260
Rb (ppm)	146	164	148	130	76	104
Sr (ppm)	52	66	79	66	66	59

Table 2 (continued)

Member	4	4	4	4	4b	5
Sample	26/8/7	26/8/9	27/8/1A	27/8/1B	27/8/1C	27/8/2
SiO ₂	72.50	78.60	72.20	75.65	63.90	76.70
Al ₂ O ₃	12.56	10.77	13.46	11.66	13.17	12.24
Fe ₂ O ₃	0.75	0.40	0.20	0.48	1.47	1.20
FeO	0.26	0.38	0.18	0.62	0.88	0.76
CaO	1.50	0.50	1.65	1.75	5.52	1.20
MgO	0.18	0.19	0.15	0.41	2.14	0.82
Na ₂ O	0.80	0.42	1.50	1.78	0.04	3.27
K ₂ O	9.13	7.35	8.59	5.27	6.14	2.08
TiO ₂	0.06	0.04	0.07	0.07	0.06	0.13
P ₂ O ₅	0.00	0.02	0.01	0.00	0.02	0.00
MnO	0.01	0.02	0.02	0.02	0.07	0.02
S	0.750	0.082	0.026	0.007	0.018	0.064
CO ₂	1.91	0.56	1.34	1.36	4.35	0.40
H ₂ O+	0.36	0.62	0.38	0.83	-	-
H ₂ O	0.42	0.67	0.41	0.93	2.23	1.18
Total	100.83	100.00	99.81	100.01	100.01	100.06
Ba (%)	0.270	0.185	0.184	0.222	0.175	0.240
Rb (ppm)	180	129	141	133	252	69
Sr (ppm)	86	46	79	79	159	171

Table 2 (continued)

Member	6		Upper section			
Sample	27/8/3A	27/8/4	27/8/5	27/8/6	27/8/7	27/8/8
SiO ₂	75.90	66.05	77.45	66.05	71.85	69.90
Al ₂ O ₃	12.96	14.33	12.20	15.12	13.36	14.92
Fe ₂ O ₃	0.35	1.72	1.16	2.58	2.33	2.28
FeO	0.34	2.78	0.40	2.36	1.12	1.12
CaO	0.49	3.44	0.56	3.21	1.21	2.50
MgO	0.24	3.49	1.06	2.09	1.14	1.45
Na ₂ O	0.83	1.83	2.70	1.19	2.86	1.38
K ₂ O	8.16	2.79	2.64	3.78	2.96	3.49
TiO ₂	0.11	0.68	0.22	0.76	0.57	0.54
P ₂ O ₅	0.00	0.15	0.02	0.17	0.08	0.08
MnO	0.03	0.09	0.02	0.08	0.07	0.07
S	0.024	0.044	0.002	0.151	0.101	0.123
CO ₂	-	0.25	0.27	0.50	0.84	0.64
H ₂ O+	0.54	-	-	-	-	-
H ₂ O	0.61	2.15	1.12	2.28	1.45	1.83
Total	100.04	99.79	99.82	100.32	99.94	100.32
Ba (%)	0.290	0.220	0.140	0.285	0.301	0.175
Rb (ppm)	106	119	111	117	100	106
Sr (ppm)	66	129	72	340	61	189

Table 2 (continued)

Member	Upper section					
Sample	27/8/9	27/8/10	27/8/11	27/8/12	27/8/13	27/8/14
SiO ₂	76.10	75.65	73.65	73.10	73.60	75.05
Al ₂ O ₃	11.76	132.6	14.04	13.42	13.84	14.02
Fe ₂ O ₃	1.07	1.27	1.96	1.46	0.80	1.43
FeO	0.88	0.60	0.32	1.04	0.36	0.44
CaO	0.68	0.16	1.65	0.59	0.54	0.20
MgO	1.28	0.68	0.75	0.92	1.02	0.56
Na ₂ O	2.35	3.10	2.42	4.62	3.00	4.98
K ₂ O	3.02	3.78	3.42	2.44	3.60	2.01
TiO ₂	0.44	0.18	0.25	0.37	0.10	0.09
P ₂ O ₅	0.06	0.01	0.02	0.06	0.01	0.09
MnO	0.03	0.02	0.03	0.03	0.02	0.03
S	0.007	0.030	0.054	0.019	0.012	0.063
CO ₂	0.90	0.19	0.27	0.64	0.50	0.28
H ₂ O ⁺	-	-	-	-	-	-
H ₂ O	1.22	0.92	1.09	1.17	1.24	0.91
Total	99.80	99.85	99.92	99.88	98.64	100.15
Ba (%)	0.185	0.234	0.313	0.166	0.220	0.255
Rb (ppm)	89	99	112	69	109	68
Sr (ppm)	66	44	96	72	56	50

Table 2 (continued)

Member	Upper section	
	Sample	27/8/15
SiO ₂	70.30	74.35
Al ₂ O ₃	12.84	12.06
Fe ₂ O ₃	3.46	0.68
FeO	1.00	1.62
CaO	0.82	0.36
MgO	1.29	2.49
Na ₂ O	3.43	4.00
K ₂ O	3.20	1.70
TiO ₂	0.74	0.48
P ₂ O ₅	0.12	0.08
MnO	0.05	0.05
S	0.031	0.007
CO ₂	0.72	0.08
H ₂ O+	-	-
H ₂ O	1.44	1.54
Total	99.44	99.50
Ba (%)	0.065	0.050
Rb (ppm)	106	51
Sr (ppm)	79	38

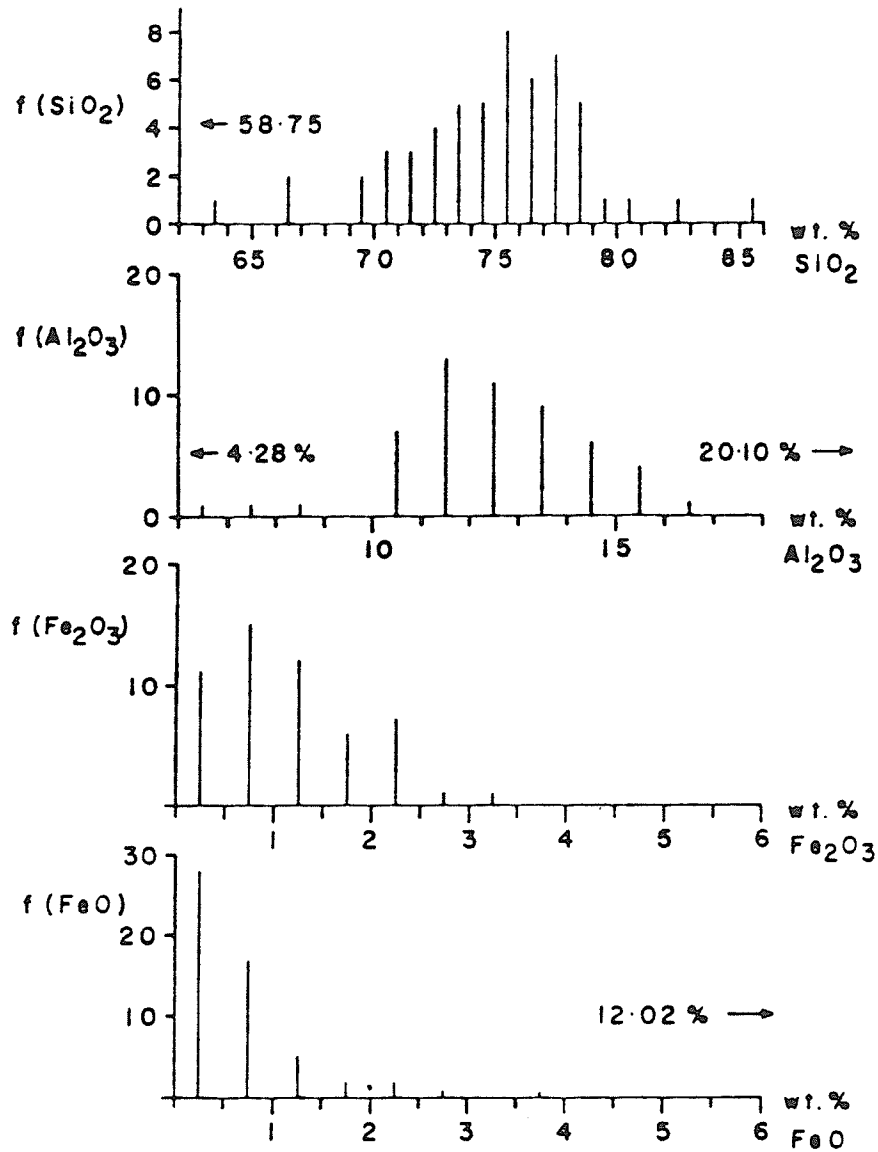


Figure 9. Frequency variation diagrams for SiO_2 , Al_2O_3 , Fe_2O_3 and FeO . Frequencies expressed in number of samples. Values with arrows indicate sample falling outside compositional field of diagram.

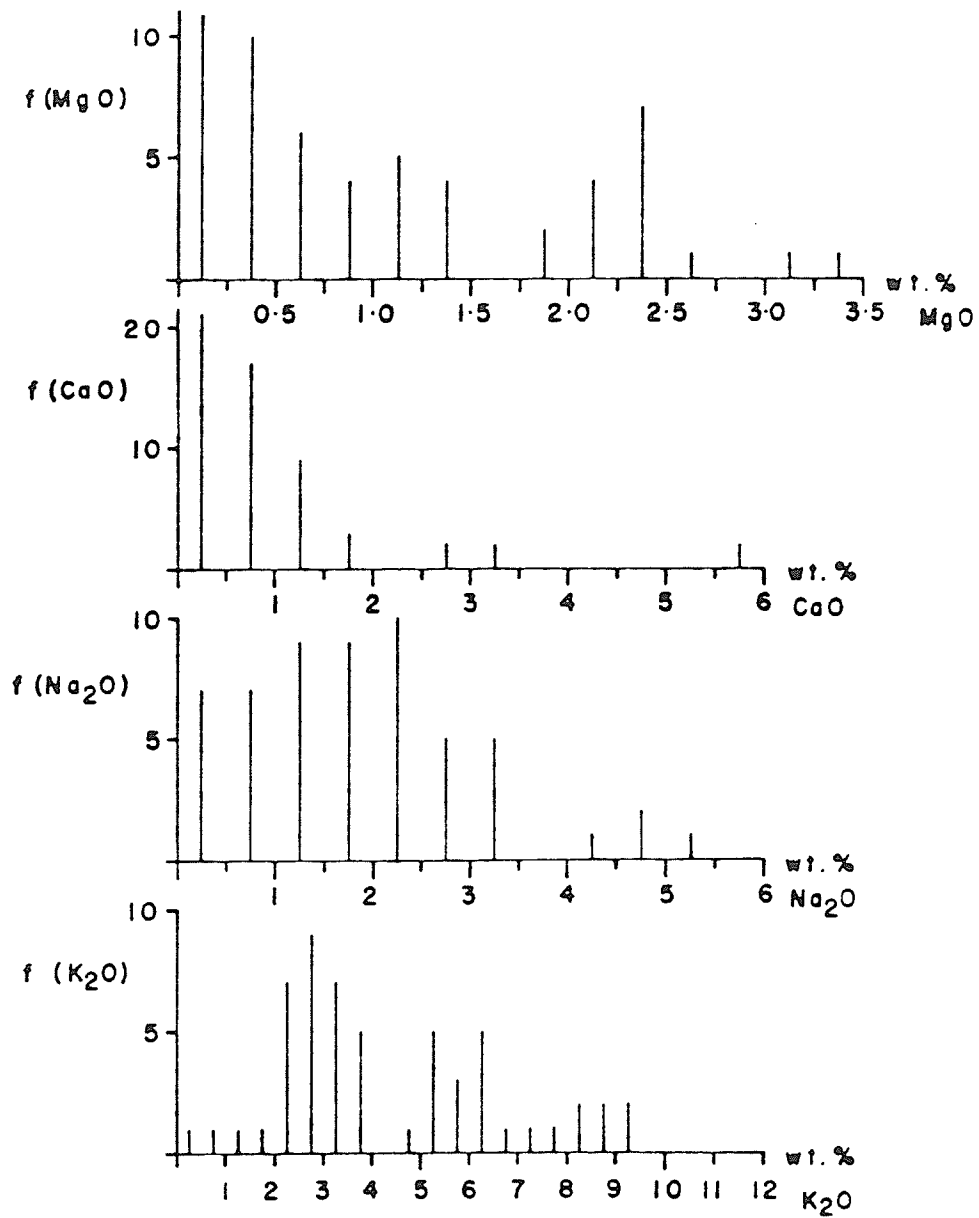


Figure 10. Frequency variation diagrams for MgO, CaO, Na₂O and K₂O. Frequencies expressed in number of samples.

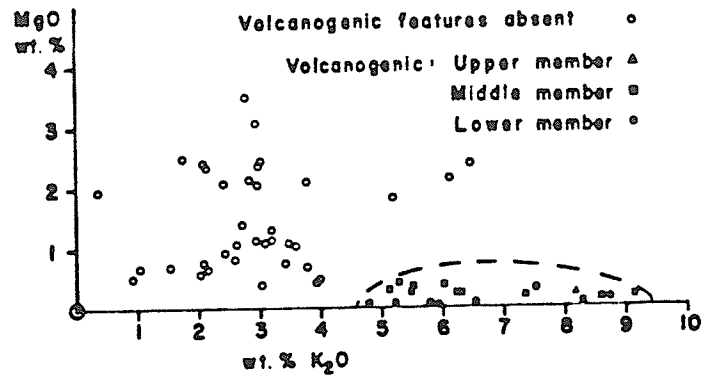


Figure 11. K₂O-MgO diagram for the Klondike Formation. The volcanogenic members (2, 4 and 6) plot separately from the blastomylonites.

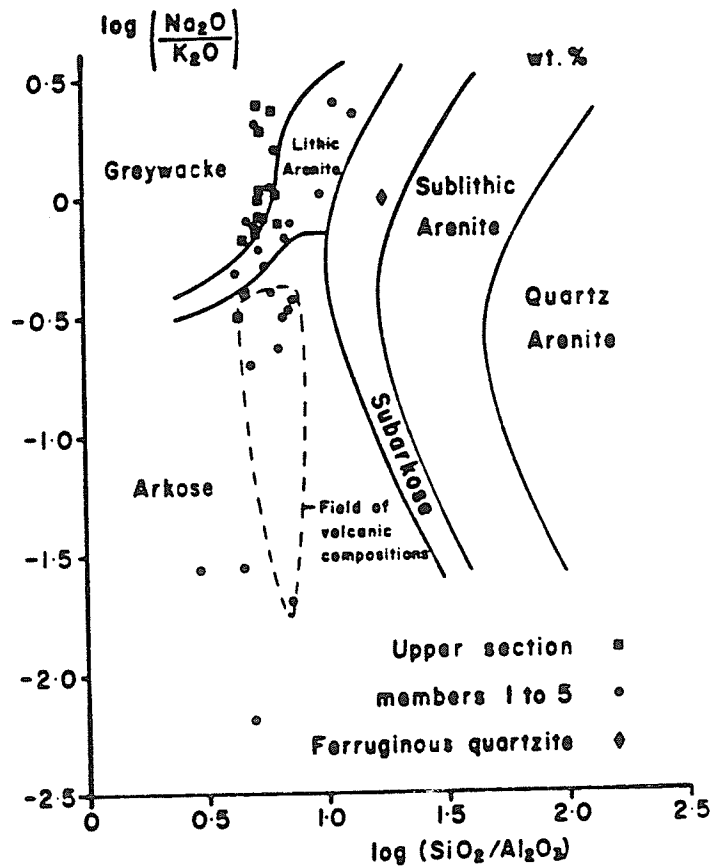


Figure 12. Chemical classification of Klondike Formation metasedimentary rocks (after Pettijohn et al., 1973). The compositional field of the Klondike Formation metavolcanic rocks is shown for comparison. "Upper section" refers to section lying above

those members of the Klondike Formation exhibiting textures suggestive of a volcanic origin are also distinguishable chemically from the rest of the formation. The K_2O - MgO plot is not reliable where metavolcanics have a slightly higher content of Mg minerals. This method is, therefore, useful only with felsic volcanics.

An attempt was made to classify the metasedimentary members of the Klondike Formation, using a plot of $\log (SiO_2/Al_2O_3)$ against $\log (Na_2O/K_2O)$, after Pettijohn et al. (1973). The plot is shown in Figure 12, with the compositional field of the volcanics added for comparison. The metasedimentary samples of the Klondike Formation plot in a trend from arkose through lithic arenite to the greywacke field, away from the compositional range of the volcanic rocks. This suggests that the metasedimentary rocks were derived from rocks similar to the metavolcanics, suffering leaching of potassium and progressive admixture of magnesian clay minerals to produce the chemical bimodality.

Members 2, 4 and 6 of the Klondike Formation appear to be metavolcanic units, distinguishable from the enclosing blastomylonites by their petrographic and chemical characteristics. Samples from these members were classified on the basis of normative composition, using a conventional system of nomenclature (Irvine and Baragar, 1971).

Normative analyses were carried out on 19 chemical analyses from the metavolcanic members, using the RENORM computer programme. This programme was designed for rapid application of the Irvine and Baragar classification to any suite of volcanic rocks. A brief description of the programme is presented in Appendix C, with a list of the parameter configurations used. Six runs were made.

The results from Run 3 are presented in Appendix D, beneath the appropriate chemical analyses. Figures 13 to 16 document the classification process. Figure 13 assigns the suite to the subalkaline family, Figure 14 to the calc-

alkaline series. Figures 15 and 16 assign a name and chemical series to each sample. Tie lines indicate the variance in classification introduced by significant amounts of carbonate. It is probable that the carbonate, and therefore the calcium, is secondary; CO_2 was therefore assigned as a permitted component in the norm calculation. The author concludes that the protomylonitic members are volcanics of rhyolitic composition, with a low initial calcium concentration.

4.3 SUMMARY OF CHEMISTRY

The protomylonitic members of the Klondike Formation are chemically distinct from the enclosing blastomylonites and are interpreted as calc-alkaline rhyolites, potassium-poor, in a succession of quartzofeldspathic sediments with minor ferruginous quartzites. The quartzofeldspathic sediments are classified chemically as ranging from arkoses to greywackes and are possibly derived from the metarhyolites or chemically equivalent rocks.

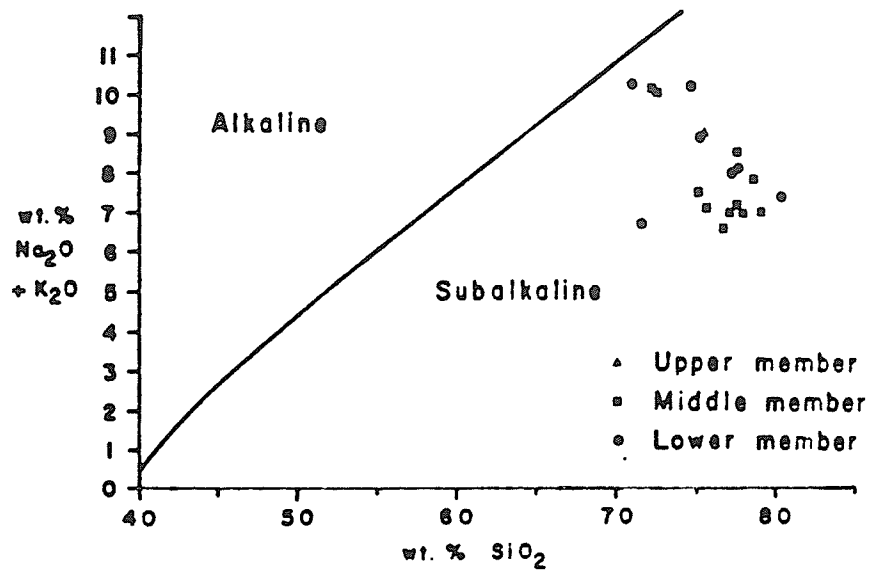


Figure 13. MacDonald diagram for volcanogenic samples.

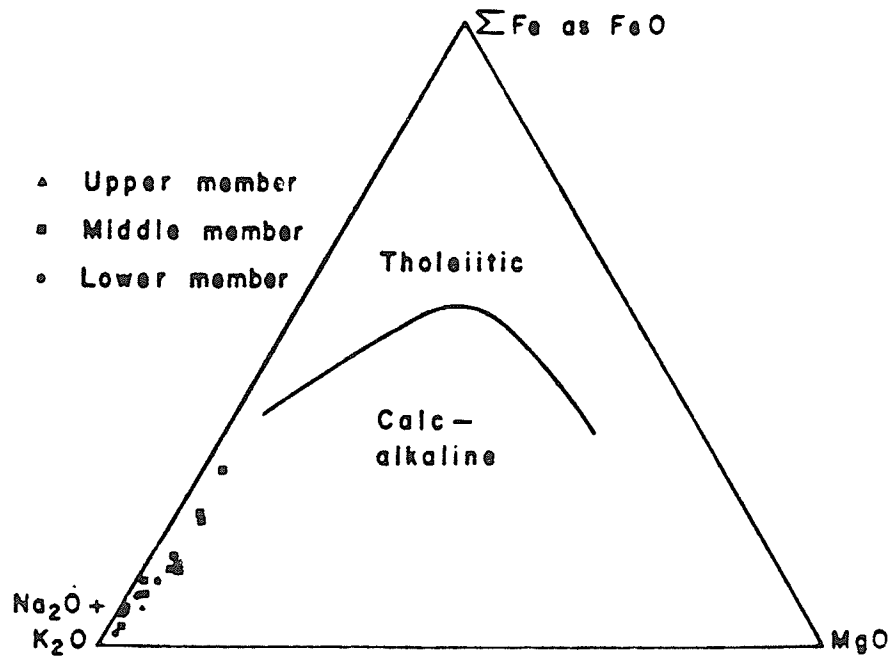


Figure 14. AFM diagram for volcanogenic samples. Plots in weight percent.

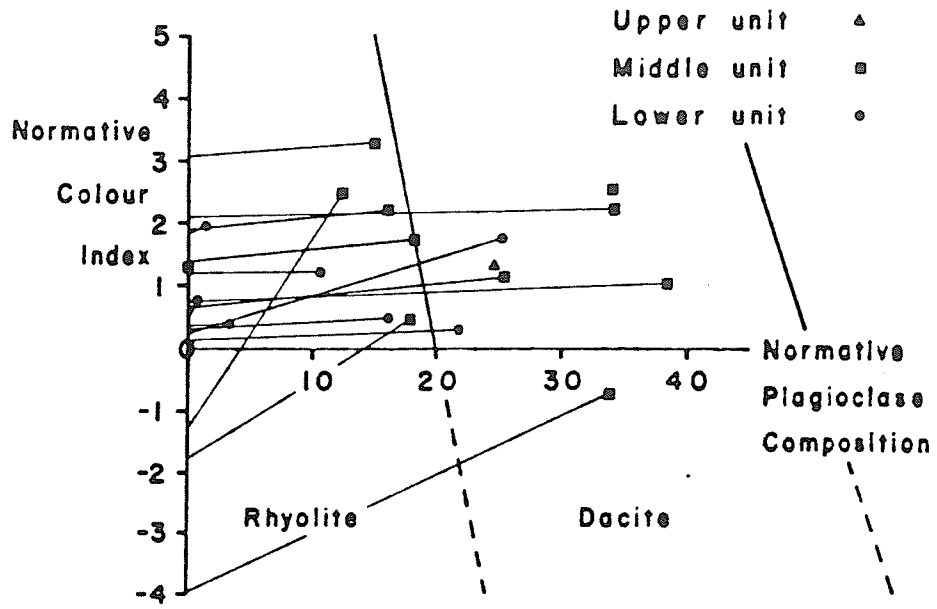


Figure 15. Normative plagioclase composition against normative colour index. Plots in cation percent.

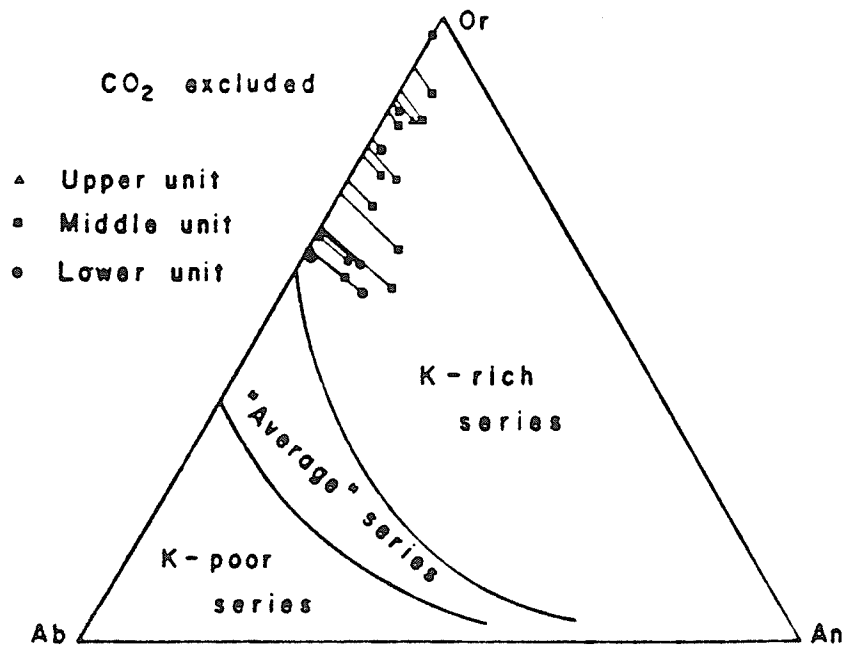


Figure 16. Or-Ab-An diagram. Plots in cation percent.

Chapter V

ISOTOPIC STUDIES5.1 PREVIOUS STUDIES

K-Ar isotopic ages hitherto reported for igneous and metamorphic rocks in the Yukon Crystalline Terrain (Lowdon, 1961, 1962; Lowdon et al., 1963; Leech et al., 1964; Wanless et al., 1965, 1966, 1967, 1968, 1970, 1972) are summarised in Tempelman-Kluit and Wanless (1975). Two further publications (Wanless et al., 1978, 1979) present further K-Ar data. The results of Rb-Sr and U-Pb studies are presented, respectively, by leCouteur and Tempelman-Kluit (1976) and Tempelman-Kluit and Wanless (1980). In addition, an Rb-Sr isotopic age on metamorphic rocks is included in a study of the Clinton Creek asbestos mine (Htoon, 1979).

Isotopic ages obtained for metamorphic rocks of the Yukon Crystalline Terrain are listed in Table 3. Sample locations are plotted on Figure 17. Results from the plutonic rocks are too numerous to be listed here; the reader is referred to the appropriate paper for a more comprehensive treatment.

Isotopic studies using the U-Pb method indicate a diversity in ages for the 'Pelly Gneiss' unit. Several units have been, inadvertently, assigned to this unit as reported by Tempelman-Kluit and Wanless (1980) and it is questionable as to whether the name 'Pelly Gneiss' is still valid. U-Pb zircon ages obtained for two of the three samples are Lower and Middle Palaeozoic, considerably greater than K-Ar dates from the same samples. The third age is a Triassic age, from a sample of the Klotassin Suite.

K-Ar ages from metamorphic and plutonic rocks in the Yukon Crystalline Terrain define three thermal events (Tempelman-Kluit and Wanless, 1975). These are related to the intrusion of three generations of plutons; the "pink quartz monzonite" suite (160-170 Ma), the Coffee Creek quartz monzonite

Table 3

Previous Isotopic Ages of Metamorphic Rocks

Location	Lithology	Method	Age (Ma)	Ref ¹
63°47'30"N 140°28'00"W	Gneissic biotite-quartz monzonite with K-feldspar augen (Pelly Gneiss)	Bi Zr	98±4 375±6	1 2
63°54'00"N 138°52'00"W	Quartz-muscovite schist (Klondike Schist)	Mu	138±11	1
61°17'00"N 138°07'00"W	Plagioclase-biotite-garnet schist (Kluane Schist)	Bi	140±11	1
61°14'00"N 136°57'00"W	Quartz-biotite schist (Biotite Schist unit)	Bi	147±12	1
62°47'30"N 138°16'15"W	Strongly foliated biotite granodiorite (Pelly Gneiss)	Bi Zr	164±6 276±5	1 2
62°55'30"N 138°27'20"W	Biotite-muscovite schist (Pelly Gneiss)	Mu Bi	168±6 137±5	1 1
62°46'45"N 138°18'30"W	Strongly foliated biotite- muscovite-quartz diorite (Pelly Gneiss)	Bi Mu	161±6 160±6	1 1
64°07'00"N 140°48'00"W	Quartz-muscovite schist (Klondike Schist)	Bi	175±14	1
62°53'30"N 138°51'00"W	Quartz-feldspar-biotite hornblende gneiss (Pelly Gneiss)	Bi Hb	187±10 181±28	1 1
63°06'45"N 139°29'30"W	Biotite-muscovite granodiorite gneiss (Pelly Gneiss)	Bi Mu	182±8 178±7	1 1
64°02'00"N 140°23'20"W	Foliated biotite granodiorite (Pelly Gneiss)	Bi	202±16	1
64°25'00"N 140°40'00"W	Quartz-muscovite schist, quartz-biotite-muscovite schist, "greenstone" and amphibolite	Rb Mu Hb Hb	256±22 245±8 278±10 191±7	3 3 3 3

Bi = K-Ar Biotite
Mu = K-Ar Muscovite
Hb = K-Ar Hornblende

Zr = U-Pb Zircon
Rb = Rb-Sr Whole rock

¹ References: 1 = Tempelman-Kluit and Wanless, 1975
2 = Tempelman-Kluit and Wanless, 1980
3 = Htoon, 1979



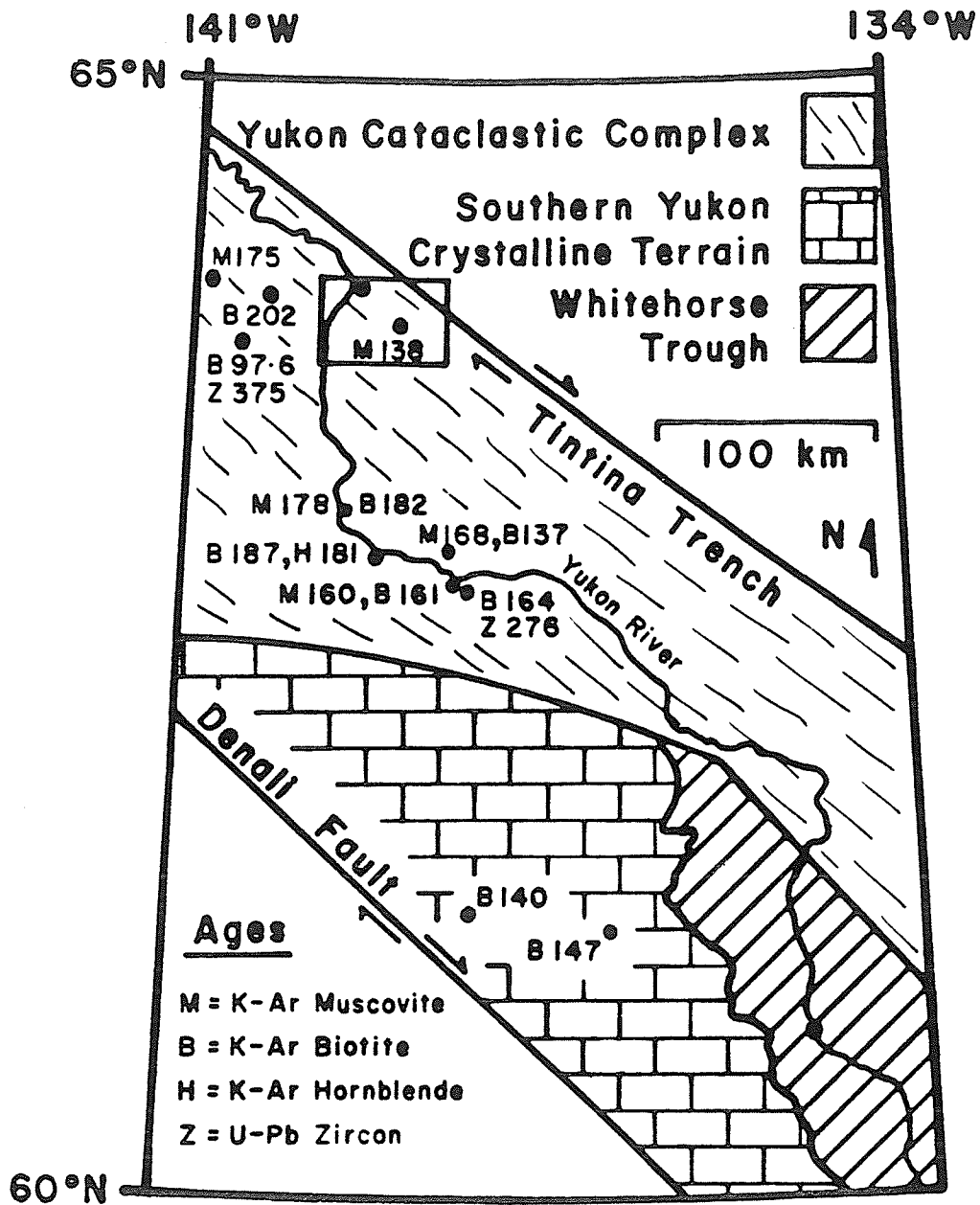


Figure 17. Previous isotopic ages of metamorphic rocks in the Yukon Cataclastic Complex, from Tempelman-Kluit and Wanless (1975).

(90-100 Ma) and the Nisling Range Alaskite (50-60 Ma). Later isotopic studies on the intrusive rocks, using the Rb-Sr method (LeCouteur and Tempelman-Kluit, 1976; Morrison et al., 1979), confirmed these ages and suggested an age of emplacement of 190 Ma for the Klotassin quartz diorite.

5.2 ISOTOPIC AGE OF THE KLONDIKE FORMATION METARHYOLITES

Rb-Sr isotopic studies were conducted on the Klondike Formation, as part of the present study, to determine an age of formation for the unit. Seven samples were selected from the metavolcanic members in the type section (Fig. 7). All had been petrographically and chemically analyzed and appeared least altered of the samples examined.

Isotopic Analysis

A detailed account of chemical preparation is given in Appendix B. Briefly, the samples were digested in hydrofluoric and nitric acids, then spiked with solutions of standard isotopic composition. The spiked samples were homogenized in 6.2N HCl. Rb was removed from samples for Sr analysis by passing these through ion exchange columns. All samples were evaporated to dryness.

The mass spectrometry is described in detail by Cheung (1978). Isotopic measurements were made on a triple filament, single focusing, mass spectrometer having a 25 cm radius tube and a 90° sector magnet. Signals were measured using a Cary VRE (model 401) and recorded with an HP model 5326B timer-counter DVM.

Rb and Sr concentrations were determined by isotope dilution mass spectrometry and $^{87}\text{Sr}/^{86}\text{Sr}$ ratios were measured on spiked samples. During the study, several analyses of the E and A SrCO₃ standard (lot 492 327) gave an average value of 0.7083 ± 0.0003 (one sigma) for the $^{87}\text{Sr}/^{86}\text{Sr}$ ratio when normalized to an $^{86}\text{Sr}/^{88}\text{Sr}$ value of 0.1194.

On the basis of replicate determinations on samples and standards, the errors used in calculating the ages and initial ratios are 0.8% for the $^{87}\text{Rb}/^{86}\text{Sr}$ ratios and 0.07% for the $^{87}\text{Sr}/^{86}\text{Sr}$ ratio (one sigma). Errors quoted for the age and initial ratio are at the one sigma level. The age was calculated using the method of York (1966) from the REGROSS programme of Brookes et al. (1972). An ^{87}Rb decay constant of $1.42 \cdot 10^{-11} \text{yr}^{-1}$ (Steiger and Jager, 1977) was used in the age calculation.

Analytical Results

Isotopic compositions and concentrations for each sample are presented in Table 4. Figure 18 is a plot of $^{87}\text{Rb}/^{86}\text{Sr}$ against $^{87}\text{Sr}/^{86}\text{Sr}$. Statistical regression of the data gives an age of 202 ± 11 Ma and an initial $^{87}\text{Sr}/^{86}\text{Sr}$ ratio of 0.7140 ± 0.0001 . The mean square of weighted deviates is 0.83, indicating that this line is an isochron.

5.3 DISCUSSION

The age obtained here for the Klondike Formation is in reasonable agreement with previously reported K-Ar ages. The high initial ratio for the suite indicates that the age is one of metamorphism, rather than an age of formation and probably marks the end of cataclasis and greenschist facies metamorphism.

An estimate of an age of formation can be made if it is assumed that isochemical metamorphism took place, with redistribution of isotopes. The isochron can therefore be rotated about an estimated mean value of 8 for $^{87}\text{Rb}/^{86}\text{Sr}$ to an assumed initial $^{87}\text{Sr}/^{86}\text{Sr}$ for continental arc rhyolites of 0.704 (Carmichael et al., 1974). The rotation point at 8 is a mean value of $^{87}\text{Rb}/^{86}\text{Sr}$ for the entire suite of metarhyolite samples. An age of formation of 290 Ma is thereby derived.

It is possible that some redistribution of elements has taken place.

Table 4
Isotopic Analysis: Results

Sample number	Rb (ppm)	Sr (ppm)	$\frac{87\text{Rb}}{86\text{Sr}}^1$	$\frac{87\text{Sr}}{86\text{Sr}}^2$
26/8/6	118.88	76.07	4.5250	0.7268
26/8/7	213.49	87.60	7.0625	0.7350
26/8/9	163.06	56.87	8.3122	0.7376
27/8/1A	190.78	88.82	6.2686	0.7320
27/8/1B	175.14	87.76	5.7814	0.7307
27/8/3A	141.00	75.44	5.4178	0.7289
16/8/1	165.86	121.32	3.9583	0.7258

1. Atomic ratio
2. Normalized to an $^{86}\text{Sr}/^{88}\text{Sr}$ ratio of 0.1194.

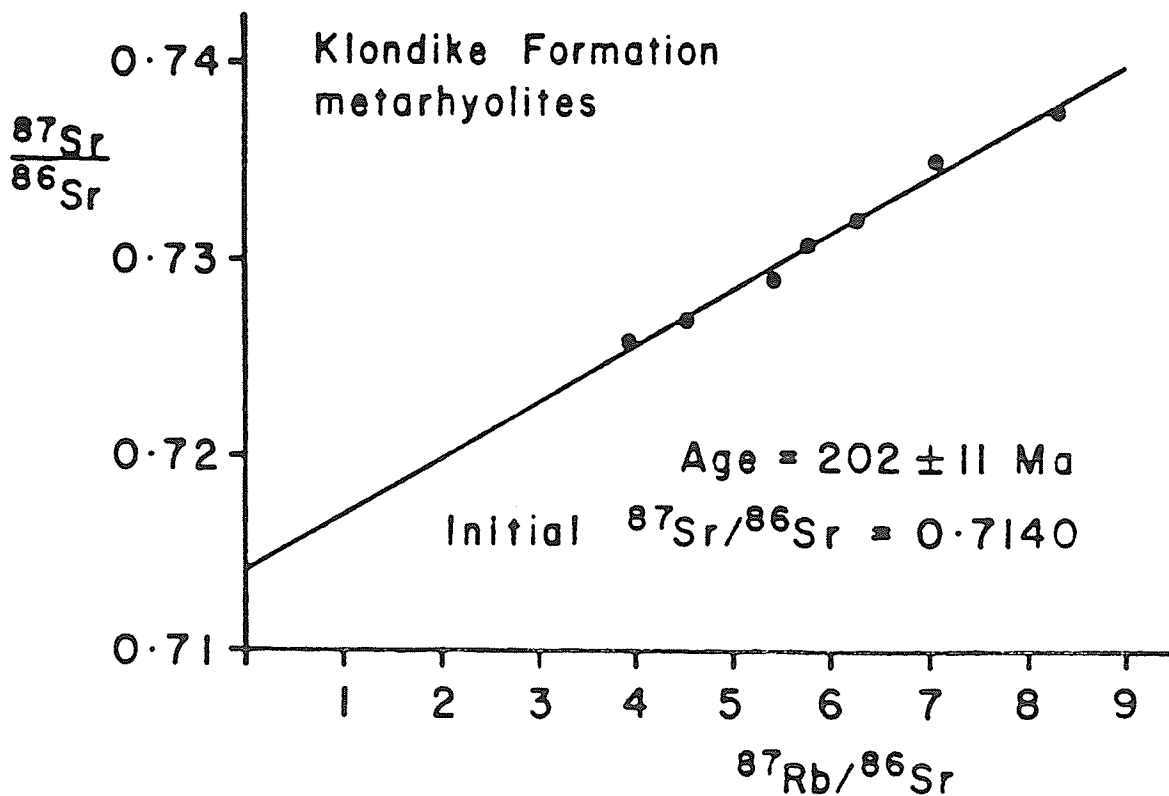


Figure 18. Rb-Sr isochron for Klondike Formation metarhyolites.

The erratic distribution of carbonate in samples and the skewed distribution of Ca suggests that extraneous Ca, and therefore Sr, was introduced during the course of metamorphism. Brooks et al. (1969) showed that vein calcite can have a small but significant affect on $^{87}\text{Sr}/^{86}\text{Sr}$ for a sample suite. Samples low in carbonate have a mean $^{87}\text{Rb}/^{86}\text{Sr}$ value of 11; an estimated primary age of 265 Ma would result from rotation about this point.

Isotopic analysis of the Klotassin suite of intrusive rocks yielded an initial $^{87}\text{Sr}/^{86}\text{Sr}$ of approximately 0.707 (Tempelman-Kluit and Wanless, 1975). In a later paper Tempelman-Kluit (1979) suggested that the Klotassin suite and Klondike Formation are genetically related; accordingly, the isochron was rotated to an initial value of 0.707. The mean for all 19 samples of the metarhyolite suite and for the low carbonate metarhyolites was used; the ages obtained were 260 Ma and 250 Ma respectively.

5.4 SUMMARY

Rb-Sr isotopic analysis of the Klondike Formation metarhyolites gave an isochron age of 202 ± 11 Ma, interpreted as an age of metamorphism. Rotation of this isochron to an assumed initial $^{87}\text{Sr}/^{86}\text{Sr}$ of 0.704 resulted in an age of 290 Ma, possibly an age of formation. The minimum age of the unit is 260 Ma. Rotation to an initial value of 0.707 yielded ages of 260 Ma and 250 Ma for the suite and low-carbonate samples, respectively.

The metamorphic age and estimated primary ages are consistent with published isotopic ages and geological age estimates. This is the first Rb-Sr whole rock age to be reported for stratigraphically coherent rocks of the Klondike Formation.

Chapter VI

CHLORITE-ACTINOLITE SCHIST ASSEMBLAGES

Assemblages in the study area which contain appreciable amounts of chlorite are of particular interest with regard to current theories of Cordilleran evolution (e.g. Tempelman-Kluit, 1979). Two "greenstone" assemblages were identified in the study area: a) the ultramafic rocks and associated amphibolites and chlorite schists of the Moosehide Assemblage and b) the chlorite-actinolite schists of King Solomon Dome and upper Bonanza Creek. The latter assemblage has hitherto been classified as part of the Klondike Schist.

6.1 MOOSEHIDE ASSEMBLAGE

The Moosehide Assemblage comprises chlorite-actinolite schists, talc schists, amphibolites and serpentinites (after McConnell, 1905). Field relationships are discussed in Chapter II. The assemblage overlies the Klondike Formation and Nasina Series on the ridge northeast of Hunker Creek (Figs. 3 and 4). The contact is marked by recrystallization of micas and the appearance of garnet in both of the underlying units.

Several samples were collected from localities along the north bank of the Klondike River (Fig. 3). Poor outcrop and extensive deformation of the assemblage precluded adequate stratigraphic control. The number of samples was inadequate for a detailed petrologic study but sufficed to gain general knowledge of the lithologies within the assemblage.

Six petrographic descriptions and four whole rock chemical analyses from a representative suite are presented in Appendix E. Norms were calculated using the RENORM computer programme.

Petrographic studies show that the rocks are part of a sheared and hydrated assemblage of mafic igneous rocks. The serpentinite comprises

unsheared pseudomorphs of antigorite after mafic minerals, indicating that hydration persisted beyond the cessation of deformation (Plate 7, Fig. 1). The pseudomorphs are separated by shear zones filled with sheared antigorite and chrysotile. The serpentinite is normatively a tholeiitic hartzburgite. Cataclastic amphibolites have the texture and mineralogy of metagabbros and metabasalts (Plate 7, Fig. 2). Actinolite has relict cores of uralitic hornblende. Plagioclase, where determined, is andesine. The amphibolites are normatively tholeiitic basalts (Figs. 19-22). A banded, quartz-rich chlorite schist is interpreted as a metasedimentary rock.

It is concluded that the Moosehide Assemblage is a metamorphosed tholeiitic assemblage of hartzburgite-gabbro-basalt-chloritic sediment, cataclastically sheared and probably overthrust upon the Klondike Formation and Nasina Series. The assemblage is structurally complex, and thus poorly understood, but it is possibly related to the Anvil Allochthon of Tempelman-Kluit (1979).

6.2 CHLORITE-ACTINOLITE SCHIST OF KING SOLOMON DOME

Green (1972) noted the presence of chlorite schist members in the Klondike Formation. Milner (1977) described a band of chlorite schist and amphibolite, with a weak magnetic signature, crossing the watershed from Hunker and Goldbottom Creeks into upper Bonanza Creek. Field work in the area indicates that the chlorite schists usually dip gently to the southwest or are flat-lying, forming ridge tops in the vicinity of King Solomon Dome (Figs. 3 and 4). Contacts with the Klondike Formation are not exposed but are possibly vertical in places, flat-lying in others.

Sample locations are shown on Figure 3. Petrographic descriptions, chemical analyses and normative calculations are presented in Appendix E.

Petrographic studies show that most of the samples are plagioclase-actinolite-chlorite schists with accessory epidote and iron-titanium oxide

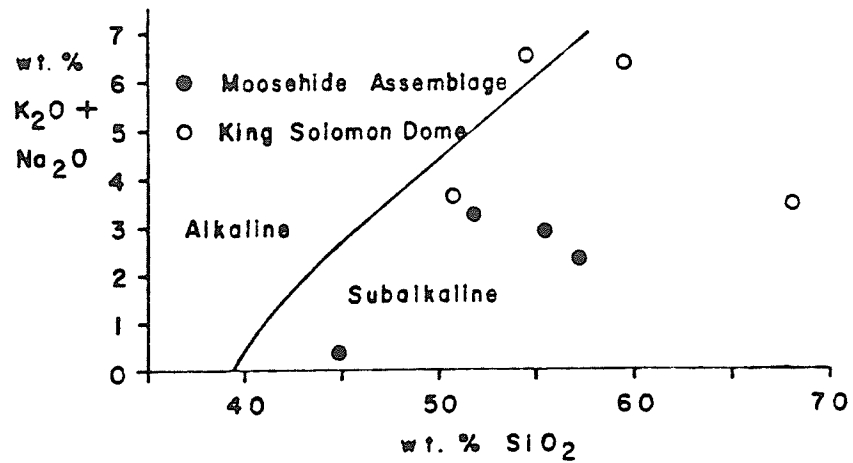


Figure 19. MacDonald diagram for chlorite schists and amphibolites.

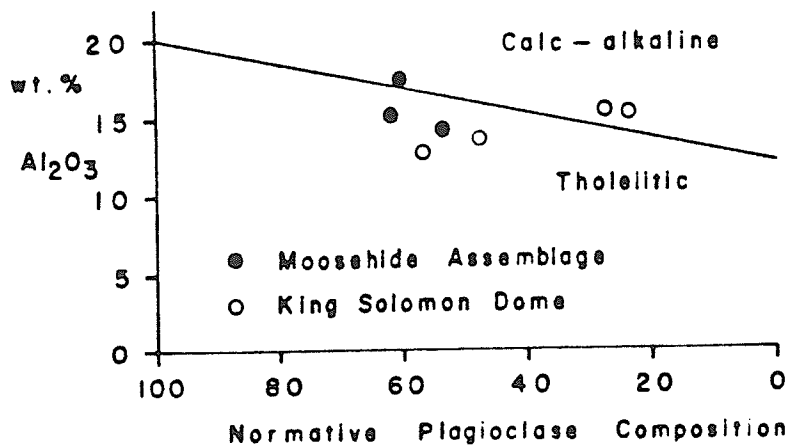


Figure 20. Normative plagioclase composition against Al_2O_3 for chlorite schists and amphibolites.

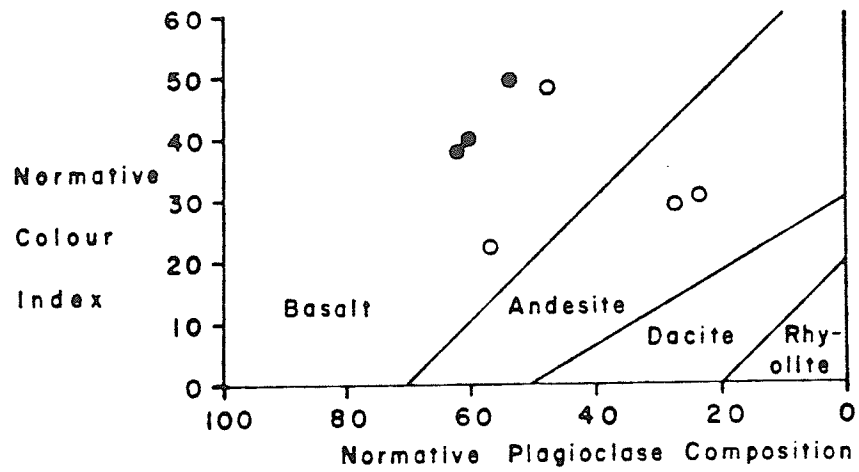


Figure 21. Normative plagioclase composition against normative colour index for chlorite schists and amphibolites. Plots in cation percent.

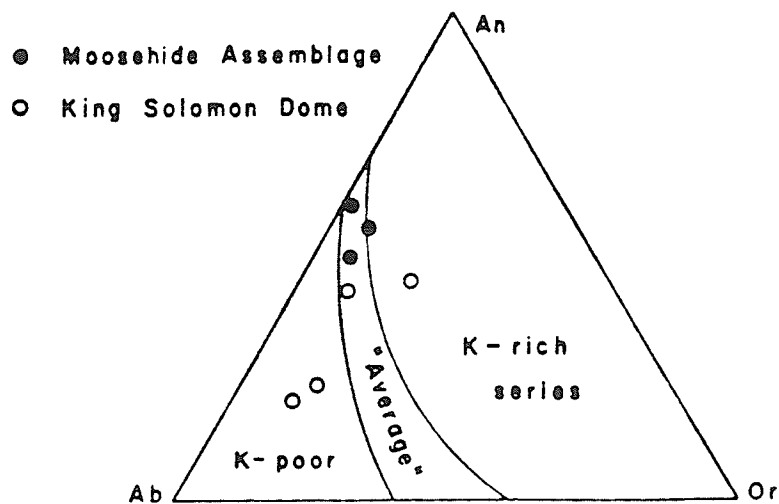


Figure 22. Or-Ab-An diagram for chlorite schists and amphibolites. Plots in cation percent.

(Plate 7, Fig. 3). Plagioclase composition ranges from An₆ to An₃₄, suggesting strong leaching of Ca. Rare mafic schists occur, with only trace amounts of plagioclase. Coarse-grained amphibolites (Plate 7, Fig. 4) retain relict hornblende at the cores of actinolite crystals (Plate 7, Fig. 5). Muscovite is a rare accessory.

A sample taken from the contact between the chlorite schists and the quartz muscovite schists of the Klondike Formation is a tectonically sheared and reworked garnet-hornblende-magnetite-plagioclase blastomylonite (Plate 7, Fig. 6). The presence of garnet, fringed by iron oxide and carbonate indicates higher metamorphic grade than in either unit and the hybrid nature of the rock suggests that the units are in tectonic contact.

Specimen 26/7/5, from Quartz Creek (Fig. 3), contains appreciable amounts of chlorite, but has a texture identical with the fragment-bearing members of the type section. The author considers this sample as a chlorite-rich variant of the Klondike Formation.

Four whole rock chemical analyses are presented in Appendix E. One sample, 26/7/5, is treated as part of the Klondike Formation. The remaining three samples are similar to the Moosehide Assemblage (Figs. 19-22).

The chlorite-actinolite schists in the area of King Solomon Dome are excluded from the Klondike Formation on the grounds of their different composition. They are reclassified as part of the Moosehide Assemblage on the basis of lithologic similarity. Chlorite-rich fragment-bearing units are retained in the Klondike Formation.

Chapter VII

CONCLUSION

The bedrock of the Klondike placer gold deposits in the Yukon Territory is here redefined as the Klondike Formation, using conventional litho-stratigraphic nomenclature. The formation comprises a 3000 m-thick cataclastically deformed sequence of bimodal blastomylonitic quartz feldspar muscovite schists, with intercalated quartz K-feldspar protomylonites near the observed base of the formation. Metamorphic grade is middle greenschist facies. The protomylonites are petrographically distinct from the blastomylonitic schists and are interpreted as minor rhyolitic volcanic members in a predominantly arkosic sedimentary succession, the latter possibly derived from erosion of the rhyolites, or genetically equivalent rocks.

Rb-Sr isotopic studies on the metarhyolites indicate an age of 202 ± 11 Ma for metamorphism of the Klondike Formation. This age is consistent with K-Ar studies conducted on the formation. Rotation of the isochron to an assumed initial $^{87}\text{Sr}/^{86}\text{Sr}$ of 0.704 yields an age of 290 Ma for formation of the rhyolites, in agreement with a U-Pb zircon age of 276 ± 5 Ma on genetically related sheared plutonic rocks. The minimum estimated age of the formation is 250 Ma.

The Klondike Formation is conformable on the structurally underlying Nasina Series, although discordant cleavages in less competent lithologies of the Nasina Series possibly reflect a low-angle thrust contact. The two formations were folded congruently during F2.

Chlorite-actinolite schists, in the area around King Solomon Dome, are associated with a serpentinite body. These have been excluded from the reclassification and assigned to the Moosehide Assemblage on the grounds of lithologic similarity.

7.1 TECTONIC SETTING

Regional models of Cordilleran evolution (Monger, 1977; Monger et al., 1972, 1978; Souther, 1977) can be correlated with North American plate motion during the Phanerozoic. The Cordilleran collage is interpreted as a series of island arcs accreted to the continental margin since late Triassic time.

Resetting of the Tintina Trench (Roddick, 1967) places the study area adjacent to the Finlayson Lake and Quiet Lake map-areas, mapped and interpreted by Tempelman-Kluit (1977a, 1977b). The regional setting of the areas is shown in Figure 1. The area was originally interpreted as a carbonate platform-back basin-foredeep assemblage overthrust by an ophiolite assemblage (Fig. 23). The Klondike Formation was interpreted as an assemblage coeval with rhyolitic volcanics on the Pelly-Cassiar Platform.

In a more recent paper Tempelman-Kluit (1979) interprets the lateral equivalent of the Klondike Formation as an allochthonous assemblage of meta-sedimentary siliceous cataclasite, the lowermost of three allochthons obducted onto the North American continental margin during the late Triassic and early to mid-Jurassic. The Nisutlin Allochthon comprises a metamorphosed sequence of immature clastic rocks, eroded from an island arc and metamorphosed in a westward dipping subduction zone. This allochthon, in the northern part of the Yukon Cataclastic Complex (Fig. 24) lies at the structural base of an obducted island arc. A model for initial rifting of the arc, westward subduction of back-arc oceanic crust and arc obduction (Tempelman-Kluit, 1979) is presented in Figure 25. The upper allochthons are interpreted as, respectively, oceanic crust (Anvil Allochthon) and plutonic root of island arc (Simpson Allochthon). The latter incorporates the Klotassin Granodiorite and part of the Pelly Gneiss (Tempelman-Kluit, 1980).

The present study on the Klondike Formation suggests that the hypothesis of island arc-continent collision provides a valid model for the origin and subsequent deformation of these rocks. The calc-alkaline rhyolites of the

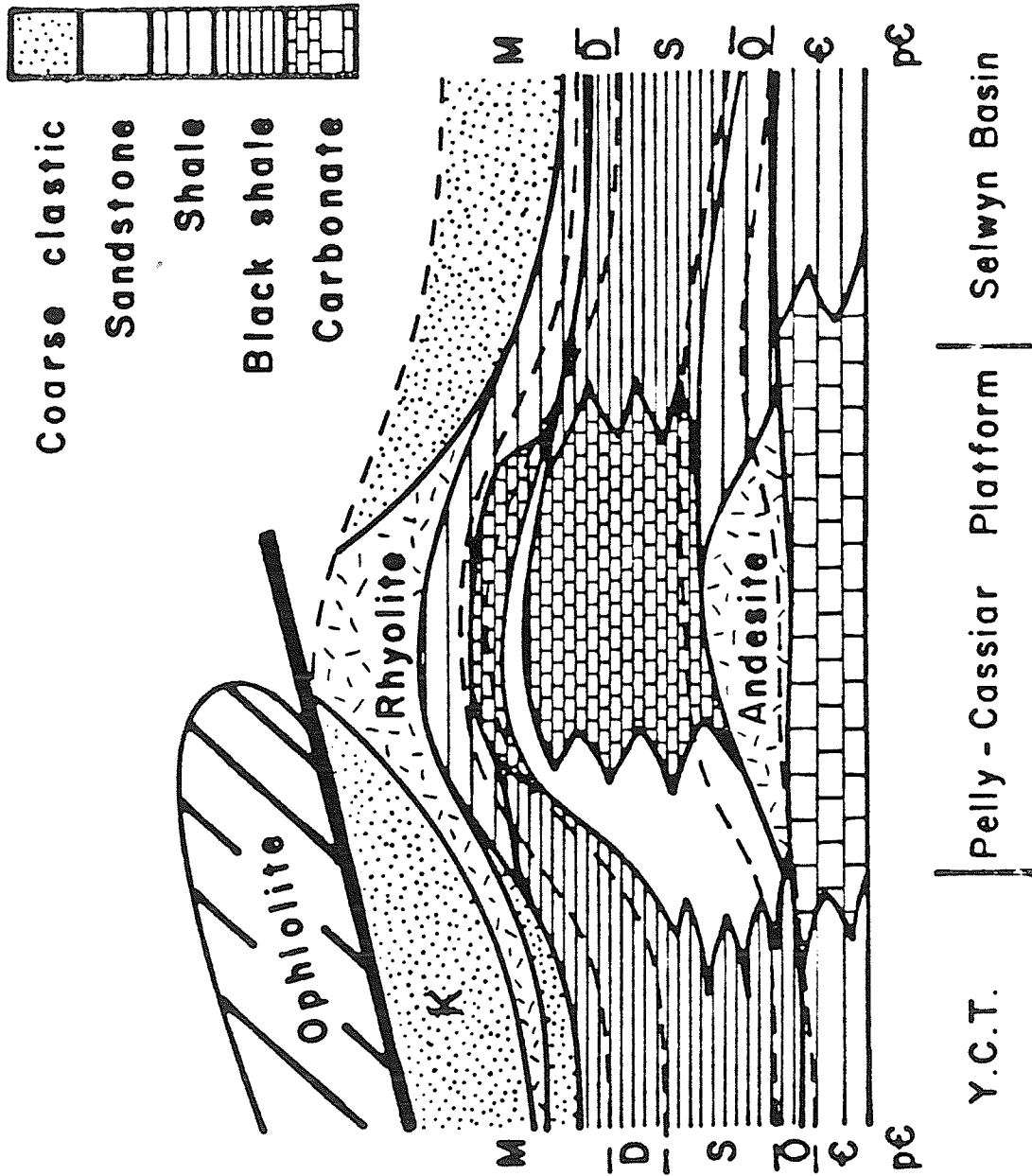


Figure 23. Idealized cross-section across the Quiet Lake and Finlayson Lake areas. K = Klondike Formation. After Tempelman-Kluit, 1977b.

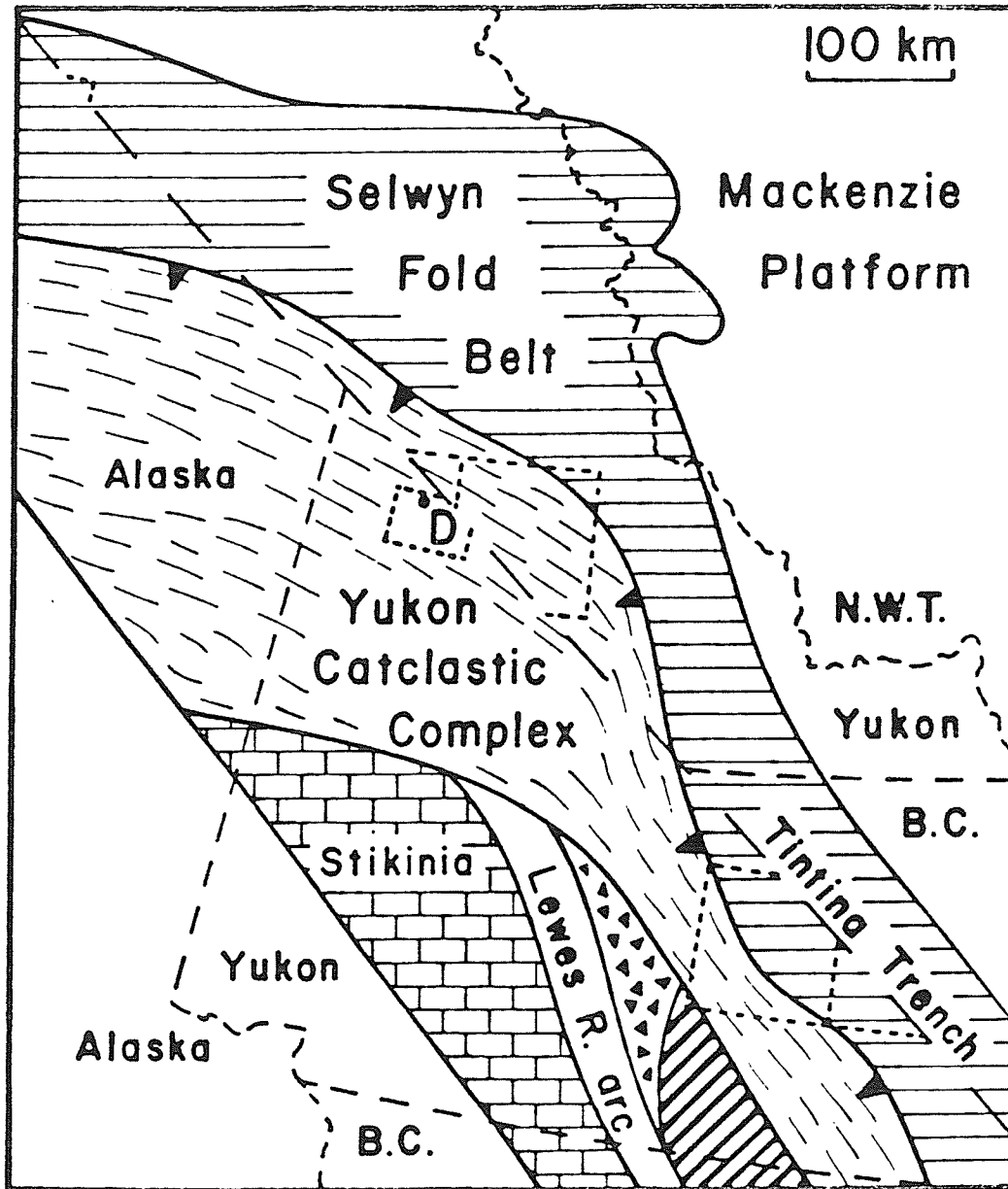


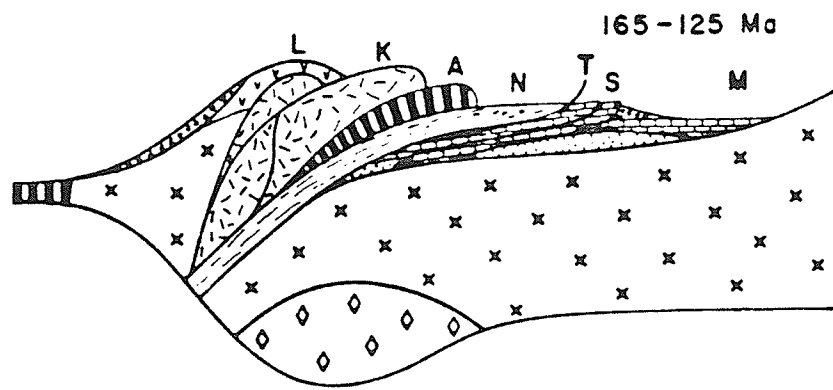
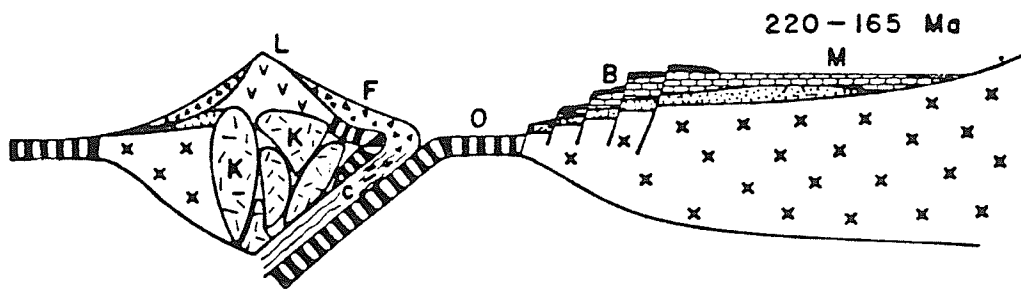
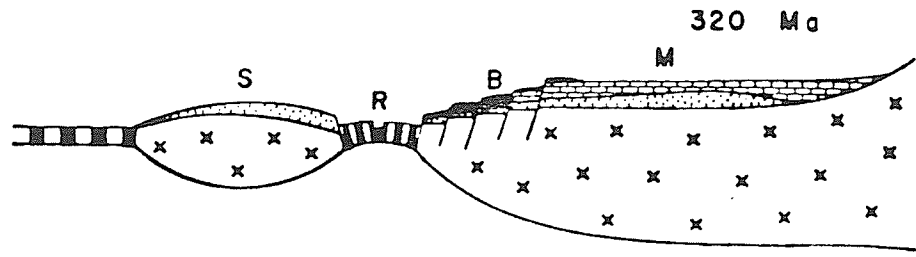
Figure 24. Regional tectonic setting of the Yukon Cataclastic Complex after resetting of the Tintina Trench (Tempelman-Kluit, 1979).

Figure 25. Model for formation of the Yukon Cataclastic Complex as a result of an island arc-continent collision (Tempelman-Kluit, 1979).

- a) Initial rifting of Stikinia (S) and formation of spreading centre (R). Eruption of basalts (B) on north American continental margin, outboard of the MacKenzie Platform (M).

- b) Closure of ocean by subduction of oceanic lithosphere (O) westward beneath Stikinia. Formation of Lewes River Arc (L) with forearc sediments and rhyolites (F) subjected to cataclasis (C).

- c) Near-complete obduction of Stikinia along Teislin Suture Zone (T). Formation of Selwyn Fold Belt (S), outboard of MacKenzie Platform. Obduction documented by emplacement of the Nisutlin (N), Anvil (A) and Simpson (K) Allochthons. Intrusion of the pink quartz monzonite suite.



Klondike Formation and their associated clastic sediments are typical of an island arc which is developing a base of continental lithosphere. The discordant cleavages in the Nasina graphitic phyllites suggest overthrusting of the Klondike Formation. Greenschist facies metamorphism possibly overprinted the conventional blueschist metamorphism developed in the trench (Erdmer, 1981). The ages of formation and metamorphism for the Klondike Formation are consistent with initiation of back-arc subduction and arc obduction, respectively.

7.2 RECOMMENDATIONS FOR STUDY

Future studies in the Yukon Crystalline Terrain may be assigned to three types, all concentrated on reconstruction of the initial disposition of the various lithologic assemblages. Stratigraphic studies should include precise documentation of the Nasina Series, well exposed in the Yukon River near the type section of the Klondike Formation. Detailed structural studies on the basal contacts of the Klondike Formation and Moosehide Assemblage will determine whether these contacts are tectonic, and might, in part, unravel the apparently severe deformation of the latter. Petrologic studies on the Moosehide Assemblage will facilitate its classification, possibly as part of the Anvil Allochthon.

Studies on the Klondike Formation are, as yet, incomplete. The upper part of the type section should be studied in detail, with regard to petrogenesis and to the origin of the quartz-plagioclase fragments. The appropriate division of the "Pelly Gneiss" should be considered, both as a parent for the fragments and as a coeval unit, genetically related to the Klondike Formation. More Rb-Sr and U-Pb isotopic ages are necessary on both units. In the light of more data, the Klondike Formation and related rocks may then be assigned to their correct context within the Cordilleran tectonic collage.

REFERENCES CITED

- American Commission on Stratigraphic Nomenclature, 1961: Code of Stratigraphic Nomenclature. American Association of Petroleum Geologists Bulletin, v.45, pp. 645-665.
- Bostock, H.S., 1942: Ogilvie Map-sheet. Geological Survey of Canada, Map 711A.
- _____ 1957: Yukon Territory: Selected field reports of the Geological Survey of Canada, 1898-1933. Geological Survey of Canada Memoir 284, 650p.
- Brooks, C., Hart, S.R. and Wendt, I., 1972: Realistic use of two-error regression treatments as applied to rubidium-strontium data. Reviews of Geophysics and Space Physics, v.10, pp.551-577.
- _____, Krogh, T.E. and Davis, G.L., 1969: Carbonate contents and $^{87}\text{Sr}/^{86}\text{Sr}$ ratios of calcites from Archaean metavolcanics. Earth and Planetary Science Letters, v.6, pp.35-38.
- Cairnes, D.D., 1914: The Yukon-Alaska international boundary between Porcupine and Yukon Rivers. Geological Survey of Canada Memoir 67, 161p.
- Carmichael, I.S.E., Turner, F.J. and Verhoogen, J., 1974: Igneous Petrology. McGraw-Hill, 739p.
- Cheung, S.P., 1978: Rubidium-Strontium whole-rock ages from the Oxford Lake-Knee Lake Greenstone belt, northern Manitoba. M.Sc. thesis, University of Manitoba, 41p.
- Cockfield, W.E., 1921: Sixtymile and Ladue Rivers area, Yukon. Geological Survey of Canada Memoir 123, 60p.
- Erdmer, P., 1981: Comparative studies of cataclastic allochthonous terranes in south central Yukon: new evidence for continental suturing. Geological Association of Canada Abstracts 1981, p.A17.
- Gleeson, C.F., 1970: Heavy mineral studies in the Klondike, Yukon Territory. Geological Survey of Canada Bulletin, v.173, 63p.

- Green, L.H., 1972: Geology of Nash Creek, Larsen Creek and Dawson map-areas, Yukon Territory. Geological Survey of Canada Memoir 364, 157p.
- Htoon, M., 1979: Geology of the Clinton Creek asbestos deposit, Yukon Territory. M.Sc. thesis, University of British Columbia.
- Hughes, O.L., Campbell, R.B., Muller, J.E. and Wheeler, J.O., 1969: Glacial limits and flow patterns, Yukon Territory south of 65 degrees north latitude. Geological Survey of Canada Paper 68-34, 9p.
- Irvine, T.N. and Baragar, W.R.A., 1971: A guide to the chemical classification of the common volcanic rocks. Canadian Journal of Earth Sciences, v.8, pp.523-548.
- Kanasewich, E.R., Havskov, J. and Evans, M.E., 1978: Plate tectonics in the Phanerozoic. Canadian Journal of Earth Sciences, v.15, pp.919-955.
- LeCouteur, P.C. and Tempelman-Kluit, D.J., 1976: Rb-Sr ages and a profile of initial $^{87}\text{Sr}/^{86}\text{Sr}$ ratios for plutonic rocks across the Yukon Crystalline Terrain. Canadian Journal of Earth Sciences, v.13, pp.319-330.
- Leech, G.B., Lowdon, J.A., Stockwell, C.H. and Wanless, R.K., 1964: Age determinations and geological studies - Report 4 Geological Survey of Canada Paper 63-17, 140p.
- Lowdon, J.A., 1961: Age determinations and geological studies - Report 1 Geological Survey of Canada Paper 60-17, 51p.
- _____ 1962: Age determinations and geological studies - Report 2 Geological Survey of Canada Paper 61-17, 127p.
- _____, Stockwell, C.H., Tipper, H.W. and Wanless, R.K., 1963: Age determinations and geological studies - Report 3 Geological Survey of Canada Paper 62-17, 140p.
- McConnell, R.G., 1889: Report on an exploration in the Yukon and MacKenzie basins, N.W.T. Geological and Natural History Survey of Canada Annual Reports, v.14 (1888-1889).

- _____, 1905: Report on the Klondike gold fields. Geological Survey of Canada Annual Report 14, Part B, pp.1B-71B.
- Mertie, J.B., Jr. 1937: The Yukon-Tanana region, Alaska. United States Geological Survey Bulletin, v.872, 276pp.
- Milner, M.W., 1977: Geomorphology of the Klondike placer goldfields, Yukon Territory. Ph.D. thesis, University of British Columbia.
- Monger, J.W.H., 1977: Upper Palaeozoic rocks of the western Canadian Cordillera and their bearing on Cordilleran evolution. Canadian Journal of Earth Sciences, v.14, pp.1832-1859.
- _____, Richards, T.A. and Paterson, I.A., 1978: The hinterland belt of the Canadian Cordillera: new data from northern and central British Columbia. Canadian Journal of Earth Sciences, v.15, pp.823-830.
- _____, Souther, J.G. and Galbriese, H., 1972: Evolution of the Canadian Cordillera: a plate-tectonic model. American Journal of Science, v.272, pp.577-602.
- Morrison, G.W., Godwin, C.I. and Armstrong, R.L., 1979: Interpretation of isotopic ages and $^{87}\text{Sr}/^{86}\text{Sr}$ initial ratios for plutonic rocks in the Whitehorse map area, Yukon. Canadian Journal of Earth Sciences, v.16, 1988-1997.
- Pettijohn, F.J., Potter, P.E. and Siever, R., 1973: Sand and Sandstone. Springer-Verlag, New York, 618p.
- Roddick, J.A., 1967: Tintina Trench. Journal of Geology, v.75, pp.23-33.
- Souther, J.G., 1977: Volcanism and tectonic environments in the Canadian Cordillera: a second look. In: Volcanic Regimes in Canada (ed. Baragar, W.R.A., Coleman, L.C. and Hall, J.M.): Geological Association of Canada Special Paper 16, pp.3-24.
- Spurr, J.E., 1897: Geology of the Yukon gold district, Alaska. U.S. Geological Survey 18th Annual Report Part 3, pp.87-392.

Steiger, R.H. and Jager, E., 1977: Subcommittee on geochronology: convention on the use of decay constants in geo- and cosmochronology. *Earth and Planetary Science Letters*, v.36, pp.359-362.

Tempelman-Kluit, D.J., 1974: Reconnaissance geology of Aishihik Lake, Snag and part of Stewart map-areas, west-central Yukon. *Geological Survey of Canada Paper 73-41*, 97p.

_____ 1976: The Yukon Crystalline Terrain: enigma in the Canadian Cordillera. *Geological Society of America Bulletin*, v.87, pp.1343-1357.

_____ 1977a: Quiet Lake (105F) and Finlayson Lake (105G) map areas, Yukon. *Geological Survey of Canada Open File 486*.

_____ 1977b: Stratigraphic and structural relations between Selwyn Basin, Pelly-Cassiar Platform and Yukon Crystalline Terrain in the Pelly Mountains, Yukon. In: *Report of Activities, Part A*, *Geological Survey of Canada Paper 77-1A*, pp.223-227.

_____ 1979: Transported cataclasite, ophiolite and granodiorite in Yukon: evidence of arc-continent collision. *Geological Survey of Canada Paper 79-14*, 27p.

_____ and Wanless, R.K., 1975: Potassium-argon age determinations of metamorphic and plutonic rocks in the Yukon Crystalline Terrain. *Canadian Journal of Earth Sciences*, v.12, 1895-1909.

_____ 1980: Zircon ages for the Pelly Gneiss and Klotassin granodiorite in western Yukon. *Canadian Journal of Earth Sciences*, v.17, pp.297-306.

Wanless, R.K., Stevens, R.D., laChance, G.R. and Delabio, R.N., 1970: Age determinations and geological studies: K-Ar isotopic ages: Report 9 *Geological Survey of Canada Paper 69-2A*, 78p.

-
- 1972: Age determinations and geological studies: K-Ar isotopic ages: Report 10 Geological Survey of Canada Paper 71-2, 96p.
-
- 1978: Age determinations and geological studies: K-Ar isotopic ages: Report 13 Geological Survey of Canada Paper 77-2, 60p.
-
- 1979: Age determinations and geological studies: K-Ar isotopic ages: Report 14 Geological Survey of Canada Paper 79-2, 67p.
- Wanless, R.K., Stevens, R.D., laChance, G.R. and Edmonds, C.M., 1967: Age determinations and geological studies: K-Ar isotopic ages: Report 7 Geological Survey of Canada Paper 66-17, 120p.
-
- 1968: Age determinations and geological studies: K-Ar isotopic ages: Report 8 Geological Survey of Canada Paper 67-2A, 141p.
- Wanless, R.K., Stevens, R.D., laChance, G.R. and Rimsaite, J.Y.H., 1965: Age determinations and geological studies: K-Ar isotopic ages: Report 5 Geological Survey of Canada Paper 64-17, 155p.
-
- 1966: Age determinations and geological studies: K-Ar isotopic ages: Report 6 Geological Survey of Canada Paper 65-17, 101p.
- Winkler, H.G.F., 1979: Petrogenesis of Metamorphic Rocks. Springer-Verlag, New York, 348p.
- York, D., 1966: Least squares fitting of a straight line. Canadian Journal of Physics, v.44, 1079-1086.

PHOTOGRAPHIC PLATES

Plate 1

- Fig. 1. The area to the north of King Solomon Dome, characteristically poor in outcrop. The valley of the Tintina Trench (dashed line) separates the dissected Yukon Plateau physiographically and geologically from the Ogilvie Mountains in the background.
- Fig. 2. Entrenchment of the Yukon River at Dawson City (foreground). The type section of the Klondike Formation lies on the far bend of the river, to the southwest of Dawson City.

1



2

Type section

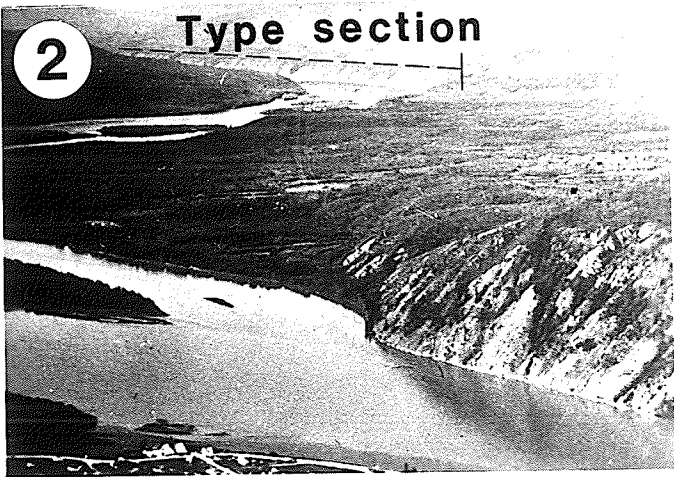


Plate 2

- Fig. 1. Parallelism of S1 cleavage and S0 compositional layering in rocks of the Klondike Formation. The dark bands are ferruginous quartzites in quartz muscovite feldspar blastomylonite. Photograph from the type section.
- Fig. 2. Close-up of compositional layering and S1 cleavage in type section.
- Fig. 3. Discordant S0 and S1 in graphitic phyllites of the Nasina Series. Photograph from mouth of Bonanza Creek, right bank.
- Fig. 4. Non-parallelism of S1 to compositional layering in mica schist (top) contrasts with parallelism observed in competent quartzite (bottom). Photograph from right bank of Yukon River, 5 km north of Dawson City.
- Fig. 5. Shear zones in graphitic phyllites of Nasina Series. Photograph from mouth of Bonanza Creek, right bank.
- Fig. 6. High-angle reverse fault (F) in type section, dislocating the contact between members 1 and 2 of the Klondike Formation by 40 m.

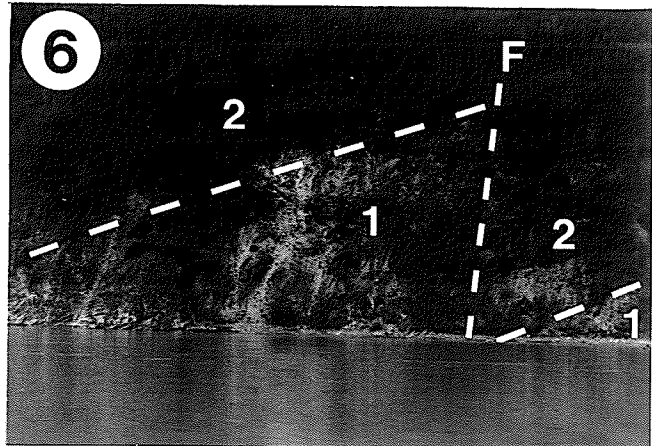
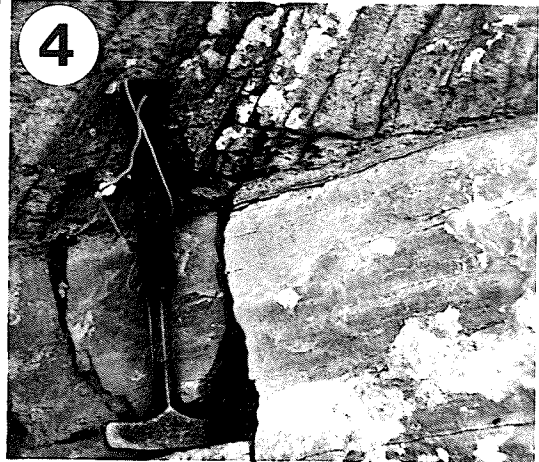
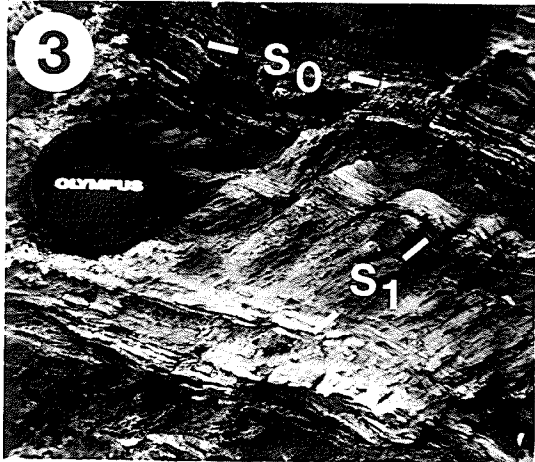
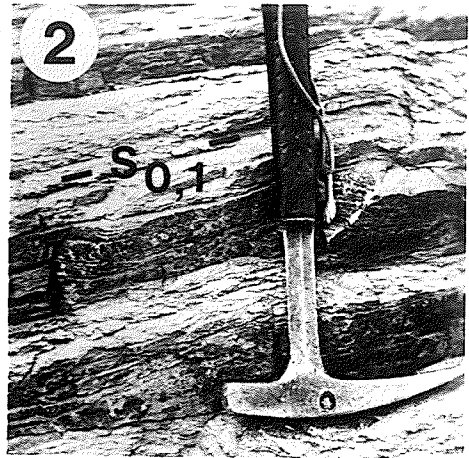
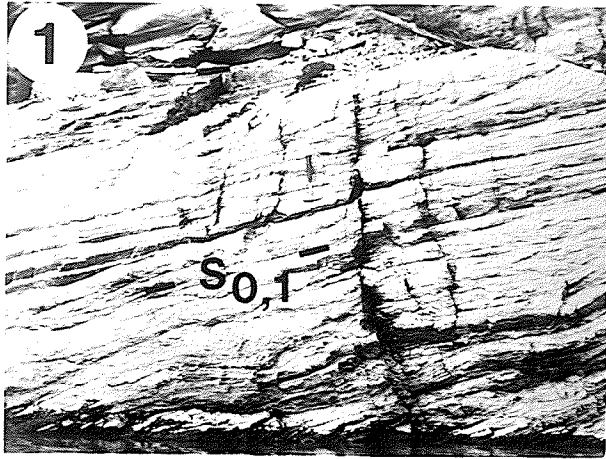
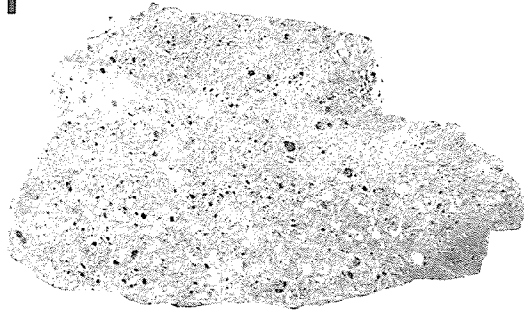


Plate 3

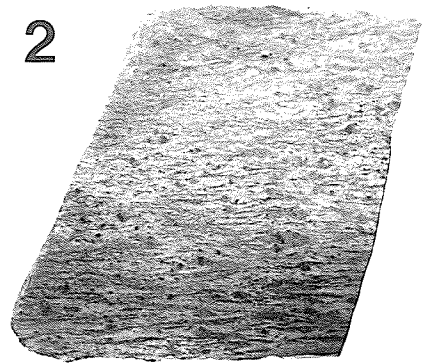
- Fig. 1. Hand specimen of bimodal quartz muscovite feldspar blastomylonite, stained with sodium cobaltinitrite.
- Fig. 2. Hand specimen of quartz K-feldspar protomylonite, stained with sodium cobaltinitrite.
- Fig. 3. Blastomylonite, showing F2 refolding of S1 cleavage. The matrix of quartz-plagioclase (Q-P) has an S1 cleavage defined by lepidoblastic mica (M). Scale bar 2.0 mm (plane polarised light).
- Fig. 4. Deformation of plagioclase grain (P) by F2 (crossed polars). Scale bar 1.0 mm.
- Fig. 5. Quartz fragments (Q) in blastomylonite internally recrystallized, with sutured grain boundaries (crossed polars). Scale bar 2.0 mm.
- Fig. 6. Compound fragment, comprising equigranular quartz (Q) and plagioclase (P), in blastomylonite (crossed polars). Scale bar 1.0 mm.

1



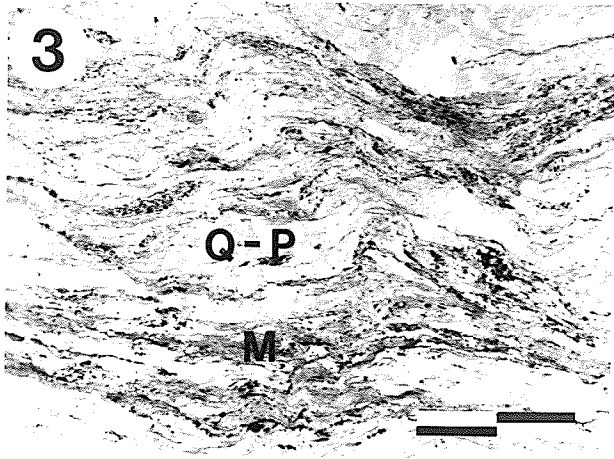
5 cm

2

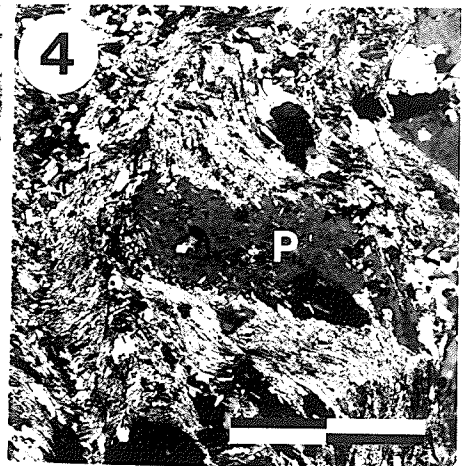


5 cm

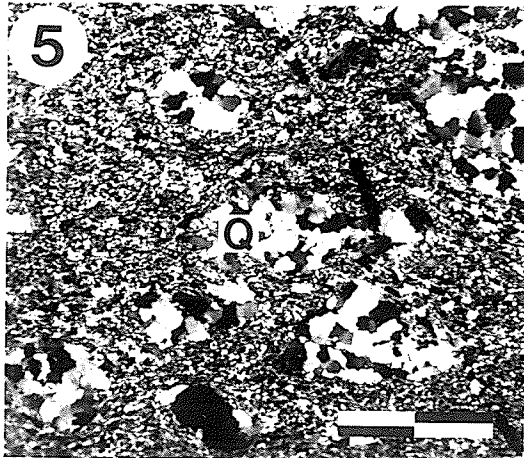
3



4



5



6

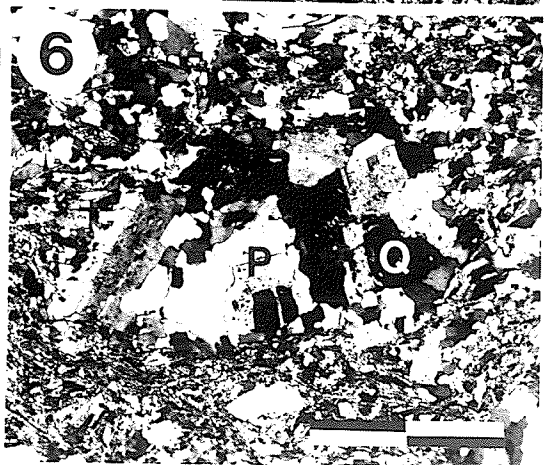


Plate 4

- Fig. 1. Protomylonite, showing fine-grained, almost isotropic matrix (crossed polars). Scale bar 2.0 mm.
- Fig. 2. Close-up of unrecrystallized matrix, which appears to show a devitrification texture (crossed polars). Scale bar 0.1 mm.
- Fig. 3. Relict spherulitic texture in protomylonite matrix (crossed polars). Scale bar 0.2 mm.
- Fig. 4. Devitrified glass fragment in the pressure shadow of a quartz crystal (crossed polars). Scale bar 0.2 mm.
- Fig. 5. Embayed quartz grain in protomylonite. Note partial recrystallization of quartz and unrecrystallized matrix within the embayment (crossed polars). Scale bar 1.0 mm.
- Fig. 6. Strained quartz crystal, embayed, with unrecrystallized matrix filling the embayment (crossed polars). Scale bar 1.0 mm.

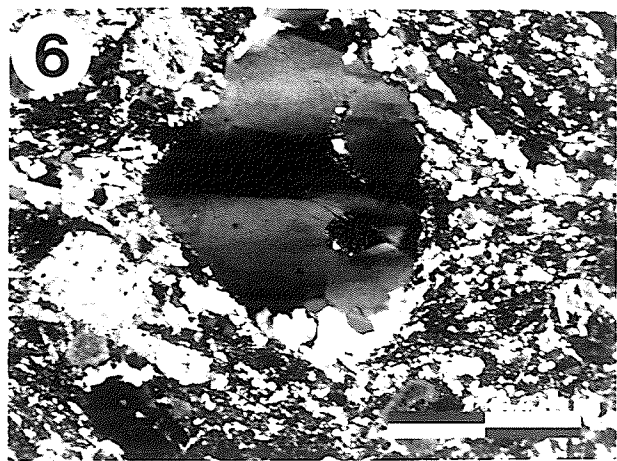
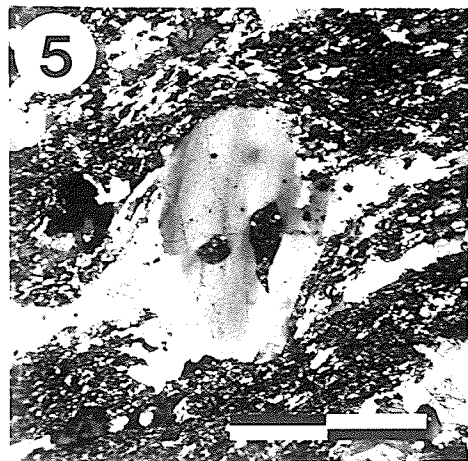
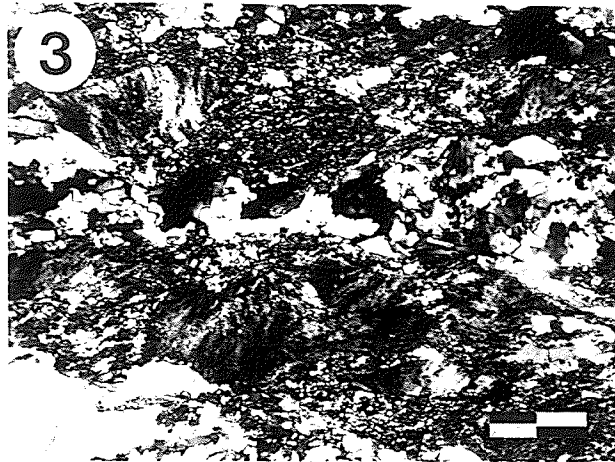
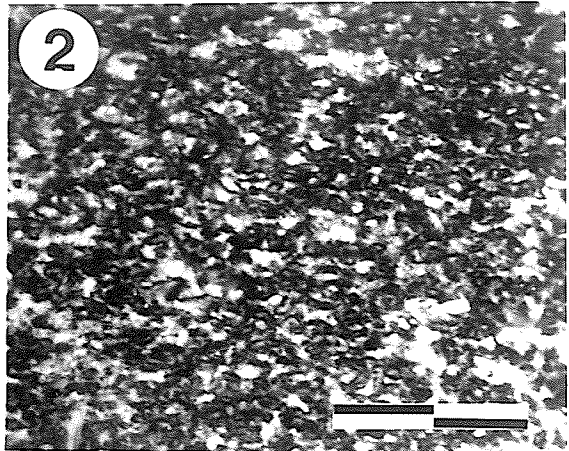
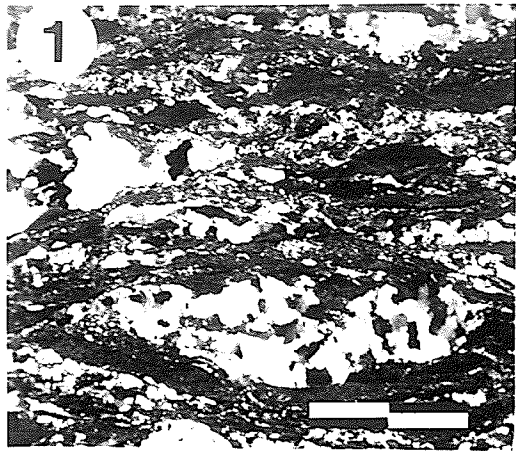


Plate 5

- Fig. 1. Elongate K-feldspar in protomylonite, rimmed with relict matrix (crossed polars). Scale bar 1.0 mm.
- Fig. 2. Embayed K-feldspar in protomylonite with relict matrix filling embayment (crossed polars). Scale bar 1.0 mm.
- Fig. 3. Embayed K-feldspar in protomylonite, marginally recrystallized (crossed polars). Scale bar 1.0 mm.
- Fig. 4. Embayed K-feldspar in protomylonite with embayments filled with relict matrix; the K-feldspar is also rimmed with relict matrix and peripherally recrystallized (crossed polars). Scale bar 0.2 mm.
- Fig. 5. K-feldspar, twinned according to the Baveno law, exsolving albite (crossed polars). Scale bar 1.0 mm.
- Fig. 6. Compound fragment of quartz and plagioclase with a thin rim of relict matrix (crossed polars). Scale bar 1.0 mm.

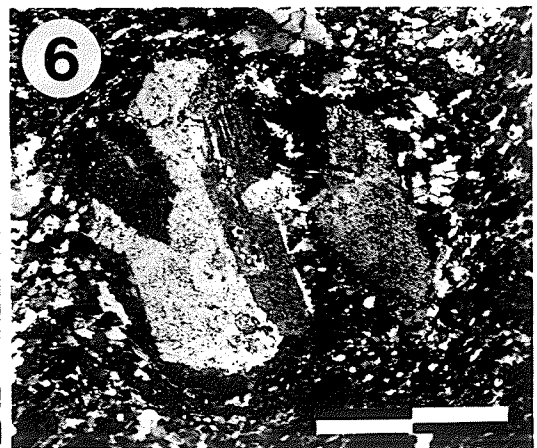
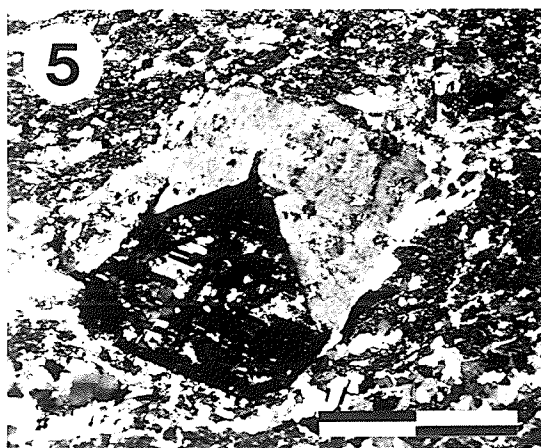
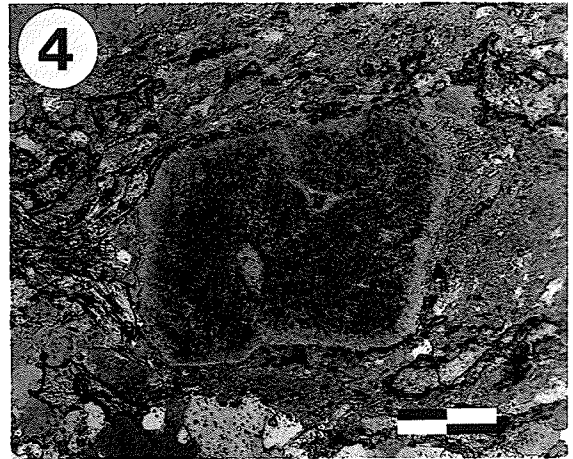
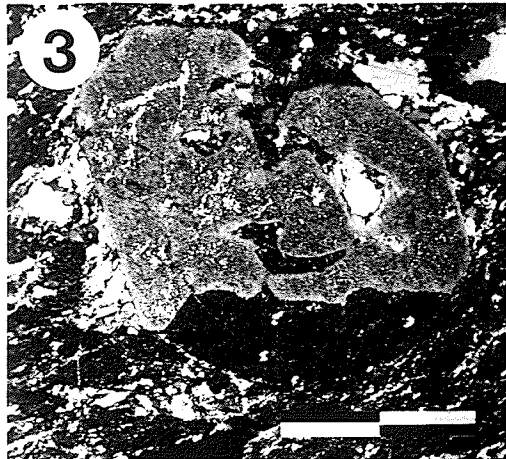
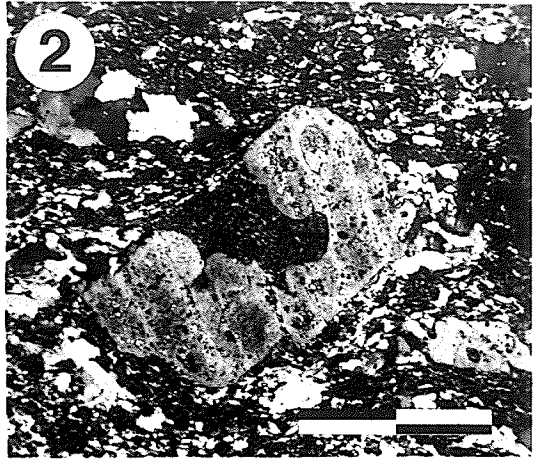
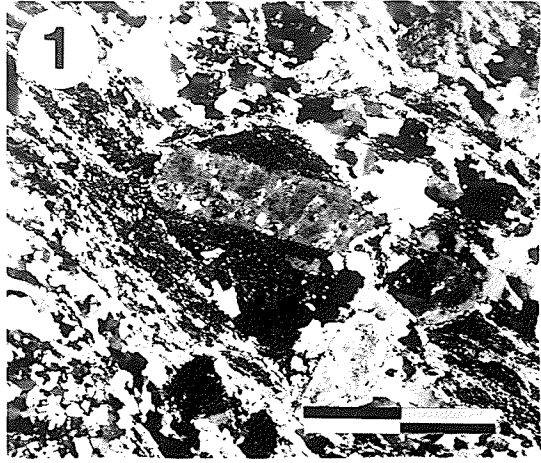


Plate 6

- Fig. 1. Banded ferruginous quartzite (plane polarised light).
Scale bar 2.0 mm.
- Fig. 2. Chlorite (Chl)-carbonate (Cb) aggregate is banded
ferruginous quartzite (plane polarised light). Scale bar
1.0 mm.
- Fig. 3. Retrograde reaction of actinolitic amphibole (A) to
ferroan dolomite (D)-quartz (Q) (plane polarised light).
Scale bar 0.2 mm.
- Fig. 4. Chlorite (C=, after biotite (B), and muscovite (M) in
blastomylonite. Note absence of garnet and staurolite
(plane polarised light). Scale bar 0.1 mm.

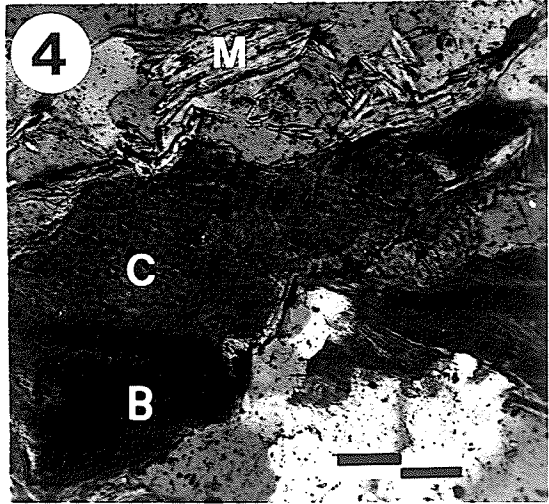
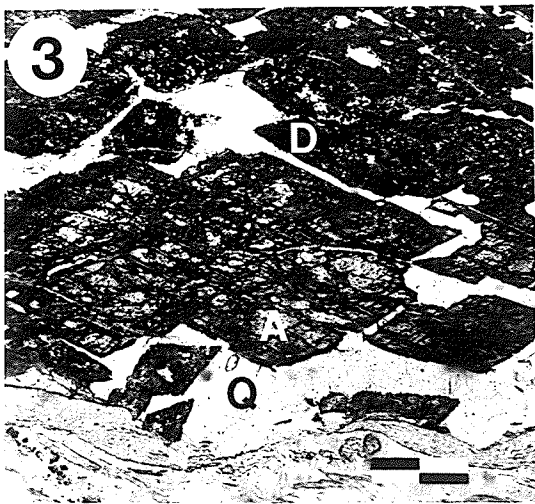
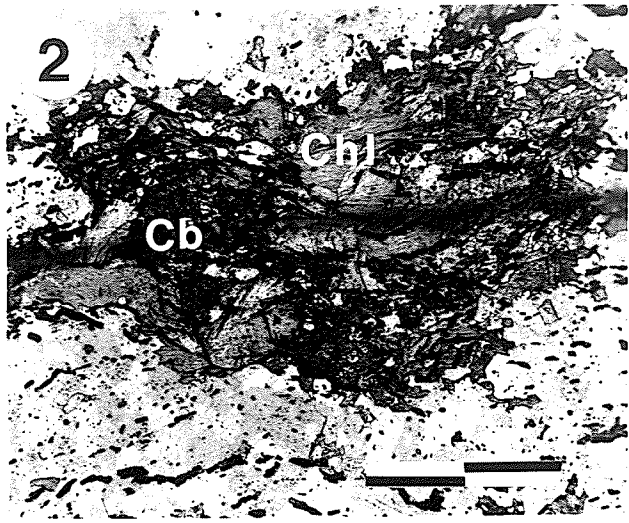
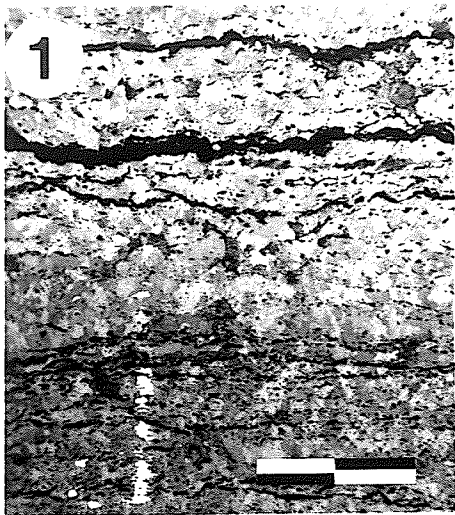
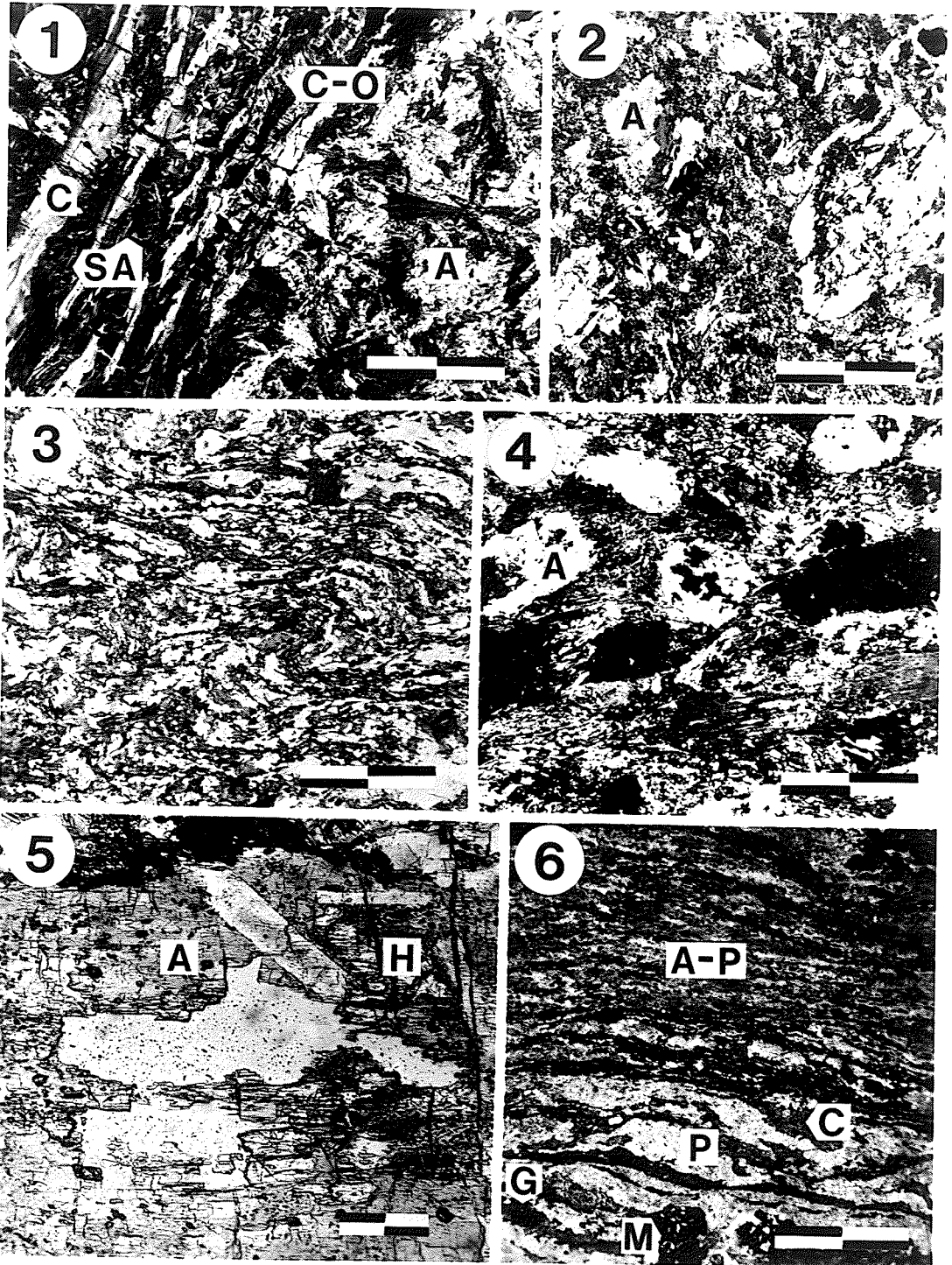


Plate 7

- Fig. 1. Sheared serpentinite (sample 4/6/1) from Moosehide Assemblage. Areas of antigorite (A) are bounded by sheared antigorite (SA) with veins of chrysotile (C) and chrysotile-iron titanium oxide (C-0). Crossed polars; scale bar 2.0 mm.
- Fig. 2. Cataclastic amphibolite (sample 27/5/3A) with large amphibole (A) crystalloblasts (crossed polars). Scale bar 2.0 mm.
- Fig. 3. Mylonitized metabasalt (sample H-62) from Upper Bonanza Creek. The light areas are granoblastic albite-quartz; darker areas comprise biotite, chlorite, epidote and actinolite. Plane polarised light; scale bar 2.0 mm.
- Fig. 4. Cataclastic amphibolite (sample H-119) from Upper Bonanza Creek with large actinolite grains (A). Crossed polars; scale bar 2.0 mm.
- Fig. 5. Relict hornblende (H) in actinolite (A); sample H-119 (plane polarised light). Scale bar 0.2 mm.
- Fig. 6. Garnet (G)-magnetite (M)-albite (P)-actinolite (A) - chlorite (C) blastomylonite (plane polarised light). Scale bar 2.0 mm.



Appendix A

PETROGRAPHIC DESCRIPTIONS OF KLONDIKE FORMATION

Samples taken from the lower part of the type section have been assigned to discrete members, in order to present petrographic data concisely. Members were defined on the basis of stratigraphic height and petrographic similarity. This designation is informal as individual members cannot be traced for any distance in the field.

Where a single, lithologically distinct, bed was included in a member, the bed was classified as part of the member. Such a bed is described by a subscript a, b, c ...; "a" having the lowest stratigraphic height. A separate description is included for each "submember".

Modes are visual estimates. Variations in modal composition occur within members but the mineral assemblages exhibit little or no variation. Where small grain size precluded accurate estimates, the material was counted ensemble as "matrix". Subsequent staining with sodium cobaltinitrite indicated that the material is dominantly K-feldspar.

A.1 MEMBER 1

Stratigraphic height: 0-200 m

Blastomylonitic schist

Modes in Table A-1

Crystalloblasts of quartz and sodic plagioclase (0.1-0.4 mm) form the matrix. Lepidoblastic muscovite (0.2-0.4 mm) forms an S1 cleavage, deformed by a later (F2) event. Areas of finer grain size denote cataclastic shear zones. The matrix occasionally exhibits sutured grain boundaries.

Clast-like fragments of quartz and plagioclase (0.5-4.0 mm) occur, comprising as much as 20% of the rock. Quartz is recrystallized with pre-metamorphic marginal textures obscured; some samples exhibit rare embayments.

Table A-1

Member 1: modes

Sample number	Coarse fraction										Matrix						
	Comp	Qz	Plag	%An	Qz	Fsp	Mu	Ch1	Bi	Act	Ep	Ap	C03	Ox	Py		
14/8/1		15			45	8	30							2	Tr		
14/8/2	5	5	5	22	55	15	15							Tr			
14/8/3		5			65	5	25							Tr			
14/8/4		10	10	26	35	20	15			1	Tr			6	3		
14/8/5		10			20	20	50				Tr			Tr	Tr		
14/8/6		5	5	30	30	30	30							Tr			
14/8/7					40	40	20							Tr			
14/8/9		5	5	26	50	15	20	2					3	Tr			
14/8/11		5	5	26	30	35	10	5		2				3	5		
14/8/12		5	5	30	35	30	20							5	Tr		
14/8/13			5	24	45	10	40								Tr		
14/8/14	5	5	5	35	55	5	25						Tr	Tr			
16/8/3A		5			50	30	15							Tr			
16/8/3B		2			50	10	30			4			2	2			
16/8/6		10	5	6	40	35	10*							Tr	Tr		
16/8/7					55	15	20*						8	2			

Table A-1 (cont'd)

Sample number	Coarse fraction										Matrix									
	Comp	Qz	Plag	%An	Qz	Fsp	Mu	Chl	Bi	Act	Ep	Ap	C03	Ox	Py					
16/8/8					45	10	30						15	Tr						
16/8/9A	10		5	6	45	10	15						15	Tr						
16/8/10		5			50	15	20	5					3	2						
16/8/11					40	20	30*						Tr	10						
16/8/12B		5			55	10	25						3	2						

* Possible interlamination of chlorite

Plagioclase (An₂₆) is peripherally albitized with no relict textures. Rare compound fragments of interlocking quartz and plagioclase (An₂₆) occur.

A.2 MEMBER 2

Stratigraphic height: 200-275 m

Protomylonitic granofels

Modes in Table A-2

Relict matrix (0.03-0.05 mm) contains rare spherulites and is variably recrystallized to granoblastic quartz and alkali feldspar (0.3 mm). Lepidoblastic muscovite (0.3 mm) is oriented parallel to S₁. Fracturing of the matrix replaces folding due to low mica contents.

Rounded grains of quartz and euhedral to subhedral K-feldspar (1-4 mm) exhibit well-developed magmatic embayments. The embayments are filled with unrecrystallized matrix; the grains occasionally exhibit unrecrystallized matrix along their margins. K-feldspar is twinned on the Carlsbad Law, is sericitized and exhibits albite exsolution.

Fragments of quartz-plagioclase (An₂₆), 1-2 mm, are extremely rare. The fragments exhibit unrecrystallized matrix along their margins. Plagioclase is marginally albitized and clouded by alteration.

Submember 2a

Stratigraphic height: 230-250 m

Blastomylonitic schist

Crystalloblastic matrix of quartz and plagioclase (0.2-0.3 mm) with lepidoblastic muscovite forming the S₁ cleavage. The S₁ cleavage is refolded by F₂. Quartz fragments (1-2 mm), with marginal textures obscured by recrystallization, are the only coarse component.

Table A-2
Member 2: modes

Sample number	Coarse fraction										Matrix				
	Comp	Qz	Kfsp	Plag	%An	Fine	Qz	Fsp	Mu	Sph	Carb	Ox	Py		
16/8/1		2	3	Tr	-	70	10		Tr		15				
16/8/2		3		7	-	70	15		5			Tr			
16/8/4			5			20	30	20	25			Tr	Tr		
16/8/5		5	5	5	26	55	10	15	5			Tr	Tr		
16/8/9B		10	5	1	-	50	20	10	2		1	1	Tr		
16/8/12A		5	10			65	10		8		1	1	Tr		
16/8/15A		4	5	1	34	65	15		10	Tr			Tr		
16/8/15B		5	5			65	10		15			Tr			
16/8/16		5	5			65	18		5		2	Tr	Tr		
16/8/17A		10	5			40	20	10	10		3	1	1		
					submember 2a										
16/8/14		5				35	33	33	25		2	Tr			
16/8/15C		5				15	Tr	75			3	2			

A.3 MEMBER 3

Stratigraphic height: 275-490 m

Blastomylonitic schist

Modes in Table A-3

The matrix comprises crystalloblastic quartz and plagioclase (0.1-0.3 mm) with lepidoblastic muscovite (0.5 mm) imparting an S1 cleavage refolded by F2. Anhedral carbonate, Fe-Ti oxides and leucoxene (0.1 mm) are accessory. Carbonate-quartz intergrowths (1-2 mm), after actinolite porphyroblasts, occur in carbonate-rich samples.

Rare rounded quartz fragments (1-4 mm) are frequently recrystallized. Sutured grain boundaries occur in both fragments and matrix. Feldspar fragments are absent.

Submember 3a

Stratigraphic height: 470 m

Ferruginous quartzites

Mode in Table A-3

Granoblastic quartz (0.3 mm) occasionally exhibits sutured grain boundaries. Quartz crystalloblasts enclose elongate grains of iron oxide (0.05-0.1 mm) which form bands (S0). Muscovite and feldspar are present only in trace amounts. Chlorite-carbonate-epidote intergrowths (0.5-1.0 mm) are possibly reaction products after garnet. Fragments are absent.

A.4 MEMBER 4

Stratigraphic height: 490-600 m

Protomylonitic granofels

Modes in Table A-4

A relict matrix (0.03-0.05 mm) contains rare spherulites and fragments

Table A-3

Member 3: modes

Sample number	Coarse fraction										Matrix						
	Comp	Qz	Plag	%An	Qz	Fsp	Mu	Chl	Bi	Act	Ep	Ap	C03	Ox	Py		
16/8/17B					40	5	50						2/2	1			
17/8/1A					55	10	30						3	2			
17/8/1B	5				55	20	15	1					2/1	1			
25/8/1	5				40	15	40	Tr					Tr	Tr			
25/8/2	20				40		37						2	1			
25/8/3					45	10	40						1	4			
25/8/4					55	10	30*						2	3			
25/8/5C					55	5	40*							Tr			
					submember 3a												
25/8/5A					65	2		10				3	10	10			
25/8/5B					70	Tr	Tr	10			3	2	2	15			

*Possible interlaminations of chlorite carbonate as leuocarbonate/siderite.

Table A-4

Member 4: modes

Sample number	Coarse fraction										Matrix					
	Comp	Qz	Kfsp	Plag	%An	Fine	Qz	Fsp	Mu	Sph	Carb	Ox	Py			
25/8/6		15				30	30		20	3	2					
25/8/7		9	1			40	20		25	2	3					
26/8/1		10				30	20		15	3	2	Tr				
26/8/2		10				50	30		5		5					
26/8/3		10	1				30	35	20	3	1					
26/8/6		4	1			30	40	10	10	2	3	Tr				
26/8/7		5	5			60	15		5	5	2	3				
26/8/9		5				60	25		10	Tr	Tr					
27/8/1A		10	5			60	10		10	5	Tr					
27/8/1B		9	1			45	20		20	5	Tr					
27/8/1D		5	5			40	30		15	5	Tr					
					submember 4a											
26/8/5	Tr			Tr	Ab		50	15	30	Tr	Tr					
26/8/8					submember 4b		40	10	45	0/5	Tr					
27/8/1C		5					30		55		10					

Carbonate as leucocarbonate/siderite

of devitrified glass (0.5 mm). Staining of this matrix with sodium cobalt-nitrite indicated that it is dominantly K-feldspar. Recrystallized matrix comprises granoblastic quartz and alkali feldspar (0.2 mm) with a weak S1 cleavage imparted by oriented lepidoblasts of muscovite (0.1-0.3 mm). Late (F2) fractures are filled with quartz and carbonate.

Rounded quartz grains, euhedral to subhedral K-feldspar and rare plagioclase (1-3 mm) are present. Plagioclase is altered to muscovite and carbonate. Quartz and K-feldspar are strongly embayed and rimmed by relict matrix.

Submember 4a

Stratigraphic height: 540-560 m

Blastomylonitic schist

Quartz and minor plagioclase (0.1-0.4 mm) form a sutured matrix. Oriented lepidoblasts of muscovite (0.5 mm) form a penetrative S1 cleavage, refolded by F2. Quartz-carbonate aggregates (1 mm) are alteration after actinolite porphyroblasts. Quartz and albite fragments are rare.

Submember 4b

Stratigraphic height: 590 m

Blastomylonitic schist

A granoblastic matrix of quartz and carbonate (0.4 mm) is transected by cataclastic shear zones of lepidoblastic muscovite (0.5 mm). The S1 cleavage is refolded by F2. Fragments are rare.

A.5 MEMBER 5

Stratigraphic height: 600-850 m

Blastomylonitic schist

Modes in Table A-5

A granoblastic quartz-plagioclase matrix (0.2 mm) exhibits an S1 cleavage, imparted by oriented lepidoblastic muscovite (0.1-0.5 mm). The cleavage is refolded by F2.

Rounded quartz fragments (1-3 mm), flattened parallel to S1, have their marginal textures obscured by recrystallization. Plagioclase (An32), 1-2 mm in size, is also present.

Table A-5
Member 5: modes

Sample number	Coarse fraction				Matrix										
	Comp	Qz	Plag	%An	Qz	Fsp	Mu	Chl	Bi	Act	Ep	Ap	CO3	Ox	Py
27/8/2	5	5	32	35	30	20*					5		Tr	Tr	
27/8/3B				45	5	45							2/3		

* Possible interlamination of chlorite
Carbonate as leucocarbonate/siderite

A.6 MEMBER 6

Stratigraphic height: 850-870 m

Protomylonitic granofels

Mode in Table A-6

Relict matrix (0.03-0.05 mm), stained with sodium cobaltinitrite, is an intergrowth of quartz and K-feldspar. Recrystallized matrix comprises crystalloblastic quartz and K-feldspar (0.1-0.3 mm) with minor oriented lepidoblastic muscovite (0.2 mm). Quartz fills fractures (F2). Graphite is a finely-disseminated accessory.

Rounded quartz and subhedral microcline (1-2 mm) are fractured and exhibit rare embayments. Microcline is extensively sericitized.

Table A-6
Member 6: mode

Sample number	Coarse fraction					Matrix								
	Comp	Qz	Kfsp	Plag	%An	Fine	Qz	Fsp	Mu	Sph	CO3	Ox	Py	Gr
27/8/3A		10	5			55	15		10		2	Tr		3

A.7 UPPER SECTION

Stratigraphic height: 850 m+

Blastomylonitic schists

Modes in Table A-7

The matrix comprises crystalloblastic quartz and albite (0.2-0.5 mm), frequently exhibiting sutured grain boundaries. Lepidoblastic muscovite and, rarely, amphibole impart a penetrative S1 cleavage refolded by F2. Sphene, biotite and increasingly calcic plagioclase appear higher in the section. Pistacite forms as much as 10% of the matrix.

Quartz fragments are as much as 7 mm in diameter. Many are recrystallized some with sutured internal grain boundaries. They are frequently flattened tectonically, with long cross-sections parallel to S1.

Table A-7
Upper Section: modes

Sample number	Coarse fraction											Matrix						
	Comp	Qz	Plag	%An	Qz	Fsp	Mu	Chl	Bi	Act	Ep	Sph	Ap	C03	Ox	Py		
27/8/4	5	Tr		32	25	10	30			25	4	1						
27/8/5					55	25	20				Tr				Tr			
27/8/6		15		25	35	10	30*				5	5						
27/8/7	10	5		27	30	20	30*	1	1			3			Tr			
27/8/8	10	5		31	30	20	25			10					Tr			
27/8/9	5	5		34	40	20	25		Tr			1		0/3	1			
27/8/10	2				38	45	15								Tr	Tr		
27/8/11	5	5		32	35	30	20				5	Tr			Tr			
27/8/12		10		34	45	30	15		Tr			Tr			Tr	Tr		
27/8/13					40	28	30					Tr		2	Tr			
27/8/15	5	5		33	30	30	7		Tr			3		Tr	Tr	Tr		
27/8/16	5	5		36	35	30	7		5	13					Tr			

* Possible interlaminations of chlorite

Carbonate as leucocarbonate/siderite

Table A-8

Stratigraphic Height of Samples from the Type Section

Height (m)	Samples
3110	27/8/16
3110	27/8/15
3080	27/8/14
3060	27/8/13
3020	27/8/12
2950	27/8/11
2940	27/8/10
2650	27/8/9
2600	27/8/8
1900	27/8/7
1600	27/8/6
1170	27/8/5
1135	27/8/4
860	27/8/3A, 27/8/3B
840	27/8/2
590	27/8/1A, 27/8/1B, 27/8/1C, 27/8/1D
575	26/8/9
570	26/8/7
565	26/8/6
555	26/8/5
540	26/8/4, 26/8/8
525	26/8/3
510	26/8/2
500	26/8/1
490	25/8/7
485	25/8/6
475	25/8/5A, 25/8/5B, 25/8/5C
470	25/8/2, 25/8/3, 25/8/4
395	25/8/1
325	17/8/1A, 17/8/1B
275	16/8/17A, 16/8/17B, 16/8/17C
270	16/8/16
245	16/8/15A, 16/8/15B, 16/8/15C
240	16/8/14
210	16/8/1, 16/8/2, 16/8/4, 16/8/5
200	16/8/12A, 16/8/12B, 16/8/9A, 16/8/9B
0-200	14/8/1, 14/8/2, 14/8/3, 14/8/4, 14/8/5, 14/8/6, 14/8/7, 14/8/9, 14/8/11, 14/8/12, 14/8/13, 14/8/14, 16/8/3A, 16/8/3B, 16/8/6, 16/8/7, 16/8/8, 16/8/9A, 16/8/10 16/8/11

Appendix B

PROCEDURES FOR WHOLE ROCK ANALYSIS AND
ISOTOPE DILUTION

B.1 WHOLE ROCK ANALYSIS

Samples were trimmed of weathered surfaces and passed through a jaw crusher. Fragments were screened for steel-grazed surfaces, then ground to -200 mesh, using a disc grinder.

H₂O- values were determined by heating aliquots to constant weight at 110°C. Total H₂O and CO₂ were measured by heating in an induction furnace using oxygen. H₂O was collected on Anhydron, CO₂ on Ascarite. SO₂ values, from which S was determined, were obtained using an automatic titrator.

FeO aliquots were decomposed in a 1:4 mixture of HF and H₂SO₄. FeO was then determined by titration with potassium dichromate using sodium diphenylamine sulphonate as an indicator.

Na₂O, MgO, P₂O₅, Rb, Sr and Cs aliquots were dissolved in platinum crucibles using HF, H₂SO₄ and HNO₃. P₂O₅ values were measured by absorption of the molydivanadophosphoric acid complex at 430 nm., using a Unicam SP 500 spectrophotometer. Na₂O, MgO, Rb, Sr and Cs values were determined using a Perkin Elmer 303 Atomic Absorption Spectrophotometer.

Single weighed aliquots were heated to 1100°C in platinum crucibles with Li2B4O7 and La2O3. The resulting beads were made up to 2.1000 gm with H3B03, ground to -200 mesh and compressed at a pressure of 50000 psi to obtain discs. These were analysed simultaneously for SiO₂, Al₂O₃, Fe as FeO, Ca, K, Ti, Mn and Ba on a multi-channel ARL X-ray spectrometer.

B.2 SAMPLE PREPARATION FOR RB-SR ISOTOPIC ANALYSIS

Rb and Sr concentrations were determined by atomic absorption during whole rock chemical analysis. Samples were weighed in aluminium foil boats

Table B-1
 Methods, Precision and Replicability of Chemical Analysis

Constituent	Method	Concentration	Instrument precision	Replicability
SiO ₂	XRF	59.60	±0.12	±0.20
Al ₂ O ₃	XRF	9.34	±0.05	±0.13
*Fe ₂ O ₃	XRF	10.08	±0.017	±0.03
FeO	Titration	10.92	-	±0.04
CaO	XRF	10.22	±0.02	±0.07
MgO	AAS	4.04	±0.04	±0.10
Na ₂ O	AAS	4.20	±0.01	±0.05
K ₂ O	XRF	2.69	±0.01	±0.01
TiO ₂	XRF	0.48	±0.02	±0.02
P ₂ O ₅	Spectrophotometry	0.20	±0.01	±0.01
MnO	XRF	0.41	±0.01	±0.01
S	Combustion	0.185	±0.003	±0.005
CO ₂	Combustion	1.15	±0.05	±0.12
*H ₂ O	Combustion	1.60	±0.03	±0.06
Ba	XRF	0.015	±0.005	±0.005
Rb	XRF	228 ppm	±1.0	±2.0
Sr	XRF	260 ppm	±5.0	±8.0
Cs	AAS	820 ppm	±5.0	±13.0

* Total concentration expressed as ...

Concentration in weight percentages unless stated
 precision and replicability in units of measurement

on an electric balance, transferred to 100 ml Teflon beakers and digested overnight in a 4:1 mixture of 49% HF and 70.9% HNO₃. The solutions were then evaporated to mush, dissolved in double-distilled water and evaporated to dryness.

Samples were spiked with the appropriate volume of ⁸⁷Rb or ⁸⁴Sr spike solution. The spiked samples were equilibrated by refluxing in 6.2N HCl for two hours, then evaporated to dryness. Samples for Rb isotopic analysis were transferred in solution to 10 ml Pyrex beakers, evaporated and baked.

Samples for Sr isotopic analysis were redissolved in 6.2N HCl and centrifuged to remove undissolved material. They were then passed through ion exchange columns packed with cation exchange resin (Biograd Analytical Grade Cation Exchange Resin, hydrogen form, AG 50W-X12, 200-400 mesh). The first 40 ml was discarded; the following 95 ml was collected and and evaporated to dryness. It was necessary to elute samples twice (because of high Rb levels), the second time discarding the first 50 ml. Samples were then evaporated, transferred to 10 ml beakers and evaporated to dryness.

Appendix C

RENORMC.1 FUNCTION

The purpose of this programme is to compute the normative mineral composition of a rock from the chemical analysis for major oxides. The programme is intended to be particularly relevant for volcanic rocks but will compute norms for other igneous rocks. It is a hybridization of three pre-existing norm-calculation programmes and includes the variations in calculation by means of options.

The calculation method was derived by T.N. Irvine and W.R.A. Baragar (1971) from the earlier CIPW and Barth-Niggli norms. Both weight percent and percent cation equivalents are calculated. The programme includes algorithms for assignation of a name based on the Irvine and Baragar classification and for calculation of indices and ratios used in petrology.

C.2 PROCESSING LOGIC

The processing logic of the programme is:

- 1) Read in the title, parameter and format cards.
- 2) Print out the options selected.
- 3) Read in the data.
- 4) Reorder the oxides if necessary.
- 5) Apply iron and carbon dioxide options to the data.
- 6) Normalize the oxide (weight %) values to 100%.
- 7) Print out the original data and the normalised results.
- 8) Compute cation equivalents (mol.%) for the oxides and renormalize.
- 9) Compute normative composition in cation equivalents.
- 10) Convert normative composition to weight % of each mineral and normalize.
- 11) Print out normative composition in weight % and mole %.

- 12) Compute and print mineral ratios and indices in cation equivalents and weight %.
- 13) Assign a name according to the Irvine and Baragar classification.

Normative composition is assumed to be water-free. The normative minerals are derived from the chemical analyses in the order: calcite, apatite, pyrrhotite, chromite, ilmenite, feldspars, corundum, potassium metasilicate, acmite, sodium metasilicate, magnetite, haematite, wollastonite, enstatite, ferrosilite, diopside, hedenbergite, quartz, forsterite, fayalite. If quartz is deficient, nepheline, leucite, larnite and kaliophilite may be formed from more saturated minerals.

C.3 OPTIONS

The standard defaults in the programme may be overridden to suit the user's requirements. If all defaults are used, data is expected on cards in the order: Sample number - SiO_2 - Al_2O_3 - Fe_2O_3 - FeO - CaO - MgO - Na_2O - K_2O - TiO_2 - P_2O_5 - MnO - S - NiO - CrO_3 - CO_2 - H_2O . CO_2 is included in the norm calculation, H_2O is removed and ferric iron is adjusted to be less than $\text{TiO}_2+1.5$. The rock is assigned a name according to the Irvine-Baragar classification.

The options are:

- a) Variable input format.
- b) Input data on cards or discs.
- c) Oxides in any order.
- d) CO_2 may be removed.
- e) Ferric iron/ferrous iron may be adjusted so that ferric iron is less than $\text{TiO}_2+1.5\%$.
- f) All ferric iron may be converted to ferrous iron.
- g) A separate output of normative mineral composition for later processing.
- h) A separate output of normalised volatile-free composition for later

processing with optional user-defined format.

- i) A separate output of ratios and indices for later processing.
- j) Suppression of assigned name.

C.4 OUTPUT

Printed output comprises:

- a) Parameters and options selected for the data.
- b) A table of oxide weight percentages and normalized weight percentages after the options have been applied.
- c) Normative mineral composition, in weight % and mole % normalized to 100%.
- d) Petrologic indices and ratios, in weight % and mole %.
- e) The assigned rock name (unless suppressed).

Optional output, stored on files, comprises:

- a) Normalized volatile-free composition.
- b) Normative mineral composition in mole %.
- c) Some of the petrologic indices and ratios.

Appendix D

NORMATIVE CALCULATIONS ON KLONDIKE FORMATION

Normative calculations were carried out using the RENORM programme (Appendix C). Petrographic studies suggested that calcite, and therefore Ca, is not a primary component of the volcanogenic rocks; accordingly, CO₂ was a permitted component. Adjustment of ferric iron was carried out after preliminary runs assigned the volcanogenic rocks to the calc-alkaline suite. Further information on parameter selection is presented in Table D-2.

Table D-1

Normative Analyses of Klondike Formation

Oxides are in weight %, normative minerals in cation %.

Sample						
number	14/8/15	16/8/1	16/8/2	16/8/12A	16/8/15A	16/8/16
SiO ₂	77.70	71.55	80.30	74.65	70.90	75.20
Al ₂ O ₃	12.58	10.36	10.95	13.36	15.67	13.06
Fe ₂ O ₃	0.26	0.00	0.10	0.57	0.96	0.38
FeO	0.32	0.36	0.08	0.40	0.40	0.20
MgO	0.07	0.07	0.08	0.14	0.31	0.09
CaO	0.06	5.58	0.13	0.30	0.15	0.84
Na ₂ O	2.27	1.88	2.10	1.40	2.67	2.32
K ₂ O	5.78	4.78	5.22	8.73	7.52	6.53
TiO ₂	0.10	0.12	0.10	0.15	0.17	0.12
P ₂ O ₅	0.02	0.02	0.00	0.00	0.06	0.02
MnO	0.01	0.10	0.01	0.02	0.01	0.03
S	0.01	0.00	0.01	0.01	0.02	0.12
CO ₂	0.20	4.65	0.12	0.24	0.22	0.73
q	40.10	39.65	45.85	30.98	24.54	34.40
c	2.89	2.31	2.07	1.78	3.47	2.41
or	35.04	28.68	31.86	52.58	45.15	39.24
ab	20.89	17.12	19.46	12.80	24.34	21.16
an	0.00	0.00	0.00	0.00	0.00	0.00
di	0.00	0.00	0.00	0.00	0.00	0.00
he	0.00	0.00	0.00	0.00	0.00	0.00
en	0.20	0.20	0.23	0.39	0.87	0.25
fs	0.00	0.00	0.00	0.00	0.00	0.00
wo	0.00	0.00	0.00	0.00	0.00	0.00
ru	0.03	0.07	0.04	0.00	0.00	0.21
mt	0.00	0.00	0.00	0.61	0.11	0.00
il	0.09	0.03	0.06	0.21	0.24	0.24
hm	0.19	0.00	0.07	0.00	0.61	0.27
ap	0.04	0.04	0.00	0.00	0.13	0.04
po	0.04	0.00	0.04	0.04	0.07	0.04
carb	0.50	11.93	0.31	0.62	0.57	1.88

Table D-1 (cont'd)

Sample							
number	16/8/17A	25/8/6	25/8/7	26/8/1	26/8/2	26/8/3	26/8/4
SiO ₂	77.25	77.10	76.70	79.00	77.60	77.90	75.10
Al ₂ O ₃	11.66	11.56	11.30	11.74	11.04	11.24	11.02
Fe ₂ O ₃	0.38	1.53	1.98	1.41	0.39	0.49	0.55
FeO	0.10	0.64	0.92	0.72	0.90	0.58	0.64
MgO	0.04	0.25	0.25	0.38	0.25	0.08	0.34
CaO	1.03	0.21	0.40	0.58	0.28	0.16	1.35
Na ₂ O	2.01	0.66	1.05	1.43	0.75	0.17	1.43
K ₂ O	5.92	6.30	5.49	6.02	6.24	8.28	5.51
TiO ₂	0.13	0.14	0.23	0.13	0.06	0.09	0.06
P ₂ O ₅	0.01	0.03	0.05	0.01	0.02	0.14	0.02
MnO	0.03	0.01	0.03	0.01	0.02	0.03	0.04
S	0.08	0.01	0.00	0.78	0.04	0.03	0.01
CO ₂	0.87	1.29	0.39	1.32	0.34	0.16	1.10
q	40.60	47.71	47.75	41.39	48.20	43.15	45.36
c	2.17	4.13	4.15	3.20	3.50	2.27	3.02
or	35.85	38.59	34.07	36.39	38.40	51.14	33.44
ab	18.48	6.14	9.89	13.12	7.01	1.59	13.17
an	0.00	0.00	0.00	0.00	0.00	0.00	0.00
di	0.00	2.24	0.00	0.02	0.00	0.00	0.00
he	0.00	0.00	0.00	0.00	0.00	0.00	0.00
en	0.11	0.00	0.72	0.00	0.72	0.23	0.96
fs	0.00	0.00	0.10	0.00	0.65	0.30	0.46
wo	0.00	1.19	0.00	0.00	0.00	0.00	0.01
ru	0.21	0.12	0.00	1.48	0.00	0.00	0.00
mt	0.00	0.00	1.90	0.42	0.54	0.59	0.00
il	0.24	0.04	0.34	2.77	0.09	0.13	0.09
hm	0.27	1.10	0.00	1.01	0.00	0.00	0.00
ap	0.02	.07	0.11	0.02	0.04	0.31	0.04
po	0.28	0.04	0.00	2.77	0.14	0.11	0.04
carb	2.25	3.38	1.04	3.41	0.90	0.42	2.86

Table D-1 (cont'd)

Sample						
number	26/8/6	26/8/7	26/8/9	27/8/1A	27/8/1B	27/8/3A
SiO ₂	77.60	72.50	78.60	72.20	75.65	75.90
Al ₂ O ₃	11.58	12.56	10.77	13.46	11.66	12.96
Fe ₂ O ₃	0.65	0.75	0.40	0.20	0.48	0.35
FeO	0.50	0.26	0.38	0.18	0.62	0.34
MgO	0.29	0.18	0.19	0.15	0.41	0.24
CaO	0.80	1.50	0.50	1.65	1.75	0.49
Na ₂ O	1.98	0.80	0.42	1.50	1.78	0.83
K ₂ O	5.13	9.13	7.35	8.59	5.27	8.16
TiO ₂	0.50	0.06	0.04	0.07	0.07	0.11
P ₂ O ₅	0.00	0.00	0.02	0.01	0.00	0.00
MnO	0.01	0.01	0.02	0.02	0.02	0.03
S	0.10	0.75	0.08	0.03	0.01	0.02
CO ₂	0.77	1.91	0.56	1.34	1.36	-
q	43.62	31.12	45.92	28.57	38.67	36.59
c	3.09	1.49	2.40	1.87	0.00	2.10
or	31.06	54.37	45.17	51.65	32.09	49.73
ab	18.20	7.23	3.92	1.87	16.45	7.68
an	0.00	0.00	0.00	0.00	8.49	2.51
di	0.00	1.89	0.00	0.00	0.25	0.00
he	0.00	0.00	0.00	0.00	0.11	0.00
en	0.82	0.00	0.55	0.42	1.04	0.68
fs	0.00	0.00	0.00	0.00	0.48	0.11
wo	0.00	0.94	0.00	0.00	0.00	0.00
ru	0.31	1.35	0.07	0.00	0.00	0.00
mt	0.00	0.00	0.00	0.00	0.52	0.38
il	0.09	2.62	0.09	0.09	0.10	0.16
hm	0.46	0.53	0.29	0.14	0.00	0.00
ap	0.00	0.00	0.04	0.02	0.00	0.00
po	0.36	2.62	0.29	0.11	0.04	0.07
carb	1.99	4.86	1.47	3.45	3.54	-

Table D-2

Parameter Echo for Norm Calculation Programme

-
1. Input data is on cards.
 2. Oxide data is expected in program order.
 $\text{SiO}_2\text{-Al}_2\text{O}_3\text{-Fe}_2\text{O}_3\text{-FeO-CaO-MgO-Na}_2\text{O-K}_2\text{O-TiO}_2\text{-P}_2\text{O}_5\text{-MnO-S-NiO-Cr}_2\text{O}_3\text{-CO}_2\text{-H}_2\text{O}$.
 3. CO_2 is a permitted component.
 4. All ferric iron is not converted to ferrous iron.
 5. Ferric iron is adjusted to be less than $\text{TiO}_2 + 1.5$, the excess being converted to ferrous iron.
 6. No separate output of normative mineral composition on TAPE3.
 7. No separate output of normalized volatile-free composition on TAPE4.
 8. No separate output of ratios on TAPE5.
 9. The appropriate name for the normative composition will be given according to the Baragar-Irvine classification.
 10. The input data format is the default - A5, 16F4.2 - no decimal points.
-

Appendix E

CHLORITE SCHISTS AND SERPENTINITESE.1 PETROGRAPHIC DESCRIPTIONSMoosehide Assemblage

Sample 4/6/1

Cataclastic serpentinite

Mode: Antigorite	45%
Sheared iron stained antigorite	40%
Chrysotile	5%
Iron-titanium oxide	10%

Subhedral laths of antigorite (1-2 mm) are in 10-15 mm aggregates pseudomorphous after rounded olivine. These are unsheared and bounded by zones of cataclasis comprising sheared iron-stained antigorite with discontinuous stringers of iron-titanium oxide (0.5 mm) and chrysotile (0.2-0.5 mm).

Sample 27/5/3A

Coarse-grained cataclastic amphibolite

Mode: Plagioclase (An ₃₇)	40%
Actinolite with relict uralite	35%
Epidote (zoisite)	25%

Large plagioclase phenocrysts (AN₃₇) and actinolite (17 mm) are fractured by cataclasis. Relict hornblende is enclosed by the actinolite. The matrix comprises granoblastic zoisite, plagioclase and actinolite (0.4 mm). Accessory minerals are absent.

Sample 27/5/3B

Cataclastic amphibolite

Mode: Actinolite	35%
Plagioclase	20%
Quartz	15%
Epidote	15%
Chlorite	10%
Sphene	5%

Actinolite (0.1 mm) is rotated and fractured, chlorite (0.2 mm) folded in a granoblastic matrix of plagioclase and quartz (0.1-0.3 mm). Plagioclase composition was not determinable. Anhedra epidote, sphene and iron-titanium oxide are disseminated accessory phases.

Sample 27/5/5

Cataclastic amphibolite

Mode: Actinolite	40%
Plagioclase	20%
Epidote	20%
Chlorite	15%
Quartz	5%
Sphene	Trace

Subhedral porphyroblasts (1-4 mm) of actinolite are rotated and fractured in a granoblastic matrix of quartz and plagioclase with crystalloblasts of actinolite and lepidoblasts of chlorite. The fine grain size (0.1-0.2 mm) precludes determination of plagioclase composition. The fabric is randomly oriented. Aggregates of epidote (0.5-1.0 mm) and fractured anhedra of sphene (0.5-1.0 mm) occur.

Sample 29/7/3

Blastomylonitic schist

Mode: Plagioclase (An6)	35%
Actinolite	30%

Chlorite	20%
Epidote	10%
Quartz	5%
Pyrite	Trace

Actinolite and chlorite (0.2 mm) form a lepidoblastic matrix with intersertal albite, quartz and epidote. Subhedral pyrite (2 mm) is rare. Quartz-epidote veins parallel the S1 cleavage. Minor brittle fractures are associated with S2.

Sample 29/7/4

Blastomylonitic schist

Mode: Quartz	35%
Chlorite	35%
Epidote	30%
Iron-titanium oxide	Trace

Epidote (0.1 mm) is disseminated in a granoblastic quartz matrix (0.2 mm). Penetrative bands (1-3 mm) rich in oriented lepidoblastic chlorite (0.2-0.3 mm) impart S1 and S0. S2 cleavage is weak, fractures absent.

King Solomon Dome Assemblage

Samples H-21, H-60, H-62, H129

Blastomylonitic schists

Modes: Plagioclase (An15 to An34)	40-45%
Amphibole	10-25%
Chlorite/biotite	10-25%
Epidote (Pistacite)	10-20%
Sphene/leucoxene	1-5%

An oriented matrix of lepidoblastic chlorite, altered to biotite, and actinolite, after hornblende, encloses anhedral plagioclase and epidote

(0.1-0.3 mm). The F2 deformation has folded and fractured S1 cleavage. Sphene and leucoxene (0.1-0.3 mm) are accessory phases.

Sample H-65

Blastomylonitic schist

Mode: Actinolite	60%
Chlorite	40%
Sphene	Trace

Chlorite and actinolite (0.2-0.4 mm) are oriented to form the S1 cleavage. The actinolite frequently encloses relict green hornblende. Rare euhedral sphene is associated with chlorite. The S1 cleavage is folded and fractured by F2.

Sample H-119

Cataclastic amphibolite

Mode: Green hornblende	50%
Plagioclase (An33)	25%
Chlorite	10%
Muscovite	5%
Epidote	5%
Sphene	5%

Rounded fractured anhedral hornblende (1-5 mm) are separated by penetrative shear zones comprising granoblastic andesine and epidote (0.1 mm). S1 cleavage is defined by oriented lepidoblasts of chlorite and muscovite (0.2 mm) and by laths of hornblende (0.5 mm). The large hornblende crystals are rimmed by chlorite and sphene.

Sample 20/8/3

Blastomylonitic schist

Mode: Albite	30%
Chlorite	30%
Epidote	10%
Carbonate	10%
Quartz	10%
Muscovite	10%
Iron-titanium oxide	Trace

Albite and quartz (0.2 mm) form a crystalloblastic matrix with bands, 0.5 mm in width, rich in carbonate and epidote. Lepidoblastic chlorite and muscovite (0.2 mm) define an S1 cleavage parallel to this compositional layering. F2 fractures are filled with carbonate.

Sample H-16

Banded garnetiferous blastomylonite

Mode: Plagioclase (An33)	60%
Brown hornblende	15%
Chlorite	10%
Garnet	5%
Carbonate	5%
Magnetite	4%
Apatite	1%
Epidote	Trace

A granoblastic matrix of plagioclase (0.3 mm) contains bands (0.5 mm) rich in brown hornblende (0.1-0.3 mm). Enrolled garnet (0.1-0.3 mm) and magnetite (2 mm) occur in the bands. Garnet is fractured and marginally altered to carbonate and chlorite. Aggregates of chlorite (0.5 mm) and disseminated iron-titanium oxide after garnet occur. Epidote and apatite

accessory. S0 and S1 have been folded during F2.

Sample 26/7/5

Bimodal blastomylonitic schist

Mode: Quartz fragments	10%
Quartz	20%
Muscovite	20%
Chlorite	20%
Plagioclase	15%
Epidote	10%
Carbonate	2%
Actinolite	2%
Iron-titanium oxide	1%

Lepidoblastic muscovite and chlorite (0.3 mm) impart an S1 cleavage to a crystalloblastic matrix of quartz, albite and epidote (0.2 mm) with accessory actinolite, carbonate and iron-titanium oxide. Quartz fragments, as much as 4 mm, are recrystallized, with sutured grain boundaries. The S1 cleavage has been refolded by F2.

E.2 CHEMICAL ANALYSES AND NORMATIVE CALCULATIONS

Chemical analysis of eight samples was carried out, using analytical techniques described in Appendix B. Lithologies present in the Moosehide Assemblage are represented by samples 4/6/1, 27/5/3A, 27/5/3B and 27/5/5; those in the King Solomon Dome area by samples H-119, 30/7/30, 20/8/3 and 26/7/5. Analytical results and normative analyses (using RENORM) are presented in Table E-1. Programme parameters are also listed (Table E-2).

Table E-1

Normative Calculations on Greenschists

Oxides in weight %, normative minerals in cation %

Moosehide Assemblage

Sample				
number	4/6/1	27/5/3A	27/5/3B	27/5/5
SiO ₂	39.50	49.85	55.25	53.60
Al ₂ O ₃	0.70	16.75	14.64	12.76
Fe ₂ O ₃	8.41	3.88	4.47	2.94
Feo	1.38	3.38	4.86	5.58
MgO	38.20	7.60	6.70	10.15
CaO	0.04	11.60	7.95	8.35
Na ₂ O	0.00	2.43	2.05	2.23
K ₂ O	0.34	0.69	0.20	0.56
TiO ₂	0.12	0.10	0.66	0.52
P ₂ O ₅	0.00	0.03	0.05	0.03
MnO	0.09	0.16	0.17	0.18
S	0.00	0.00	0.00	0.00
CO ₂	0.83	0.91	0.08	0.05
q	0.00	0.00	10.20	2.67
c	0.29	0.00	0.00	0.00
or	2.06	4.20	1.24	3.40
ab	0.00	22.45	19.23	20.55
an	0.20	33.72	31.51	23.77
di	0.00	13.39	4.38	10.32
he	0.00	6.86	3.11	4.53
en	19.84	6.02	17.13	23.60
fs	2.60	3.09	12.14	10.36
fo	66.16	6.66	0.00	0.00
fa	8.68	3.41	0.00	0.00
il	0.17	0.14	0.96	0.74
ap	0.00	0.07	0.11	0.06

King Solomon Dome Assemblage

Sample				
number	H-119	30/7/30	20/8/3	26/7/5
SiO ₂	48.45	52.65	55.10	65.85
Al ₂ O ₃	12.99	14.68	14.28	12.28
Fe ₂ O ₃	2.66	3.90	3.21	2.74
FeO	7.00	6.40	3.56	2.70
MgO	10.75	4.40	4.33	4.48
CaO	8.60	5.75	5.83	4.63
Na ₂ O	2.60	5.00	4.40	1.78
K ₂ O	0.86	1.28	1.50	1.55
TiO ₂	1.42	2.38	0.59	0.60
P ₂ O ₅	0.29	0.55	0.14	0.14
MnO	0.19	0.17	0.12	0.10
S	0.00	0.00	0.00	0.00
CO ₂	0.12	0.02	2.76	0.54
q	0.00	0.00	2.98	28.96
c	0.00	0.00	0.00	0.00
or	5.26	7.81	9.47	9.67
ab	24.13	46.30	42.17	16.86
an	21.95	14.27	15.79	22.09
di	11.27	4.55	6.37	0.59
he	4.89	4.61	4.96	0.35
en	8.14	4.74	9.59	12.75
fs	3.53	4.80	7.51	7.55
il	2.05	3.42	0.88	0.88
ap	0.63	1.19	0.31	0.31

Table E-2

Parameter Echo for Norm Calculation Programme

-
1. Input data is on cards.
 2. Oxide data is expected in programme order
 $\text{SiO}_2\text{-Al}_2\text{O}_3\text{-Fe}_2\text{O}_3\text{-FeO-Cao-MgO-Na}_2\text{O-K}_2\text{O-TiO}_2\text{-P}_2\text{O}_5\text{-MnO-S-NiO-Cr}_2\text{O}_3\text{-CO}_2\text{-H}_2\text{O}$
 3. CO_2 is removed from the analysis, which is normalized to 100 per cent.
 4. All ferric iron is converted to ferrous iron.
 5. Ferric iron is unchanged.
 6. No separate output of normative mineral composition on TAPE3.
 7. No separate output of normalized volatile-free composition on TAPE4.
 8. No separate output of ratios on TAPE5.
 9. The appropriate name for the normative composition will be given according to the Baragar-Irvine classification.
 10. The input data format is the default - A5, 16F4.2 - no decimal points.
-